Universidade de São Paulo–USP
Escola de Engenharia de São Carlos
Departamento de Engenharia Mecânica
Programa de Pós-Graduação em Engenharia Mecânica

Polyana Ferreira Nunes

Evaluation of Motor Primitive-Based Adaptive Control Algorithms for Lower Limb Exoskeletons

São Carlos
2021

Polyana Ferreira Nunes

Evaluation of Motor Primitive-Based Adaptive Control Algorithms for Lower Limb Exoskeletons

Tese de doutorado apresentada ao Programa de Engenharia Mecânica da Escola de Engenharia de São Carlos como parte dos requisitos para a obtenção do título de Doutor em Ciências.

Área de concentração: Dinâmica e Mecatrônica

Orientador: Adriano Almeida Gonçalves Siqueira

VERSÃO CORRIGIDA

São Carlos
2021

Ficha catalográfica elaborada pela Biblioteca Prof. Dr. Sérgio Rodrigues Fontes da EESC/USP com os dados inseridos pelo(a) autor(a).

Ferreira Nunes, Polyana
F781e Evaluation of Motor Primitive-Based Adaptive Control Algorithms for Lower Limb Exoskeletons / Polyana Ferreira Nunes; orientador Adriano Almeida Gonçalves Siqueira . São Carlos, 2021.

Tese (Doutorado) - Programa de Pós-Graduação em Engenharia Mecânica e Área de Concentração em Dinâmica e Mecatrônica -- Escola de Engenharia de São Carlos da Universidade de São Paulo, 2021.

1. Rehabilitation Robotics. 2. Motor Primitives. 3. Exoskeleton. 4. Lower Limbs. 5. Biomechatronics. I. Título.

Eduardo Graziosi Silva - CRB - 8/8907

FOLHA DE JULGAMENTO

Candidata: Engenheira **POLYANA FERREIRA NUNES.**

Título da tese: " Avaliação de algoritmos de controle baseados em primitivas motoras para exoesqueletos de membros inferiores".

Data da defesa: 07/05/2021.

Comissão Julgadora	**Resultado**
Prof. Associado **Adriano Almeida Gonçalves Siqueira (Orientador)** (Escola de Engenharia de São Carlos/EESC-USP)	**APROVADA**
Prof. Dr. **Carlos Andrés Cifuentes García** (Escuela Colombiana de Ingenieria/ECI-Bogotá)	**APROVADA**
Prof. Dr. **Adriano de Oliveira Andrade** (Universidade Federal de Uberlândia/UFU)	**APROVADA**
Profa. Dra. **Zilda de Castro Silveira** (Escola de Engenharia de São Carlos/EESC-USP)	**APROVADA**
Prof. Dr. **Luciano Luporini Menegaldo** (Universidade Federal do Rio de Janeiro/UFRJ)	**APROVADA**

Coordenador do Programa de Pós-Graduação em Engenharia Mecânica:
Prof. Associado **Adriano Almeida Gonçalves Siqueira**

Presidente da Comissão de Pós-Graduação:
Prof. Titular **Murilo Araujo Romero**

Dedico esse trabalho aos meus pais, Elb e Nélida, ao meu esposo, Marco Aurélio, à minha irmã, Tatiana e aos meus amados sobrinhos, Carlos Eduardo e Gabriel, pelo amor incondicional e apoio.

Acknowledgments

Primeiramente a DEUS, que com sua infinita misericórdia meu ajudou a chegar até aqui, sempre me dando forças e colocando pessoas no meu caminho que foram verdadeiros anjos.

Ao meu esposo Marco Aurélio pelo amor, companheirismo, paciência, incentivo e ajuda incondicional durante todos esses anos de doutorado.

À minha família, que é a base da minha vida, sinônimo de amor, compreensão e fé. À minha mãe, por seu amor imensurável, por ter orado tanto por mim e por sempre estar presente. Ao meu pai, por ter me apoiado e por ter confiado em mim quando eu quis sair de casa pra estudar. Aos meus sobrinhos, amores da minha vida, que me proporcionam tanto carinho e amor.

Ao meu orientador, Adriano Siqueira, pela confiança e orientação. Pelas horas de reuniões tão engrandecedoras, pela compreensão nas horas difíceis e, principalmente, por não ter medido esforços para que eu chegasse até aqui.

À minha querida Flaviane, que me aproximou ainda mais de Deus. Mulher de fé, me acolheu como uma irmã. Tem uma família que é exemplo de amor pra mim.

Aos meus avós, José e Terezinha, pelo carinho e compreensão por eu ter ficado tanto tempo longe. Aos meus avós, José do Carmo (in memorian), e Lélia (in memorian), eram tão entusiasmados em me ver estudar, e sempre perguntavam quando eu terminaria. Não foi da vontade de Deus que eles estivessem aqui hoje pra eu poder respondê-los: terminei.

Aos professores do Departamento de Engenharia Mecânica da EESC/USP. Aos professores, Samuel Nogueira e Glauco A. de Paula Caurin pelas contribuições ao trabalho dadas no exame de qualificação. À professora Zilda, que sempre me tratou com muito carinho.

Aos funcionários do Laboratório de Mecatrônica e da Secretaria de Pós-Graduação do departamento de Engenharia Mecânica (em especial a Iara) que de alguma forma contribuíram para a realização deste trabalho.

Aos colegas do Laboratório de Mecatrônica pelo ótimo ambiente de trabalho e companheirismo. Meninos brilhantes: fui muito privilegiada em estar junto a eles durante esses anos.

Ao Ícaro, por todos os minutos que passamos juntos no laboratório. Entre um cafezinho e outro, estávamos lá trabalhando e dando boas gargalhadas. Como eu aprendi com esse menino! Além de ser uma pessoa generosa, é um aluno de excelência e terá um futuro brilhante.

E por fim, e não menos importante, a todos os amigos que de uma forma ou outra, também fizeram parte. Ao Wilian Leão, que foi quem me incentivou a fazer mestrado e doutorado na USP e que hoje, apesar da distância, é meu amigo irmão. À Patrícia, minha eterna melhor amiga de infância. À Helena, que, de repente, estava na minha casa tomando café comigo e abrançando minhas gatas como se fossem dela, assim nasceu uma amizade. À Mariana, inspiração de coragem, que além de amiga será minha colega de profissão.

"For, see, the winter is past, the rain is over and gone; The flowers appear on the earth; The time of the singing has come."

Song of Solomon 2:12-13

Resumo

Nunes, P. F. **Avaliação de Algoritmos de Controle Baseados em Primitivas Motoras para Exoesqueletos de Membros Inferiores**. 115 p. Tese de doutorado – Escola de Engenharia de São Carlos, Universidade de São Paulo, 2021.

A fim de auxiliar na reabilitação de indivíduos com deficiência motora, especialmente vítimas de acidente vascular cerebral a reabilitar seus movimentos, centros de pesquisa vem desenvolvendo exoesqueletos de membros inferiores e estratégias de controle para esses dispositivos robóticos. A terapia assistida por robô pode ajudar não só por fornecer suporte, exatidão e precisão durante a execução dos exercícios, mas também por ser capaz de se adaptar às diferentes necessidades do paciente, de acordo com suas deficiências. A abordagem proposta foi avaliada em um exoesqueleto de membros inferiores, no qual a articulação do joelho era acionada por um atuador elástico em série. Primeiro, para extrair as primitivas motoras, os torques do usuário são estimados por meio de um observador de distúrbio baseado em momentum generalizado combinado com um filtro de Kalman estendido. Esses dados são fornecidos ao algoritmo de controle do exoesqueleto, que, a cada fase de balanço, auxilia o sujeito a realizar o movimento desejado, a partir da análise de sua etapa anterior. Os testes foram realizados para avaliar o desempenho do controlador para um sujeito caminhando ativamente, passivamente e em uma combinação dessas duas condições. Os resultados sugerem que a assistência do robô é capaz de compensar a deficiência de peso da primitiva motora quando o sujeito exerce menos torque do que o esperado. Além disso, embora apenas a articulação do joelho tenha sido acionada, os pesos das primitivas motoras em relação à articulação do quadril foram influenciados pelo torque do robô aplicado no joelho. O robô também gerou torque para compensar eventuais movimentos assíncronos do sujeito e se adaptou a uma mudança nas características da marcha em três a quatro passos.

Palavras-chave: Reabilitação Robótica, Primitivas Motoras, Exoesqueleto, Membros Inferiores, Biomecatrônica.

Abstract

Nunes, P. F. **Evaluation of Motor Primitive-Based Adaptive Control Algorithms for Lower Limb Exoskeletons**. 115 p. Ph.D. Thesis – São Carlos School of Engineering, University of São Paulo, 2021.

In order to assist in the rehabilitation of individuals with motor disabilities, especially stroke victims, to rehabilitate their movements, research centers have developed lower limbs exoskeletons and control strategies for these robotic devices. Robot-assisted therapy can help not only by providing support, accuracy, and precision while performing exercises, but also by being able to adapt to different patient needs, according to their impairments. The proposed approach was evaluated on a lower limbs exoskeleton, in which the knee joint was driven by a series elastic actuator. First, to extract the motor primitives, the user torques are estimated by means of a generalized momentum-based disturbance observer combined with an extended Kalman filter. These data were provided to the control algorithm, which, at every swing phase, assisted the subject to perform the desired movement, based on the analysis of his previous step. Tests were performed in order to evaluate the controller performance for a subject walking actively, passively, and at a combination of these two conditions. Results suggest that the robot assistance is capable of compensating the motor primitive weight deficiency when the subject exerts less torque than expected. Furthermore, though only the knee joint was actuated, the motor primitive weights with respect to the hip joint were influenced by the robot torque applied at the knee. The robot also generated torque to compensate for eventual asynchronous movements of the subject, and adapted to a change in the gait characteristics within three to four steps.

Keywords: Rehabilitation Robotics, Motor Primitives, Exoskeleton, Lower Limbs, Biomechatronics.

List of Figures

List of Symbols

P	primitive
W	weight
X	the matrix of signals set
S	standard deviation
S^2	variance matrix
A	covariance matrix
I	identity matrix
V	EMG data
p_h	healthy primitive
w_h	healthy weight
τ	torque
K_v	virtual stiffness
θ^d	desired trajectory
$\tau_{r,imp}$	torque of the robot
$\tau_{h,max}$	maximum primitive torque
$\tau_{h,dc}$	constant torque offset
τ_{pat}	patient torque
$\tau_{pat,dc}$	constant offset value
$\tau_{max,h}$	extreme torque
$\tau_{pat,n}$	normalized torque
w_{pat}	patient weight
Δ_w	relative Error
τ_r^{k+1}	torque in the swing phase
$\tau_{r,e}$	effective torque

Summary

Chapter 1

Introduction

The number of subjects with motor disabilities has grown significantly in recent years, mainly stroke victims. And this growth is due to the increase in life expectancy of the elderly population, which increased to 75.8 years in 2016, in Brazil. The consequences of a stroke are numerous, from facial paralysis to physical damage such as loss of strength, balance and muscle tone. Such consequences can make walking, sitting, lying down difficult and, in some cases, the individual may be bedridden or need a wheelchair to get around. Robotics has played an important role in the rehabilitation of individuals with some type of motor disability through the development of devices aimed at rehabilitation, such as exoskeletons.

Robotics has played an important role in the rehabilitation of subjects with some type of motor disability from the development of devices aimed at rehabilitation, such as exoskeletons. These devices seek to promote motor cortical reorganization and consequently improve gait pattern.

1.1 Motivation

According to the World Health Organization - WHO population aging is a fact and by 2050 the number of people aged 60 or over will reach 2 billion, more than double the 900 million subjects in this age group registered in 2015 (ORGANIZATION, 2015) and the elderly will represent one fifth of the planet's population (CASTLES; HAAS; MILLER, 2013). According to Verghese *et al.* (2006) the incidence of gait disorders is higher among the elderly and can reach a prevalence of 35% and 60% in people over the age of respectively, and a very common disorder among elderly people is stroke.

Stroke was considered to be clinical symptoms of rapid evolution and/or signs of focal and sometimes global disturbances of brain function, lasting more than 24 hours or leading to death without any other apparent cause from that of vascular origin (HATANO, 1976). Its diagnosis can be confirmed through clinical examinations such as computed tomography and magnetic resonance imaging (DUNCAN *et al.*, 2003).

Worldwide, stroke is the second leading cause of death and the third long-term disability, with approximately 33 million surviving subjects being a more common disorder among elderly people (LOZANO *et al.*, 2012), (MURRAY *et al.*, 2012), (MURRAY *et al.*, 2015). Among several anomalies caused, stroke is a pathology that can lead to severe sequelae in the neuromusculoskeletal system - NME, including damage to the neural areas that control the movements of the upper and lower limbs, since it leads to the lack or excess of blood supply in the brain, prime area of the brain. Motor impairment affects about 50% of survivors, who are called hemiparetic subjects (MACKAY; MENSAH; GREENLUND, 2004).

The hemiparetic impairment is a tendency that the body has to remain in an asymmetric postural position, distributing the weight on the paretic body side. This asymmetry together with the difficulty in transferring weight to the affected side, interfere with the ability to maintain postural control, preventing orientation and stability to perform movements with the trunk and limbs (IKAI *et al.*, 2003).

Hemiparetic patients do not present swing and support phases as well defined as healthy individuals. The support phase of these patients is next to the balance phase, since the paretic side is unable to perform the circumduction, differently from the healthy side, whose movement begins with flexion, followed by abduction, extension and finally adduction. The patient also has a higher risk of falls, due to uncontrolled movements, and impaired balance and proprioception (SOMMERFELD *et al.*, 2004).

Loss of mobility is one of the biggest complaints of individuals with hemiparesis. The difficulty in carrying out daily tasks has a great impact on the lives of these subjects, with negative ramifications in the participation in their social, professional and recreational activities (ROBINSON *et al.*, 2011).

Several studies have emerged with the intention of rehabilitating and improving the quality of life of people with some type of disability. These studies suggest that the intensity of physical therapy practice, expressed by the number of repetitions and the specific training of the task, are the main drivers of motor rehabilitation after neural damage (KWAKKEL *et al.*, 1999), (LANGHORNE; BERNHARDT; KWAKKEL, 2011) e (BRKIC *et al.*, 2016).

Recovery and improvement in the quality of life of post-stroke subjects is only possible because the cerebral cortex is a set of highly interconnected neuronal cells. The morphology and function of these complex and spatially distributed networks are modulated or even controlled by the glial component of the central nervous system - CNS. The ability to adapt in response to changes in the environment is the most fundamental property of nerve tissues and forms the basis for motor learning. Neuroplasticity is the neurobiological basis of the ability to adapt and learn in a manner dependent on experience, based on repetitions (WIELOCH; NIKOLICH, 2006).

Neuroplasticity is the basic mechanism implicit in improving the functional outcome

after motor impairment. The recovery of subjects whose movements are compromised can be carried out through strengthening exercises for the affected limbs and training tasks (PEKNA; PEKNY; NILSSON, 2012). Therefore, it is urgent to develop new technologies to rehabilitate the NME system for individuals with motor disabilities and also to promote a society with active and sustainable aging.

In view of the difficulties faced by these individuals with motor disabilities and in order to recover the lost or impaired movements and, consequently, improve the quality of life of these people, several studies on rehabilitation have been carried out by researchers in the field of robotics.

A study presented by Stein (2012) on the use of robots in rehabilitation concluded that academic research in robotic rehabilitation has grown rapidly and steadily, mainly in the area of post-stroke rehabilitation where most of the published articles are presented. But despite growth since the late 1980s, robots are still not widely used in the lives of individuals in need, generating even more interest in academic research (FAZEKAS, 2013). And this has been done by research groups in the field of robotic rehabilitation (LUM *et al.*, 2002), (PATTON; MUSSA-IVALDI, 2004), (KREBS *et al.*, 2008) e (CONTRERAS-VIDAL *et al.*, 2016).

The importance of using robots in the rehabilitation of individuals with motor disabilities, mainly stroke victims, was seen positively by physiotherapists, who consider the use of robotic rehabilitation as a complement to conventional therapy (STEPHENSON; STEPHENS, 2017). And in the rehabilitation process, one of the most important tasks for health professionals is to accurately determine the levels of assistance that will act on human joints during gait. In a recent study published by (FRICKE *et al.*, 2020), the authors show apparent advantages of automatic adjustment compared to manual adjustment performed by therapists during clinical practice.

The advantage of using robotic devices compared to traditional rehabilitation approaches include: the ability to produce objective measures, such as: position, speed and strength/torque over time to evaluate and monitor patient progress, the option to customize treatments for patients with different levels of commitment and independence of patients to exercise.

The robots used in rehabilitation can be divided into therapeutic and assistance robots. Assistive robots' goal is compensation, while therapeutic robots provide task-specific training. Commonly, robotic devices are called exoskeletons, as they are coupled to the human body in order to support the musculoskeletal system allowing for increased strength, resistance and support for locomotion.

In Moreno et. al., (2011) a review of the application of several robotic technologies was proposed, among them the exoskeleton for lower limbs that aims to recover the neuromuscular movements of individuals with motor impairment through repeatability and flexibility. The study showed advantages in the use of this technology to aid the

neurorehabilitation of subjects with motor impairments.

Kong e Tomizuka (2009) e Ronsse *et al.* (2011) proposed a methodology to assist the subject in order to offer the necessary assistance according to their limitation, based on the torque estimate of the joint to perform the movement, and Kazerooni *et al.* (2005) proposed a torque estimate control from a dynamic model of the exoskeleton.

Therefore, how is it possible to develop an adaptive control strategy based on knowledge of the user's kinetic characteristics, so that the exoskeleton can react intuitively to the movement intended by the user, providing an effective rehabilitation. Several recent researches have attempted to achieve this goal (DIAZ; GIL; SANCHEZ, 2011), (YAN *et al.*, 2015), (ALIBEJI *et al.*, 2018), (BAYON *et al.*, 2017), (MAGGIONI *et al.*, 2018).

In Garate *et al.* (2016) e Garate *et al.* (2017), a new bioinspired controller based on motor primitives to assist in locomotion was developed. Using data from the literature, the authors extracted a basic set of primitives to reconstruct the joint torques. The controller used this reduced set of primitive signals together with the joint angle and ground reaction forces, to generate joint reference torques. Motor primitives can be defined as a basic set of signals that govern learned motor behaviors, and the combination of these primitives with different weights form a minimum set of components capable of reconstructing all possible muscle activations or position profiles. This was shown by the studies of Nah *et al.* (2020), who used a small number of primitives to perform different movement tasks when handling a whip.

This doctoral thesis fits exactly in this context. A bioinspired controller, based on motion motor primitives, was developed and evaluated in an exoskeleton for lower limbs, which was configured to provide partial support during gait, in knee flexion and extension, applying precise torques calculated by the control algorithm.

1.2 Background

This doctoral thesis is developed in the context of the research project 'Hybrid Adaptive Strategies for Exoskeletons of Lower Limbs' of the São Carlos School of Engineering (EESC) supported by FAPESP (process No. 2019/05937-7) and with funded by CAPES/PGPTA (Graduate Support Program and Scientific and Technological Research in Assistive Technology in Brazil). The project has the participation of researchers from: Federal University of Espírito Santo (UFES), Federal University of São Carlos (UFSCar), Federal University of Rio Grande do Norte (UFRN), University of Brasília (UnB) and the University of Queensland located in Australia.

The main objective of this research project is the development and evaluation of strategies for robotic rehabilitation of walking using adaptive control algorithms, new communication and interaction interfaces between the user and the exoskeleton control systems, as shown in Figure 1. To achieve this goal, a Robust Absolute Positioning Estimation

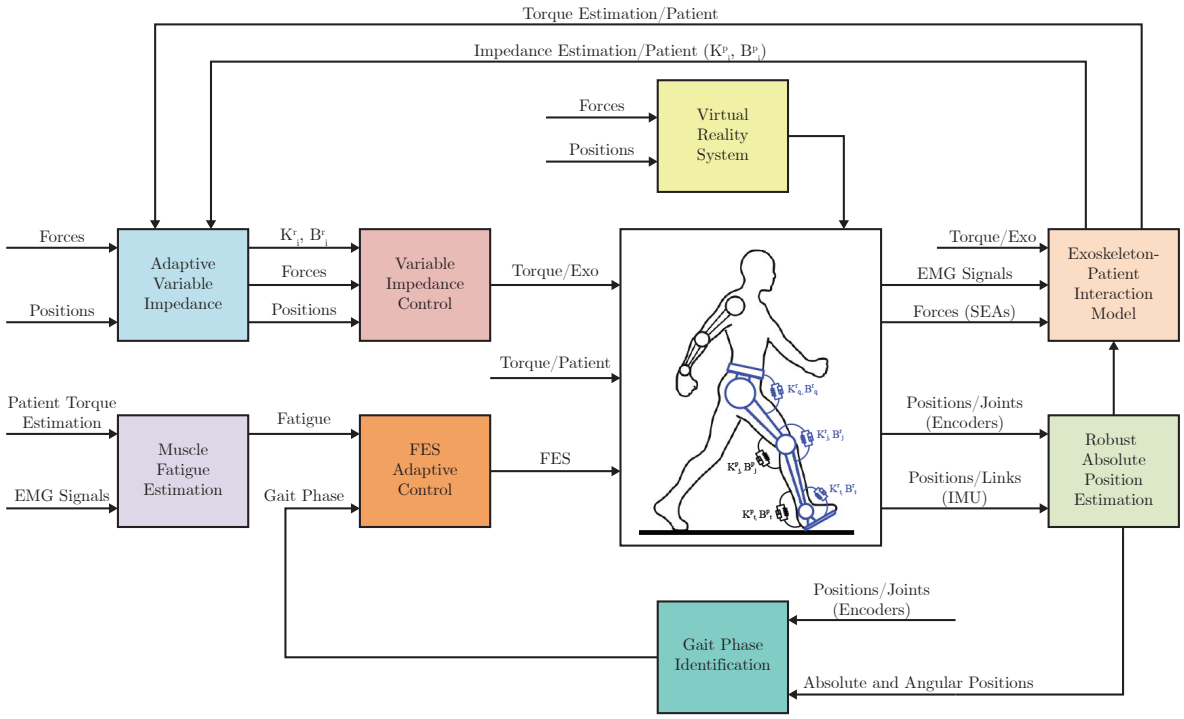

Figure 1 – Hybrid Adaptive Control Strategies for Lower Limbs Exoskeleton research project diagram. This thesis focuses on the part of the patient's torque estimation, and it presents a control strategy based on motor primitives, so that the exoskeleton helps the patient according to his needs.

system was developed to obtain the absolute angles of the patient-exoskeleton system with respect to the ground and the angular positions of all joints. The application of sensor fusion techniques based on Kalman filter and linear systems with Markovian jumps can be seen in Lambrecht *et al.* (2016), Nogueira *et al.* (2017), Nogueira *et al.* (2014). The information resulting from the previous system is used in the robot control system, which implements the Variable Impedance Control, ensuring the stability of the system composed by the user and the exoskeleton Exo Tao, Figure 2, which is the test system of the project (DOS SANTOS; CAURIN; SIQUEIRA, 2017), (DOS SANTOS; SIQUEIRA, 2014), (JUTINICO *et al.*, 2017).

The third system is to identify the current condition of the patient and the level of performance of this during the walk. For this, Patient-Exo Interaction Models were created considering muscle activation and the biomechanical characteristics of the human body, in addition to including a contact model between the patient and the robot (MOSCONI; NUNES; SIQUEIRA, 2018). This system also uses myoelectric signals obtained from the patient and measurements from the exoskeleton to estimate the force performed by the patient and the impedance parameters for each joint (PEÑA *et al.*, 2019). Using the data obtained in the previous systems, the Adaptive Variable Impedance Strategy is implemented in order to maximize the recovery of patients in the shortest possible time. Several optimization techniques are proposed and evaluated (DOS SANTOS; SIQUEIRA, 2019), (PEÑA *et al.*, 2019), (IBARRA *et al.*, 2014), (PEREZ-IBARRA *et al.*, 2018).

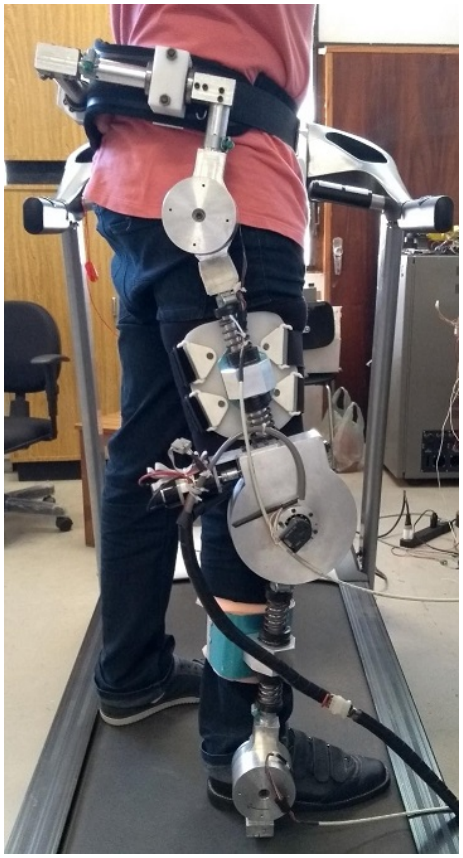

Figure 2 – Modular lower limb exoskeleton - ExoTao.

Currently, an integrated virtual reality system is being developed to interact with lower limb exoskeletons in which virtual environments are created considering walking on a treadmill and on the ground, so that the proposed adaptive strategies are evaluated in an immersive environment. A system to identify the phases of walking with inertial measurement units and contact sensors will also be part of this project. To estimate muscle fatigue, an estimation system generated by the application of FES and performed based on the estimated values of the torques, the stiffness and damping parameters provided by the Patient-Exo Interaction Models system and the electromyography signals (EMG) is also being developed. After identifying the phases of walking and estimating muscle fatigue, an adaptive FES control system will be used to define, in an adaptive way and considering optimal solutions, the periods and intensities of application of the FES.

Therefore, the development of lower limb robots for walking rehabilitation has the potential to serve not only stroke patients, but also other patients with neuromotor problems, such as multiple sclerosis, Parkinson's disease, spinal cord injury hip fracture, among others. The great potential benefit is to include a larger number of patients in motor rehabilitation programs, creating the opportunity to optimize neurorehabilitation therapies based on motor learning.

1.3 Objective

The main objective of this thesis is to develop a bioinspired robotic rehabilitation strategy based on motor primitives that assists the subject according to his needs.

As one of the advantage of using robotic devices over traditional rehabilitation approaches is the option to customizing treatments for subjects with different levels of impairment, the torque provided by the proposed strategy will act directly on the motor impairment.

Indeed, it will act on the basic movement (movement primitive) always assisting that primitive with smaller weights, that is, the motor primitive that represents the deficiency of the subject.

1.4 Contribution and Relevance of Work

In this work, it is developed, implemented and evaluated experimentally a control algorithm based on motor primitives for a modular lower limb exoskeleton, which aims to assist in the rehabilitation of individuals in an individualized way, acting in accordance with the your needs.

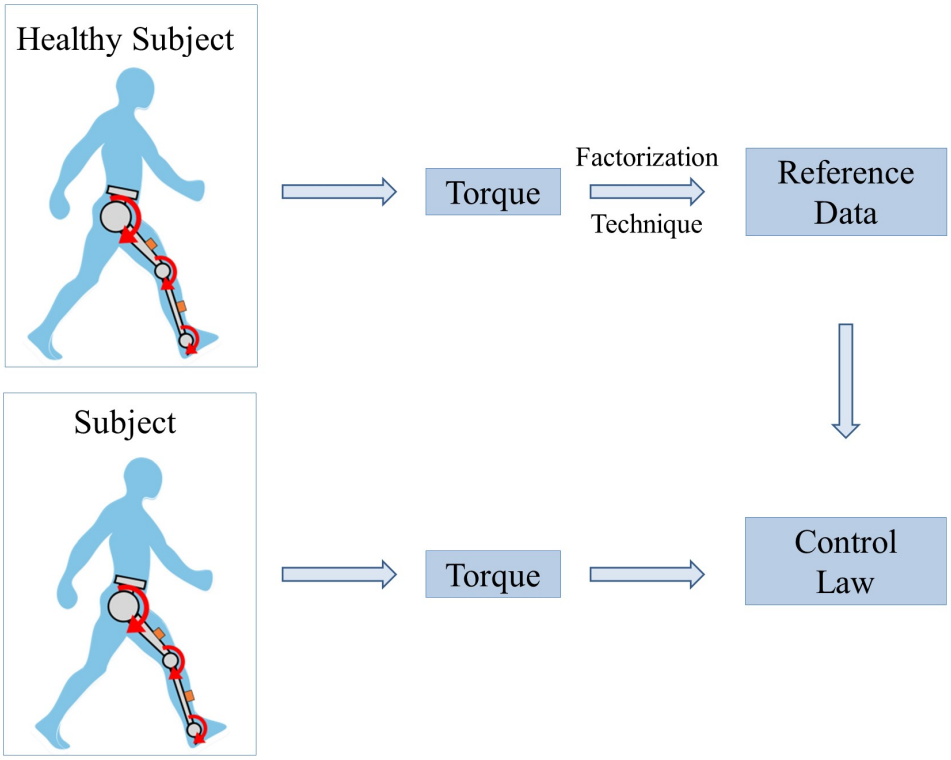

Figure 3 – Diagram of the Control Strategy based on Motor Primitives.

From the determination of the user's torques, it is possible to develop a control strategy based on the knowledge of the user's kinetic characteristics so that the exoskeleton can

react intuitively to the movement intended by the subject and, consequently, can provide collaborative assistance.

First, the motor primitives and their respective weights are extracted from four healthy individuals. To perform this first step, a torque estimation algorithm in conjunction with Principal Component Analysis was employed.

Thereafter, tests with healthy subjects wearing the right leg of the exoskeleton are performed to evaluate the performance of the controller in three different cases: when the subject is actively walking; when the subject has some torque deficiency, represented by more slowly than expected; and when there is a combination of these two cases.

In all cases, the algorithm evaluates the motor primitive weights of the current subject by comparing them with the weights of a healthy subject. When a deficiency is observed, the robot adequately exerts a complementary torque during the swing phase, in order to assist the subject to perform this movement.

The differential of this work with relation to (GARATE *et al.*, 2016) and (GARATE *et al.*, 2017) is the possibility of identifying the primitive kinetic motor of the user in an online and individualized way. Thus, it is expected that control help in the rehabilitation of individuals with different types of disabilities in the lower limbs.

1.5 Publications

Publications in Journals

NUNES, P. F.; OSTAN, I. ; SIQUEIRA, A. A. G . Evaluation of Motor Primitive-Based Adaptive Control for Lower Limb Exoskeletons. **Frontiers in Robotics and AI**, v. 7, p. 1-13, 2020.

NUNES, P. F.; PEÑA, G. G. ; DOS SANTOS, W. M. ; SIQUEIRA, A. A. G . Control of Exoskeleton for Lower Limbs and Influence on Kinetic and Muscular Properties by using Motor Primitives. **Journal of Mechanical Engineering and Biomechanics**, v. 4, p. 31-38, 2019.

Publications in Conferences

NUNES, P. F.; OSTAN, I.; SANTOS, W. M.; SIQUEIRA, ADRIANO A. G. Analysis of Matrix Factorization Techniques for Extraction of Motion Motor Primitives. **In: Congresso Brasileiro de Engenharia Biomédica - CBEB**, Espírito Santo, 2020.

NUNES, P. F.; MOSCONI, D; OSTAN, I.; SIQUEIRA, A. A. G. Control Design Inspired by Motors Primitives to Coordinate the Functioning of an Active Knee Orthosis

for Robotic Rehabilitation. **In: Congresso Brasileiro de Engenharia Biomédica - CBEB**, Espírito Santo, 2020.

NUNES, P. F.; MOSCONI, DENIS; SIQUEIRA, A. A. G. Control Design Inspired by Primitive Motors to Coordinate the Functioning of an Active Knee Orthosis for Robotic Rehabilitation. **In: X Congreso Iberoamericano de Tecnologías de Apoyo a la Discapacidad - IBERDISCAP**, Buenos Aires, 2019.

NUNES, P. F.; DOS SANTOS, W. M. ; SIQUEIRA, A. A. G . Control Strategy Based on Kinetic Motor Primitives for Lower Limbs Exoskeletons. **Symposium on Biological and Medical Systems - IFAC**, São Paulo - SP, 2018. v. 51, p. 402-406.

NUNES, P. F.; SANTOS, W. M.; SIQUEIRA, A. A. G. Análise de Técnicas de Fatoração de Matriz para extração dePrimitivas Motoras de Movimento. **In: Simpósio do Programa de Pós-Graduação em Engenharia Mecânica da EESC-USP - SIPGEM**, São Carlos, 2018.

NUNES, P. F.; PENA, G. G.; SANTOS, W. M.; SIQUEIRA, A. A. G. Influência de um Exoesqueleto sobre as Características Cinéticas e Musculares Durante a Marcha Utilizando Primitivas de Movimento. **In: 6º Encontro Nacional de Engenharia Biomecânica - ENEBI**, Águas de Lindóia - SP, 2018.

NUNES, P. F.; SANTOS, W. M. ; NOGUEIRA, A. L. ; SIQUEIRA, A. A. G. Analyzing Motor Primitives of Healthy Subjects Wearing a Lower Limb Exoskeleton. **In: International Congress of Mechanical Engineering - COBEM**, Curitiba - PR, 2017.

NUNES, P. F.; SANTOS, W. M.; NOGUEIRA, A. L.; SIQUEIRA, A. A. G. Analisando Primitivas Motoras de Sujeitos Saudáveis Usando um Exoesqueleto para Membro Inferiores. **In: Simpósio do Programa de Pós-Graduação em Engenharia Mecânica da EESC-USP - SIPGEM**, São Carlos - SP, 2017.

1.6 Thesis Organization

This doctoral thesis is divided into six chapters and an appendix, this chapter being the first, in which a general notion of the context of the work was presented.

The second chapter discusses the physiology of the muscle contraction process, from the neural cells to the action potentials that are captured by the electromyography electrodes. It also presents the theory on which this work is based, where motor primitives and

their models are discussed, and finally the primitive extraction techniques used in this thesis Principal Component Analysis (PCA) and Non-negative Matrix Factorization(NMF). Subsequently, studies on robotic rehabilitation are presented, showing the robots used in the recovery of movement and finally, the biomechanics of gait.

In the third chapter, the experimental bench with all the equipment used during the research is presented.

In the fourth chapter the bioinspired adaptive control strategy is presented and the factoring techniques used are presented.

The fifth chapter presents the results of this thesis and the discussions of all the results obtained in this work.

In the sixth and final chapter, the final considerations of this study are made.

The appendix shows the hip and knee weights during the simulation of paretic and non-paretic walking.

Chapter 2

Motor Primitives and Rehabilitation Robotics

In this chapter, it is presented a basic description of the muscular system, resulting in the formulation of the motor primitives concept. Additionaly, some researches on rehabilitation robotics are also presented.

2.1 Muscular System

Body composition consists of about 50 % of muscles, of which 40 % are skeletal muscles and about 10 % are smooth and cardiac muscles. And muscle contraction, in addition to being responsible for locomotion, is also responsible for the movement of internal organs, such as, for example, heartbeat, pulsation of arteries, the transit of food bolus through the digestive tract, among others (HALL, 2017).

According to the Figure 4, each muscle fiber is composed of numerous myofibrils, such myofibrils are made up of different types of proteins, with actin and myosin being the most abundant. Actin (Band I) is the main constituent of the thin filaments of muscle cells, with about 3000 filaments, which are long polymerized protein molecules responsible for real muscle contractions, while myosin (Band A), with filaments, makes up thicker filaments and is classified as a mechanochemical enzyme or motor protein, because it is capable of converting chemical energy into mechanical energy, used for the muscle contraction mechanism (HALL, 2017).

Myofilaments are composed of myosins and actins that have a high electronic affinity and are partially interdigitated, causing the myofibril to alternate dark and light bands, that is, the filaments are organized in such a way that the fine ones (actins) can slide over the thick ones (myosin), shortening the myofibrils, which leads to the contraction of muscle cells. This entire process occurs in the presence of Adenosine Triphosphate - ATP, which has its hydrolysis catalyzed by myosin, releasing the energy necessary for muscle to work (HALL, 2017).

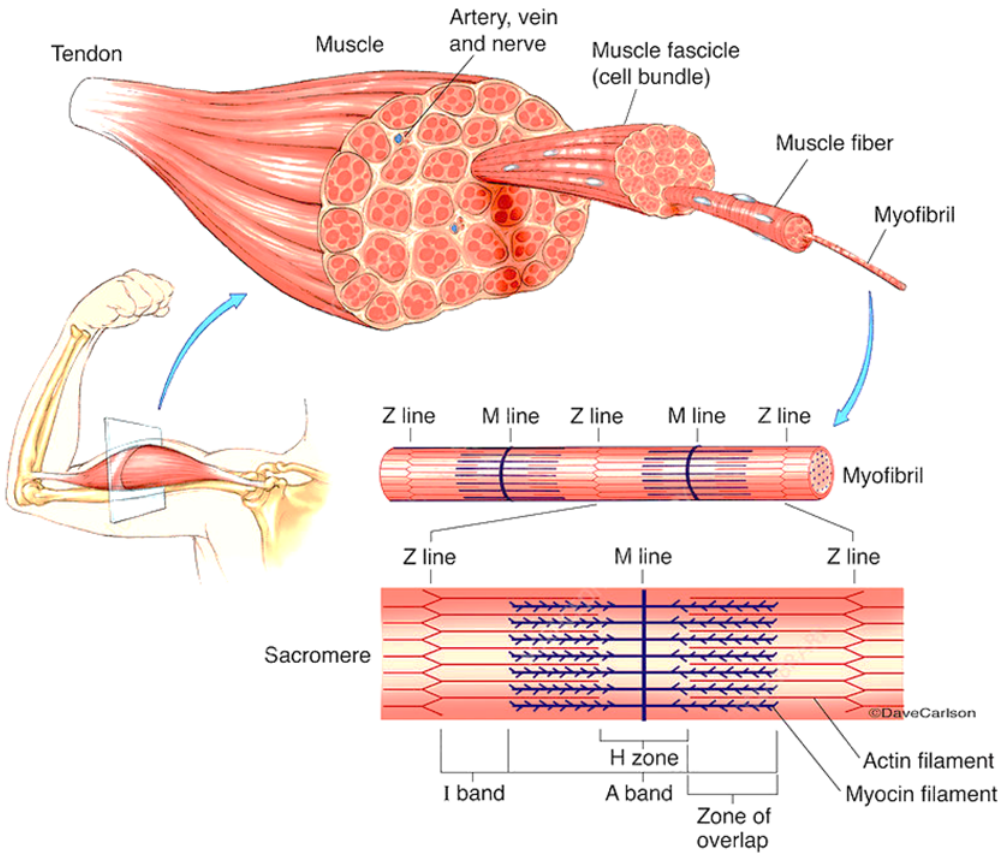

Figure 4 – Muscular Organization (HALL, 2017).

The units of actin and myosin that are repeated throughout the myofibril (or the entire muscle fiber) are called sarcomeres, which are the functional units of the muscle. The place where a sarcomere binds to the next is called Disc Z. The interposed arrangement of the actin and myosin filaments gives rise to the appearance of different bands. Band A is the portion of the sarcomere that runs the entire length of the myosin filaments, while band I contains part of the length of the actin filaments (HALL, 2017).

The length of the sarcomere is about 2 micrometers when the muscle fiber is contracted, the actin filaments overlap completely over the myosia filaments, and the ends of the actin filaments are almost starting to overlap. When the length of the sarcomere drops to 1.65 micrometers, the ends of the two actin filaments began to overlap, in addition to the overlapping of the myosin filaments (HALL, 2017).

Therefore, the length of the sarcomeres gets smaller and smaller with muscle contractions, the muscles appear more and more contracted, the ends of the myosin filaments are wrinkled and the contraction force approaches zero (HALL, 2017).

2.2 Motor Unit

The first concepts of Motor Unit - MU were studied by the British scientist Keith Lucas (1879-1916), who did a pioneering work in Neuroscience at Trinity College, Cambridge. In

his studies, he noted that increasing the intensity of a stimulus applied to a muscle nerve in an experimental animal caused a gradual increase in muscle contractions (LUCAS, 1909). In 1925, Sherrington defined MU as a basic functional element of the central nervous system and the muscle that produces movement, consisting of a motor neuron in the anterior horn of the spinal cord, its axon and the muscle fibers that the axon innervates (SHERRINGTON *et al.*, 1925).

A motor unit is the entire motoneuron, including its dendrites and axon, and the muscle fibers innervated by the axon. The identification of the motor unit was an essential discovery for the understanding of how the central nervous system - CNS controls motor production (BARBARA; CLARAC, 2011) (STUART; BROWNSTONE, 2011).

Most skeletal muscle fibers in mammals are innervated only by a single motor neuron, these fibers are called extrafusal skeletal muscle fibers and generate tension by contraction, thus allowing skeleton movement. As there are many more muscle fibers than motor neurons, individual motor axons branch off within the muscles to synapse into many different fibers that are typically distributed over a relatively wide area within the muscle, theoretically to ensure that the contractile strength of MU is spread evenly. In addition, this arrangement reduces the chance that damage to one or a few motor neurons will significantly alter the action of a muscle. As an action potential generated by a motor neuron normally causes all muscle fibers to come in contact with the threshold, a single motor neuron and its associated muscle fibers constitute the smallest unit of force that can be activated to produce movement (SQUIRE *et al.*, 2012). The Figure 5 shows the MU, composed of the motor neuron that has its branches in contact with the muscle fibers it innervates.

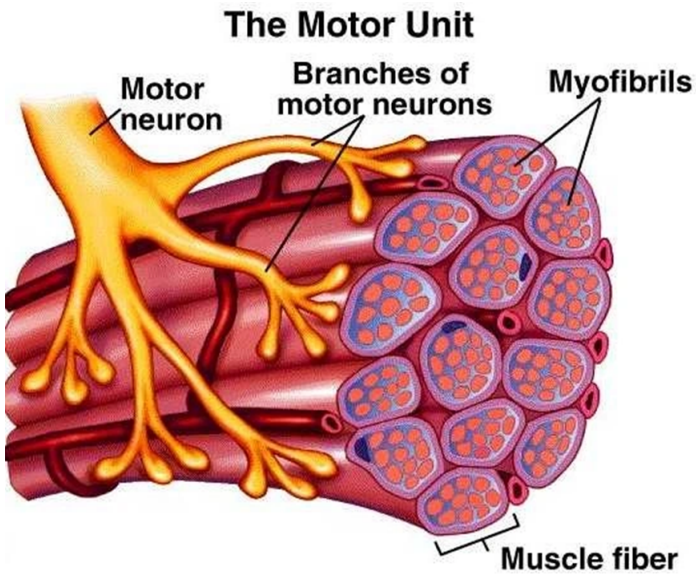

Figure 5 – Muscle fibers innervated by motor neuron - Motor Unit (HALL, 2017).

2.2.1 Motor Unit Action Potential

The action potential of the motor unit or MUAP (*Motor Unit Action Potencial*), is the linear sum of a set of action potentials sent by the alpha motor neuron to n muscle fibers, generating the depolarization of the membranes and consequently the muscle contraction. The fibers of a UM are stimulated when a motor neuron sends an action potential, however, there are small delays in these stimulations, also causing delays in contractions. These delays in muscle action potentials can occur due to two different factors: the first concerns the random nature of acetylcholine discharges at the neuromuscular junctions, and the second factor is related to the propagation time of the various branches of axons in the motor neuron (LUCA, 1979).

Muscle strength is directly related to the increase in the rate of firing of MUAPs (the greater the number of UMs stimulated, the greater the muscle strength). The increase in strength that occurs with the increase in the firing rate, reflects the sum of successive muscle contractions; the muscle fibers are activated by the next action potential before they have time to completely relax and the forces generated by the temporally overlapping contractions are added together.

The lowest firing rates during a voluntary movement are on the order of 8 times per second. As the firing rate of the individual units increases to a maximum value of 25 per second, the amount of force produced increases. At the highest firing rates, the individual muscle fibers are in a state of fused tetanus which means that the tension produced in individual UMs no longer has peaks and troughs that correspond to the individual contractions produced by the motor neuron's action potentials. Under normal conditions, the maximum rate of firing of motor neurons is less than that required for fused tetanus. However, asynchronous firing of different motor neurons provides a constant level of firing at the entrance of the muscle, which generates a change in the tension of the UMs and contraction (SQUIRE *et al.*, 2012).

The sequence of MUAPs is called the train of action potentials of the motor unit - MUAPT *(Motor Unit Action Potential Train)*. In a short period of time, several MUAPs are generated in a row that, when passing through, the muscle fibers will generate a magnetic field around them. An electrode well positioned under the muscle, located within this magnetic field, is capable of capturing the myoelectric signal referring to muscle contraction, generated from the temporal and spatial summation of all action potentials of the muscle fibers of the motor unit (MUAPTs) that spread through tissues (BASMAJIAN; LUCA, 1985).

2.2.2 Electromyography - EMG

The capture of the myoelectric signal, generated by the contraction of muscle fibers, is defined as electromyography - EMG. The first studies involving electrimographic signals,

took place in the second world war, where the capture of signals were used as a clinical diagnostic tool (CLARYS; LEWILLIE, 1992). The EMG signal can be analyzed in the domain of time and frequency. The analysis in the time domain provides parameters of the amplitude of the EMG signal, which allows the visualization of the muscle activation pattern during a contraction, while the analysis in the frequency domain is applied mainly to the study of physiological changes related to muscle fatigue (LUCA, 1997).

The set of innervated muscle fibers in the motoneuron is called the Motor Unit - UM. UMs are responsible for contraction and generate action potentials that can be measured by invasive electrodes or electrodes affixed to the skin's surface. The greater the muscular electrical activity - that is, the greater the number of action potentials (trigger rate and number of UM synchronized) that occurred during contraction and more motor units activated, higher density of the EMG signal (LUCA, 1997). As the action potentials pass through the electrodes, peaks of electrical activity are observed and captured (CLANCY; BOUCHARD; RANCOURT, 2001). The Figure 6 illustrates a schematic representation of the generation of the muscle myoelectric signal from the sum of the MUAP trains of the n motor units of this muscle (BASMAJIAN; LUCA, 1985).

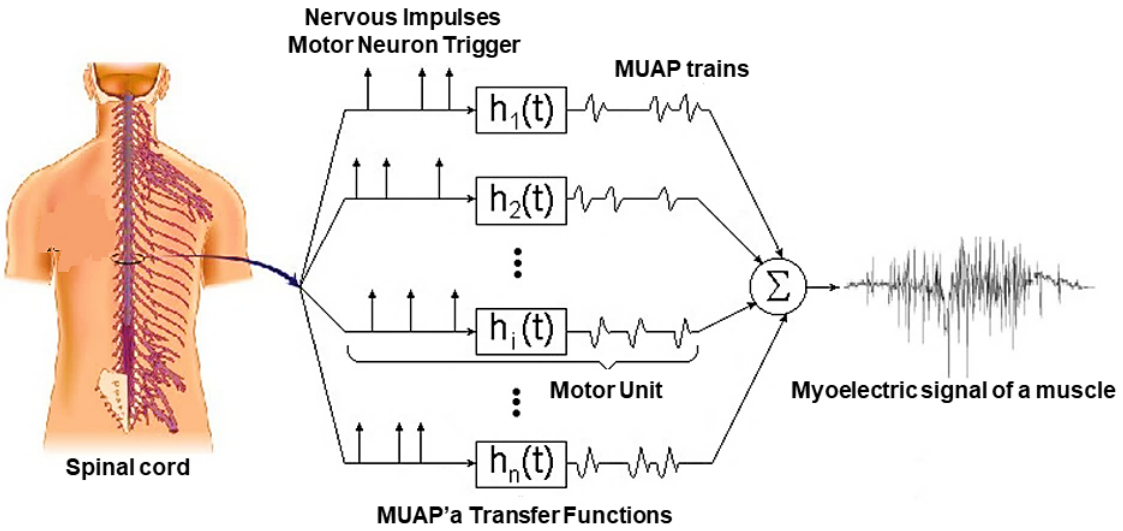

Figure 6 – Schematic representation of the muscle myoelectric signal generation (BASMAJIAN; LUCA, 1985).

The invasive electrodes have needle-type sensors that are inserted into the muscle to capture myoelectric signals. They are more used in clinical analysis because they are able to detect greater amplitudes and broader power spectra, with a frequency of up to 10 kHz (OLSON, 1998), which allows them to measure the action potential of only a single UM. Surface electromyography uses electrodes with surface sensors that are placed over the skin. They are capable of receiving signals up to 500 Hz and with amplitudes between 50muV and 5mV (BASMAJIAN; LUCA, 1985).

EMG signals are used in three major areas in Biomechanics according to (LUCA, 1997): as an indicator of muscle activation, to estimate the strength produced by the muscle, and as an index of muscle fatigue. As an indicator of the onset of muscle activity, the signal can provide the temporal sequence of one or more muscles that perform a task. Another important application of the EMG signal is to provide information about the strength contribution of individual muscles, as well as muscle groups. The resulting torque on a joint during a given task is in most cases, due to the simultaneous action of several muscles. Thus, the ability to non-invasively determine the strength contribution of individual muscles provides an enormous advantage, particularly when biomechanical models are used to describe the functioning of a musculoskeletal system (ME) structure. Finally, and given that the EMG signal displays changes over time before any change in strength, EMG has the potential to predict when the muscle has contractile fatigue (LUCA, 1997).

2.3 Motor Primitives

The concept of motor primitives has attracted much interest in neuroscience as it has become a useful and important way of describing motor behavior. Controlling the musculoskeletal system is a very complex task, since there are several biomechanical factors that are linked to movement control, so the idea of organizing the motor system in modules could be a way for the CNS to circumvent the difficulty of controlling the many degrees of freedom of the musculoskeletal system (BERNSTEIN, 1967).

It is already known that the CNS does not individually control each muscle, however can activate several combinations of motor primitives at the same time. In Lemay *et al.* (2001), it has been shown that the motor control system can produce a variety of behaviors from a limited number of motor primitives. And for that to happen, the motor primitive is used as a form of pre-motor activation that is generated by a set of neurons in the spinal cord and that recruit a muscle group during the movement (HART; GISZTER, 2010).

Due to the great number of degrees of freedom existing in the animals' bodies and in the human body, an architecture that makes the modular control of the whole spinal cord is necessary. The modules are building blocks of functional units of the spinal cord that generate a specific motor output in response with a specific muscle activity pattern, which is called by Bizzi *et al.* (2008) muscle synergies or motor primitives, and can be conceptualized at different levels of the hierarchy of the motor system: the behavioral, the kinematic, the muscular, up to the neural levels (FLASH; HOCHNER, 2005).

Therefore, motor primitives can represent building blocks for the organization of movement or a basic set of signals that, through proper recombination, are capable of generating a large set of muscle stimuli necessary for different locomotion tasks. Degallier e

Ijspeert (2010) and Turvey (2007) called motor primitives, a set of relatively independent degrees of freedom that behave as a single functional unit, reducing dimensionality with great movement flexibility.

Physiologically, primitives can be defined as a network of spinal neurons that form basic activation modules in a given set of muscles. The primitives were initially studied in animals by Tresch, Saltiel e Bizzi (1999), who described the patterns of muscular activation of the frogs' hind limbs and showed that the motor response obtained by skin stimulation of the hind limb resulted from the weighted combination of some muscular synergies. When the relative weighting of each synergy was changed, the nervous system produced a range of different motor responses. The study of motor primitives carried out by Giszter (2015) in amphibians, reptiles and mammals, concluded that the primitives of the CNS are sufficient for the initial control of movement and form a modularity similar to the biomechanics and the standard movement of these animals. The three types of motor primitives - PM addressed by the author will be cited below:

- ❏ Kinematic motor primitives - PM1: are kinematic courses of minimal strokes, which have been identified in octopuses, arthropods, frogs and other tetrapods and have strong human manipulation and reach behaviors. They are capable of capturing movement regardless of effector forces and muscle pattern and have been used successfully as a movement propagation base in robotics (SCHAAL; SCHWEIGHOFER, 2005).

- ❏ Spatial muscle synergies - PM2: they are primitive force field and neural drive motors. These primitives represent fixed values of muscle groups recruited over time. The PM2 is where a neural motor *drive* (a series of commands that trigger a motor action, indicated by the blue circle number 1 - PM) is distributed to the three muscle *motor pools* (red circles A ,C and E) which are indicated by solid blue arrows. These primitives recruit muscle activations through specific force patterns in the limb - F1.

- ❏ Temporal or time-varying muscle synergies - PM3: In this case, the primitive is defined by a variable pattern of muscle activation that can differentiate between muscles. In the temporal primitive, the relative muscular composition can change over time, illustrated in the different time courses of the M1 and M2 muscles for the S1 synergy (GISZTER, 2015).

In the same way that the motor primitives of animal movements were extracted, numerous researches have been carried out to obtain human motor primitives. In Ivanenko, Poppele e Lacquaniti (2004), EMG signals from twelve to sixteen muscles were recorded in six healthy subjects who walked on a treadmill at four different speeds. From the factoring of these electromyographic signals, it was possible to reconstruct the activity of

the muscles during the walk using only five basic patterns of muscle activation, proving the effectiveness of using the primitives in reducing the dimensionality of the data.

Also with human motor primitives, Li, Hayashibe e Guiraud (2013) investigated two approaches to estimate the torque of the ankle joint by multiple muscle activations of the Soleus, Gastrocnemius Medialis and Tibialis Anterior muscles in five healthy subjects. The first approach used all three muscle activations (using EMG) in plantar flexion and dorsal flexion as inputs to the estimation model; the second approach applied MFN to extract muscle synergy and were used to estimate the torque of the joint. In the second approach, it was also possible to evaluate the contribution of each muscle individually during the plantar flexion and dorsal flexion movements. The results showed that the two approaches were equivalent, but the second approach, which consisted of extracting the primitives, as it presented the activations of the muscles, quantitatively indicated the co-contraction ratio of the three muscles for the conduction of joint torque in the direction of plantar flexion and dorsal flexion.

In addition to the motor primitives extracted from electromyographic signals, the motor primitives can also be kinematic, dynamic and neural (FLASH; HOCHNER, 2005) (SANTELLO; BAUD-BOVY; JORNTELL, 2013), (GISZTER, 2015). The kinematic primitives were called sub-movements in studies carried out by Rohrer *et al.* (2002), who investigated changes in the smoothness of movements in the recovery of post-stroke patients. Robotic therapy devices were used to analyze five measures of smooth movement of the hemiparetic arm of 31 patients recovering from stroke.

In Grinyagin, Biryukova e Maier (2005), the kinematic and dynamic adaptability to variations in the precision of opening, strength and speed of movement of the thumb and human index finger under different conditions were analyzed. The kinematic variables were used to calculate the inverse dynamics to obtain the torques between the proximal joint of the thumb and that of the index finger. The joint angles and torques were factored by PCA in order to quantify the contributions of the joints individually in: dynamic and kinematic primitives.

Kinematic variables of positions of the hip, knee and ankle joints were used in the processing of data obtained with Inertial Measurement Units - IMUs in Nunes P. F.; Santos e Siqueira (2018). Through the inverse dynamics of OpenSim, kinetic data (hip, knee and ankle torques) were calculated in order to evaluate the influence of the exoskeleton structure on the kinetic and muscle characteristics (obtained by EMG) through the relationships between motor primitives and their respective weights for the different conditions of use of the exoskeleton.

In order to discover why the human system works so well despite its limitations, Hogan e Sternad (2012) presented a theory of sensorimotor control based on three distinct primitives: submovements, oscillations and mechanical impedances, in order to propose a structure for evaluate how humans interact physically and manipulate objects. Accor-

ding to the authors, the results showed that the use of primitives can simplify the control of physical interaction with objects and later, it was discovered that adding mechanical impedance as a class of dynamic primitives would facilitate the control of physical interaction, allowing complex tasks, including the coordination of several members, to be treated as a composite of simpler tasks (HOGAN, 2017).

In Nah *et al.* (2020), it was evaluated in simulation whether a target could be reached with a whip, which is one of the most complex tools that humans can manipulate, using a small number of dynamic motor primitives. And the results of the study showed that compositional control using motor primitives can be a strategy used by humans to have so many skills in handling objects.

At dynamic and neural levels, primitives were studied in Ronsse *et al.* (2013) and Garate *et al.* (2016). With the use of adaptive oscillators (AOs) to synchronize primitives with the individual's instantaneous walking cadence, allowing adaptation to various frequencies and stages of gait, it was developed a type of bio-inspired control. Figure 7 illustrates the torque generation scheme from dynamic primitives combined with a basic set of signals. A bio-inspired controller was developed where (a) illustrates a controller based on dynamic primitives and (b) a controller based on neural primitives. The components of the developed controllers (AOs and controllers based on motion primitives) are shown in red (GARATE *et al.*, 2016). The blue rectangle represents the algorithm that detects the motor intention of the user and the green rectangle represents the system coupled to the human orthosis. The muscles analyzed were: HFL: hip flexor; GLU: gluteus; HAM: hamstring; VAS: vastus; GAS: gastrocnemius; TA: tibialis anterior; SOL: soleus.

The use of primitives was explored in two ways: in the first, the identified motor primitives are combined with the weights to produce the desired assisted torque profiles; in the second, the identified motor primitives are combined to serve as a neural stimulus to a virtual model of the musculoskeletal system, which, in turn, produces the desired assistive torque profiles. According to the authors, the torque generated was able to adapt to the natural pattern of each individual's walk. The approach using neural-level artificial motor primitives proved to be positive for healthy individuals, according to the author, and will be used in the future in patients with pathological walking.

An investigation of the motor primitives in individuals with gait pathology, post-stroke hemiparetic patients, may provide additional information to complement the clinical assessments that are performed specifically as qualitative for the recovery of the hemiparetic patient, such as the *Fugl-Meyer* and *Wolf Motor Function*. Using IMUs to collect the upper limb positions of individuals during manual activities, Guerra *et al.* (2017) collected data from ten healthy elderly people and six chronic stroke patients and identified the functional movements of these individuals' upper limbs. In order to recognize and classify movements and assist in the rehabilitation of those hemiparetic patients, an approach using upper limb motor primitives was developed and the results showed an accuracy of

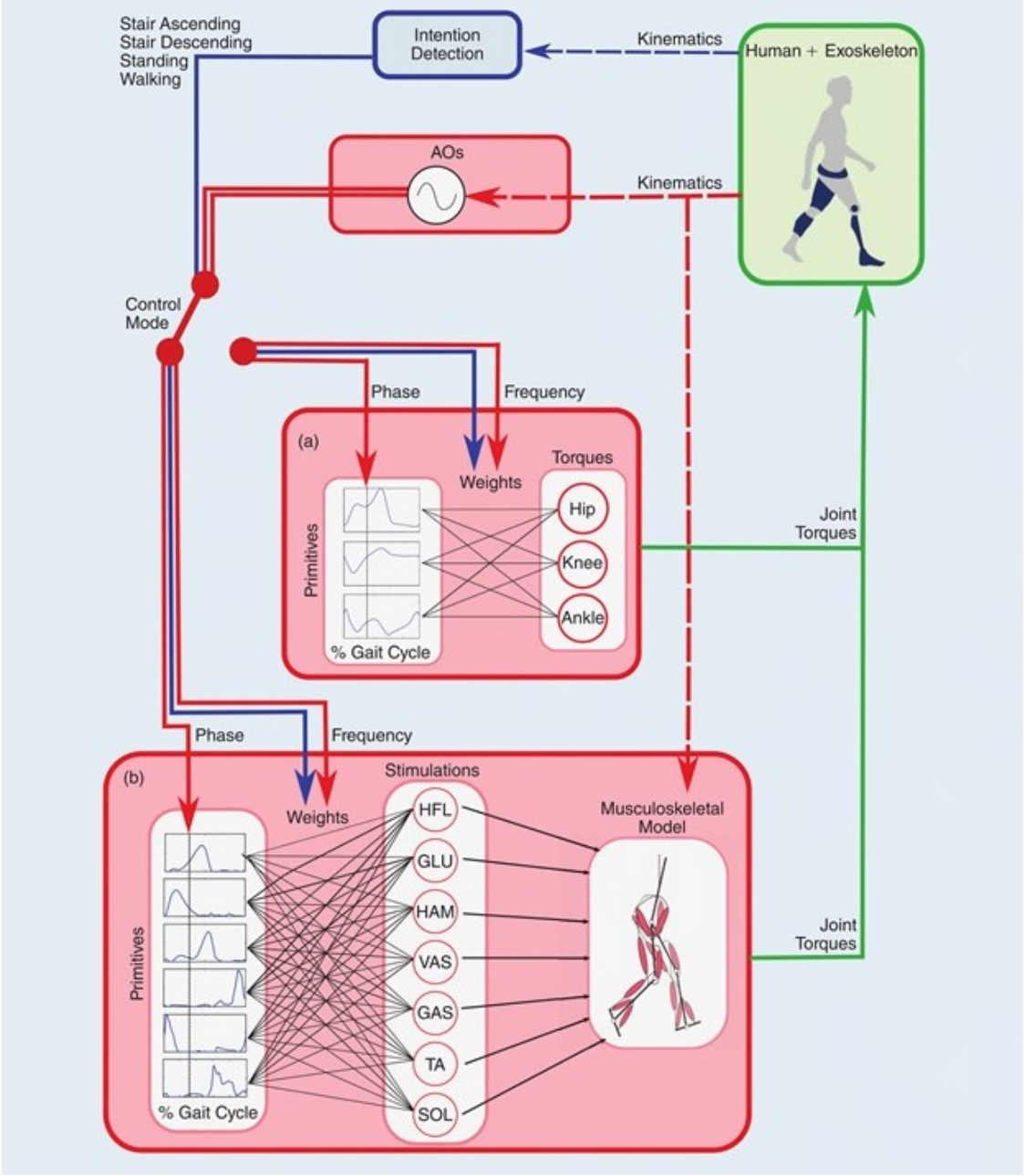

Figure 7 – A bio-inspired controller: (a) A controller based on dynamic primitives (DLMPs) and (b) a controller based on neural primitives (NLMPs) (GARATE *et al.*, 2016).

80% of the movement primitives for the control group and 79% movement patterns for patients with chronic stroke.

In post-stroke populations, Lambert-Shirzad e Loos (2017) also studied the motor synergies obtained by EMG and the kinematic joint synergies that were obtained using a *Microsoft Kinect VI* while individuals participated in video games. The aim of the study was to analyze the sample size of data necessary for an analysis of kinematic and muscular synergies in healthy populations and post-stroke populations. The relationship between the quality of the motor synergy analysis and the size of the data included in the analysis was considered.

The relationship between muscle synergies and motor functions at joint and task levels of upper limbs in post-stroke patients was evaluated by (LI *et al.*, 2017). Ten individuals who suffered a stroke and a control group of nine healthy individuals were recruited to participate in the study. EMG signals and the kinematics of the movement of patients and controls were analyzed while performing arm reach tasks. The synergies of post-stroke patients (pathological synergies) were compared with the synergies of healthy patients to evaluate deficits in neuromuscular coordination and control of these patients and, later, to offer researchers and clinicians losses in the neural organization of motor control in hemiparetic patients.

Muscle control of the lower limbs is fundamental for movement and especially the act of standing. The movement of getting up from the chair (standing) is an important daily activity and difficult to perform for those post-stroke hemiparetic patients. To analyze how healthy adults and hemiparetic patients manage to control the muscles of their lower limbs for the movement of standing, Yang *et al.* (2017) used the concept of muscle synergies. The results showed that with only four muscular synergies it is possible to represent the movement of standing.

Figure 8 illustrates the schematic design of the muscle synergy model with three synergies used to express textit 'n' muscle activations. They are composed of spatial and temporal patterns. Weights (w1, w2, w3) show a relative level of muscle activation and temporal patterns (cl, c2, c3) show the relative weighting coefficients. During movement, spatial patterns are constant, but temporal patterns change over time. Muscle activations are generated from the linear sum of the spatial and temporal patterns of muscle synergies. Muscle activations are shown in gray areas and muscle synergies 1, 2 and 3 are described in continuous lines, dashed lines and solid lines with circles.

The spatial pattern of muscle synergies was found to be common only among those healthy individuals, when compared to post-stroke patients and healthy individuals, there were changes in the weights of muscle synergies at the end of the movement.

A biomechanical analysis of gait combined with muscle synergies was also performed by Barroso *et al.* (2017). The objective was to evaluate the performance of human gait against the current *Fugl-Meyer* clinical scale and to improve the quantitative assessment of post-stroke by providing specialists with better means of functional assessment and understanding of internal mechanisms underlying post-stroke motor disabilities. In the study, gait analysis was performed during walking on the ground in nine post-stroke hemiparetic patients. Surface EMG data and joint position angles were analyzed. The number of synergies for the EMGs of the eleven muscles was approximately four for the non-paretic limb and approximately three for the hemiparetic limb. The identification of a smaller number of muscle synergies in the hemiparetic limb is associated with a greater dependence between the activation patterns of each muscle and associated with the coupling of the muscles along the limb or with the possible fusion of existing muscle

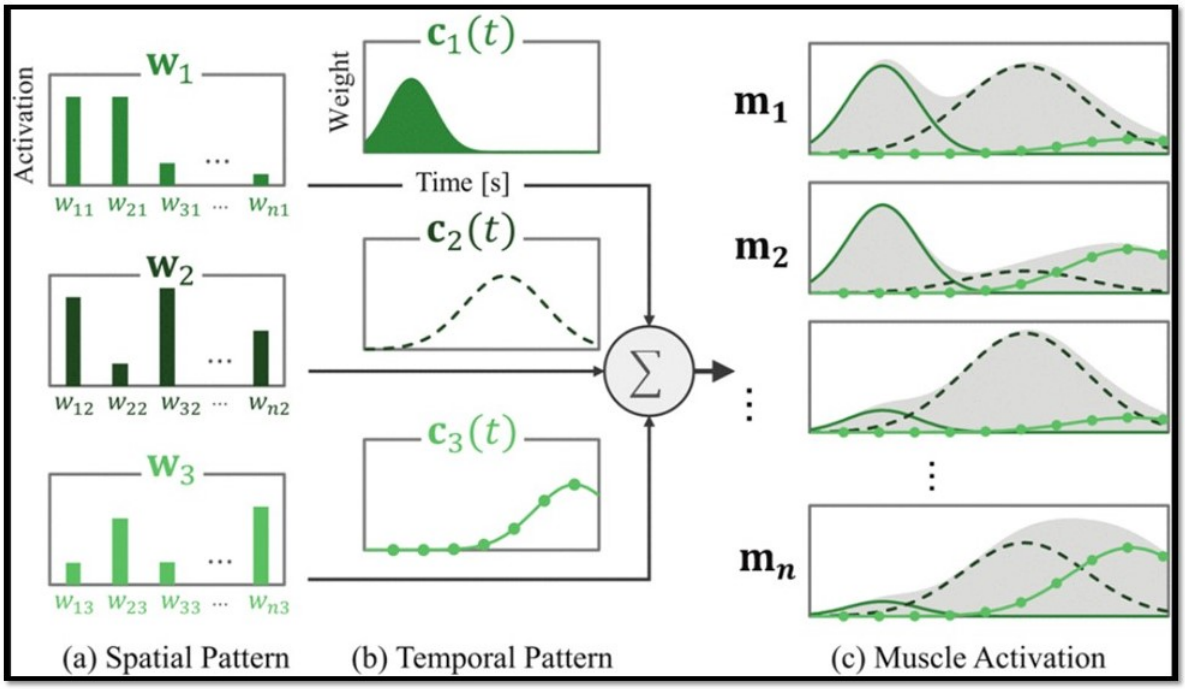

Figure 8 – Schematic drawing of the muscle synergy model, (YANG *et al.*, 2017).

synergies. The study demonstrated that it is possible to combine biomechanical and neural measures to evaluate locomotion performance in individuals with some type of neurological injury.

Without knowing the training doses necessary to enhance the recovery of hemiparetic patients, therapists must rely on intuitive amounts of training, with uncertain ramifications for recovery. However, the analysis of motor primitives can offer a view of the causes of motor disability that are preventing the individual from completing functional tasks and from this view, provide an opportunity to formulate exercises that will act on the motor impairment of each individual patient.

2.4 Models of Motor Primitives

The motor primitives were proposed as an invariant or synchronous model in time (TRESCH; SALTIEL; BIZZI, 1999), (SALTIEL *et al.*, 2001) and as a variant or asynchronous model in time (D'AVELLA; TRESCH, 2002), (D'AVELLA; SALTIEL; BIZZI, 2003). In this study, time-synchronized muscle primitives will be applied since recent research has applied motor primitives to muscle analysis with EMG and has shown evidence that they are synchronized with time (KARGO; GISZTER, 2008), (HART; GISZTER, 2010) and will be also applied, the primitive dynamics obtained by the factoring technique from the torques of the subjects.

In the literature, the matrix of a given set of signals (torques, position, EMG signal, ...) $\mathbf{X} = [\mathbf{x_1}, \mathbf{x_2}, ..., \mathbf{x_m}]$, with $\mathbf{X} \in \mathbb{R}^{t \times m}$, is decomposed as the product between the primitives

$\mathbf{P} = [\mathbf{p_1}, \mathbf{p_2}, ..., \mathbf{p_n}]$, with $\mathbf{P} \in \mathbb{R}^{t \times n}$, and their respective weights, $\mathbf{W} = [\mathbf{w_1}, \mathbf{w_2}, ..., \mathbf{w_m}]$, with $\mathbf{W} \in \mathbb{R}^{n \times m}$. The index t is the total number of samples, m represents the number of joints or muscles (or degrees of freedom), and n is the number of primitives (CHEUNG *et al.*, 2009), (BIZZI; CHEUNG, 2013), (BERGER; D'AVELLA, 2014), (ROH; RYMER; BEER, 2015), as in Equation 1:

$$\mathbf{X} = \mathbf{P} \cdot \mathbf{W}. \tag{1}$$

The computation of the primitives and their respective weights can be performed using as for example, Principal Component Analysis (PCA), Independent Component Analysis (ICA) and Non-negative Matrix Factorization (NMF) and this calculation extracts a linear combination between primitives $\mathbf{p_i}(\mathbf{t})$ and their corresponding weights $\mathbf{w_i}$ to minimize the difference between the original and reconstructed signals.

2.4.1 PCA - Principal Component Analysis

Matrix factoring has long been explored for different purposes: solving linear systems of equations, multivariate analysis, reducing data size, revealing hidden structures and representing transforms, for example. Because they are applicable to so many areas, different matrix factorization techniques have been, and still are, developed. Among them, is the Principal Component Analysis (PCA).

The PCA was proposed by (PERSON, 1901) as a procedure that uses orthogonal transformation to convert a set of observations of correlated variables into a set of unrelated variables called principal components. This technique works from the orthogonality, where the first component will be the one with the greatest variance and the second component, orthogonal to the first, the one with the second greatest variance, so the variance will decrease with each component (ABDI; WILLIAMS, 2010).

It is the most used technique in the extraction of motor primitives because it shows an accurate estimate to obtain a linear combination of these primitives and their respective weights with the aim of reducing the dimensionality and minimizing the difference between the original and reconstructed signals (NUNES *et al.*, 2020).

To extract the primitives and the weights, the average $\overline{\mathbf{X}}$ of each characteristic vector is first calculated, Equation 2, later these values are normalized and then the standard deviation is calculated $\mathbf{S}$, Equation 3. The variance matrix $\mathbf{S^2}$ is then calculated, Equation 4:

$$\overline{\mathbf{X}} = \frac{\sum_{i=1}^{m} \mathbf{x_i}}{m}. \tag{2}$$

$$\mathbf{S} = \frac{\sqrt{\sum_{i=1}^{m} (\mathbf{x_i} - \overline{\mathbf{X}})^2}}{m} \tag{3}$$

$$\mathbf{S^2} = \frac{\sum_{i=1}^{m} (\mathbf{x_i} - \overline{\mathbf{X}})^2}{m}. \tag{4}$$

The covariance calculations are between two or more dimensions, since the covariance calculated between a dimension and itself, is its own variance. Therefore, considering a second characteristic vector $\overline{\mathbf{Y}}$, after calculating the mean, standard deviation and variance, the covariance $\mathbf{A}$ can be calculated between vectors $\overline{\mathbf{X}}$ and $\overline{\mathbf{Y}}$ according to the Equation 5:

$$\mathbf{A} = \frac{\sum_{i=1}^{m} (\mathbf{x_i} - \overline{\mathbf{X}})(\mathbf{y_i} - \overline{\mathbf{Y}})}{m}. \tag{5}$$

The eigenvalues and eigenvectors of the $\mathbf{A}$ matrix will be the primitives and their weights. To calculate the eigenvalues of the covariance matrix, Equation 6 is used, where $\mathbf{P}$ are the eigenvalues, $\mathbf{I}$ is the identity matrix and $\mathbf{A}$ is the covariance matrix. The calculation of the eigenvectors $\mathbf{W}$ of the matrix $\mathbf{A}$ is done by Equation 7:

$$\mathbf{det}(\mathbf{P} \cdot \mathbf{I} - \mathbf{A}) = \mathbf{0} \tag{6}$$

$$\mathbf{A} \cdot \mathbf{W} = \mathbf{P} \cdot \mathbf{W} \tag{7}$$

where $\mathbf{A}$ is the covariance matrix and $\mathbf{W}$ is the eigenvector and $\mathbf{P}$ are the eigenvalues calculated in Equation 6, (SMITH, 2002). The higher the eigenvalue, the more significant the data of that eigenvector, and the lower the value of this eigenvalue the less significant the values of that eigenvector will be for the representation of the matrix. For the extraction of motor primitives, the eigenvalues of the covariance matrix are the primitives and the eigenvectors represent the respective weights of these primitives.

2.4.2 NMF - Non-Negative Matrix Factorization

The extraction of data by the PCA does not in any way restrict the sign of the decomposition factors. Therefore, positive and negative elements can occur both between the base vectors and in the coefficients that combine them linearly. In many applications, however, negative elements cannot be physically interpreted.

The Non-Negative Matrix Factorization - NMF is a statistical tool that imposes a non-negative restriction on the extracted factors, using second-order statistics to find the vectors that best represent the data variance. The NMF determines that the matrices $\mathbf{P}$ and $\mathbf{W}$ are non-negative and iteratively choose the best vector sets.

The non-negativity of the matrices p and w ensures that the results of the factoring are global minimums and not a local minimum, making the optimization problem convex. There is no orthogonality in base vectors located in non-negative spaces, however base vectors are required to be independent (BERRY *et al.*, 2007).

NMF was used by (AN *et al.*, 2013) to analyze the muscle primitives of seats with different heights, and (STEELE; TRESCH; PERREAULT, 2013) analyzed the impact that the number and choice of muscles have on primitive analyzes in a musculoskeletal model. This restriction is essential because muscle activations processed from EMG data always have positive values. The factoring of an EMG data set represented by the matrix $\mathbf{V}$, with $\mathbf{V} \in \mathbb{R}^{t \times m}$, in a matrix $\mathbf{W}$, with $\mathbf{W} \in \mathbb{R}^{n \times m}$, and a matrix $\mathbf{P}$, with $\mathbf{P} \in \mathbb{R}^{t \times n}$, can be presented according to the following Equation:

$$\mathbf{V} \approx \mathbf{P} \cdot \mathbf{W} \tag{8}$$

where $\mathbf{V}$ is the matrix of the EMG data set, where $\mathbf{t}$ is the number of samples and $\mathbf{m}$ is the number of muscles (or degrees of freedom). $\mathbf{P}$ is the matrix of primitives, where $\mathbf{n}$ is the number of primitives. The matrix $\mathbf{W}$ is the matrix of weights or coefficients. The values of the $\mathbf{V}$ matrix represent the activation range of each muscle at each specific moment. The values of the $\mathbf{W}$ matrix represent a fixed proportion between the muscles that make up each primitive so that the sum of each column in $\mathbf{W}$ is normalized to be equal to 1. The values in the $\mathbf{P}$ matrix represent the activation range of each primitive in the time domain. In this model, it is possible that each muscle belongs to more than one primitive. Therefore, the EMG signal of any single muscle can be attributed to simultaneous activations of several muscle primitives.

2.5 Neurorehabilitation

Neurological rehabilitation emerged as a formal method in the 1960s for the therapeutic treatment of post-stroke patients or those who presented some type of spinal cord injury with severe sequelae that affect their motor and sensory abilities. Patients with spinal cord injuries are usually treated with conventional physical therapy, whose procedures contribute to the recovery of body health and movements of these individuals. But studies have already shown that this type of physical therapy has limited effectiveness in functional rehabilitation for chronic impairments, such as those generated by stroke (PEPPEN *et al.*, 2004).

One of the most common consequences of stroke is hemiparesis, which commits members contralateral side to the affected brain, such commitment may include: muscle weakness (lack of muscle tone), lack of mobility, abnormal movement synergies, abnormal postural adjustments, loss of joint coordination and loss of sensation (LANGHORNE; BERNHARDT; KWAKKEL, 2011). However, the repair of motor deficits in post-stroke patients is possible due to the neuroplasticity of the nervous system, which makes the human brain able to reorganize itself, so that relearning offers an opportunity for motor recovery (MACKO, 2011).

The first time that the term neuroplasticity was used to describe the nervous system was in 1890 by William James, in his book *Principles of Psychology*, where the author stated that plasticity is the use of a structure strong enough to produce a influence, but weak enough not to produce everything at once (JAMES, 1984).

Neuroplasticity has also been defined as the ability of the CNS to undergo structural and functional changes in response to new experiences through physical rehabilitation, since neural plasticity is the basis for learning in the intact brain and for relearning in the brain that suffered any damage (KLEIM; JONES, 2008).

At the behavioural level, the most important parameter of task-oriented practice to induce brain plasticity is the intensity of training, defined as the amount of repetition executed for specific tasks. To induce an effective brain reorganisation, a certain threshold of training (i.e., minimum number of repetitions) needs to be reached. This effect is known as experience-dependent neuroplasticity. In animal models, it was estimated that between 1000 and 10000 repetitions of the same task (trials) are needed before a permanent change at the synaptic level can be observed, but the number of synapses and connections increases already in the initial training stages (KLEIM; JONES, 2008).

Dependent exclusively on training, the possibility of inducing a functional reorganization of the cortical circuits through neuroplasticity and, consequently, the restoration of essential functions for independence in daily activities. In the case of post-stroke patients, evidence suggests that intensive motor rehabilitation positively impacts motor recovery from hemiparesis in these patients (KWAKKEL *et al.*, 1997), (STEULTJENS *et al.*, 2003) e (TEASELL *et al.*, 2003).

Other post-stroke rehabilitation studies have also suggested that the effectiveness of post-stroke motor therapy is related to the level at which the neuromuscular system is challenged by repetitive movements (DUNCAN, 1997), (RICHARDS; POHL, 1999), (WOLDAG; HUMMELSHEIM, 2002), (BARRECA *et al.*, 2003). Thus, post-stroke individuals are able to develop neuroplasticity through specialized motor training carried out with the help of the specialist and therefore, relearning motor skills that have been lost (MANG *et al.*, 2013).

In the case of lower limbs, the main objective of the rehabilitation of post-stroke patients is to make them independent during gait and according to French *et al.* (2010), post-stroke patients who have undergone training with a greater number of repetitions, showed improvements in their activities functional.

However, specialized treatment and frequent manual interaction by the specialist is not always accessible to all patients with some type of sequelae after stroke, because it is a clinical specialty with a high cost value and most of the time unavailable in public health systems. Due to the need for new technologies to increase the efficiency of rehabilitation and improve the quality of life of patients, engineering has spared no effort to develop robotic devices.

Robotic devices make the patient more independent of the physical therapist's manual interaction, the treatment more accessible, in addition to automating therapies. With these devices, the functional neuromuscular structures that are preserved will be used during therapy by compensating for lost movements and, consequently, these structures will be able to learn motor functions to replace the damaged areas (GUTIERREZ-MARTINEZ; NUNEZ-GAONA; CARRILLO-MORA, 2014).

In a study by Mehrholz *et al.* (2015) using eight types of robotic devices for the rehabilitation of upper limbs in post-stroke patients, the effectiveness of training to improve activities of daily living, function and muscle strength was evaluated, and the acceptability and safety of the equipment by patients during therapy were also evaluated. The results showed that patients who received electromechanical and robot-assisted training were able to improve their daily activities and had their upper limb muscle strength increased.

In another study by Mehrholz Simone Thomas (2017) also with post-stroke patients, robotic devices for lower limbs (exoskeletons) were used to aid gait during rehabilitation. According to the authors, post-stroke patients who received gait training assisted by the exoskeleton device in combination with physical therapy were more likely to achieve an independent gait than those who received gait training without the device. In this study, the type of training that showed the best results was not very evident and further studies should be carried out to address issues, such as, for example, the most effective frequency and duration in assisted walking training, as well as how long the benefit can last.

Training focused on strengthening lower limbs and increasing cardiorespiratory functions (tasks aimed at improving activities related to human gait) showed the best results in increasing the quality of life of post-stroke patients (PORT *et al.*, 2007), (WEVERS *et al.*, 2009).

2.6 Rehabilitation Robotics

The race for research on active orthoses and exoskeletons began in the late 1960s, mainly between the United States and the former Yugoslavia, despite their distinct objectives. While the former focused its research mainly on the development of technologies to increase the skills of healthy human beings, often for military purposes, the latter was committed to developing assistive technologies for the rehabilitation of the disabled. The two fields of research faced numerous challenges despite the different objectives, challenges mainly related to portability and interaction with a human operator (DOLLAR; HERR, 2007).

Robotic neurorehabilitation has shown a potential for greater impact on motor recovery due to its easy implantation, due to its applicability through a wide range of motor impairment, its high reliability and its ability to provide high-dose and high-intensity

training protocols, with a greater number of movements per unit of time (infinite repetitions in a single session). In addition to the controllability of the movement provided by the robot and the reliability of the measurement, which makes them ideal instruments to help neurologists and therapists to face the challenges of neurorehabilitation (HUANG; KRAKAUER, 2009).

According to Lum *et al.* (2002), the success of applying of robotic therapy in patients with motor damage after stroke will depend on four criteria: the first and most important of all is the benefit to the patient; second, the device must improve efficiency from the current practice of therapists; thirdly, the device must be accessible to clinics, and profitable to manufacturers; and finally, the device must not increase the cost of healthcare. Other studies have also shown the short-term efficiency of the increasingly frequent use of robots in the rehabilitation of post-stroke sequelae (PRANGE *et al.*, 2006), (KWAKKEL; KOLLEN; KREBS, 2008).

To assist the movement of individuals who have some type of motor problem, the devices used can be: prostheses and orthoses, therapeutic robots and exoskeletons. The first devices (prostheses and orthoses) are designed to be used continuously by the patient, aiming to replace (in the case of prostheses) or make corrections (in the case of orthoses) of the functions. In a study conducted by Kobayashi *et al.* (2015), the gait of 10 post-stroke patients under four different conditions of plantar flexion resistance was analyzed using an articulated ankle and foot orthosis designed according to needs. The results showed that the angles and moments of the foot and ankle joints were significantly and systematically affected by the amount of plantar flexion moment of the articulated orthosis, which showed the importance of the individual construction of these orthoses due to the resistive moment of flexion of each patient.

Therapeutic robots are usually designed for the controlled execution of a sequence of movements and are usually linked to visual interfaces that serve as feedback to the patient (JIMENEZ-FABIAN; VERLINDEN, 2012). Therapeutic ankle rehabilitation, for example, given its importance in the motor recovery process, has been the focus of studies by authors such as Roy *et al.* (2009), who presented a robot called Anklebot developed in *Massachusetts Institute of Technology* (MIT) with two objectives: to provide a new therapeutic training modality and to evaluate ankle involvement, working on ankle stiffness, Figure 9. Post-stroke patients showed greater passive stiffness in the ankle joint than in relation to healthy adults, both in the sagittal plane and in the frontal plane of movement. This passive stiffness can be defined as resistance to stretching or shortening of the joint, tendon or connective tissue and happens when a passive (non-contracted) muscle is stretched.

The Anklebot is a portable ankle robot that allows normal range of motion in all three degrees of freedom - DOFs (Degree of Freedom), two of which are actuators. The movements performed are plantar flexion and dorsiflexion in the sagittal plane, obtained when the two actuators move in the same direction, and inversion and eversion in the

Figure 9 – Anklebot.

frontal plane, when the two actuators move in opposite directions. Internal/external rotation, movement not actuated, is limited at the ankle with the orientation of the foot in the transversal plane being controlled mainly by the rotation of the leg. In cases of plantar dorsiflexion/flexion and inversion/eversion movements, the Anklebot can apply up to 23 Nm for this and 15 Nm for this. Although they are values that do not support the weight of the user, the ultimate goal of the device is to provide a complementary torque to the paretic limb so that the effects of the drooping foot can be mitigated (ROY *et al.*, 2009). In Roy *et al.* (2011) studies with Anklebot were also presented, but applied in conjunction with video game. The study explored the short-term effects on ankle motor acquisition and learning in patients with chronic hemiparesis.

Another robotic device created for the rehabilitation of patients with incomplete spinal cord injury or who have suffered a stroke, is the Lokomat, Figure 10. Developed by Colombo *et al.* (2000), the device aims to move the patient on a treadmill and the patient moves using a weight compensator . The equipment is adjustable to the patient's measurements and can be used for different degrees of paresis and spasticity (COLOMBO *et al.*, 2000). Gait machines like the Lokomat or the Gait Trainer, are able to relieve the strenuous effort of the therapists during the training sessions on the treadmill since part of the patient's body weight (in this study, post-stroke patients) will be supported by the equipment (HESSE, 2008).

Until then, the patient who used Lokomat was imposed on a fixed gait pattern through position control, and it is already known that robots should not only serve as support in walking, but should also encourage patients to produce voluntary efforts maximum, ensuring that the patient is effectively walking. In Duschau-Wicke *et al.* (2010), a patient cooperation strategy was presented that allows influence on the time of movement of his legs along a physiologically significant path. The impedance control strategy creates a virtual tunnel, for the hip and knee joints, around a reference path. If the patient remains in the tunnel while walking, only the torques necessary to compensate for gravity are applied to the robot. If the patient deviates from the tunnel at a given moment in the step, the impedance control creates a force field, returning the patient close to the desired path. Some additional torques are generated by the robot to keep the patient on

Figure 10 – Lokomat exoskeleton.

the desired path over time. This support provided by the robot is a parameter defined at the beginning of the robotic therapy session by the physiotherapist.

Training tools to ensure that Lokomat and other robotic devices were used correctly, taking into account more effective interventions and reducing the likelihood of injury, were developed by Brady *et al.* (2011). In this study, the recommendation was that there should be a decrease in the guide force generated by the *Guidance Force* robot according to the evolution of the training phases.

Exoskeletons are devices attached to the human body (wearable) designed to increase the motor capacity of healthy people, supporting the musculoskeletal system and allowing for increased strength and endurance during locomotion. They are defined as active mechanical devices of an anthropomorphic nature, used by an operator and that can be adjusted to the body, working together with the movements of the operator. The term Exoskeleton is usually used to describe a device that increases the performance of a physically fit user, while the term active orthosis is used to describe a device that increases the walking ability of an individual with some pathology in the lower limbs. However, the term Exoskeleton is also used to describe assistive devices, particularly when they encompass most lower limbs (DOLLAR; HERR, 2008).

The use of wearable exoskeletons of lower limbs to assist the gait of people with motor disabilities, represents a paradigm shift beyond traditional wheelchairs. In recent times, a large number of such devices for lower limbs (and active orthoses) for assistance and rehabilitation have been developed and reported in the literature (CONTRERAS-VIDAL *et al.*, 2016), (CHEN *et al.*, 2016) and (BAYON *et al.*, 2017). The expectation of market growth (military, factory and rehabilitation/health) between 2014 and 2019 is approximately 72.5%, since these devices, in addition to improving the functions of internal organs and consequently the general health status , exoskeletons provide freedom for the patient to move and perform their daily activities while maintaining a more active lifestyle (FRISOLI

et al., 2016).

The main purpose of exoskeletons for assistance is to provide support to users who have had some type of complete spinal cord injury where there is no possibility of movement recovery. And one of the most important factors in using this type of equipment, is that recent literature reviews have shown that injured patients who received assisted electromechanical training, were more likely to resume their daily activities since the exoskeletons assist in cortical reorganization motor in order to improve the gait pattern of patients (MEHRHOLZ *et al.*, 2012).

Figure 11 – ReWalk.

The ReWalk, Figure 11, is a portable exoskeleton with a mass of approximately 23 kg and which acts on the hip and knee joints. It was developed to help individuals with SCI to stand and walk, as well as to go up and down stairs (ESQUENAZI *et al.*, 2012). When walking, the user uses two crutches and the movements are performed using command buttons and by detecting the inclination of the trunk using IMUs. These commands allow simple movements, such as executing a step or a repetitive sequence of steps. Thus, the user must always intervene to be able to move.

Figure 12 – Soft Exosuit.

Figure 12 illustrates Soft Exosuit, which was developed at Wyss Institute at Harvard, with support from the Defense Advanced Research Projects Agency - DARPA (DING *et al.*, 2014). It is a lighter and more compact device, activated by means of steel cables from

motors located at the back of the user, performing a coordinated movement of the joints of the hip, knee and ankle. As this device has a limited number of metallic parts, the support of the user and the equipment itself is compromised, therefore, this exoskeleton cannot be used by people with a high level of disability, for example, individuals with complete spinal cord injury. This solution was proposed to be used by healthy people, especially soldiers, or with mild neurological disabilities.

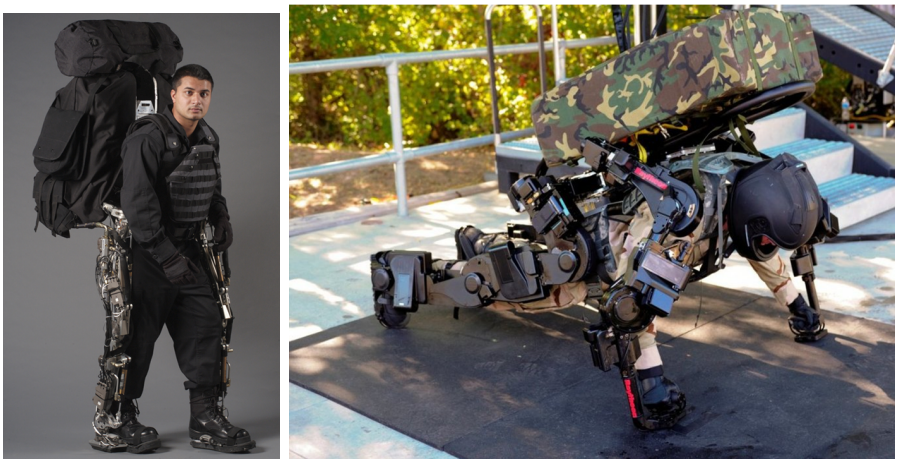

Figure 13 – BLEEX exoskeleton on the left and Exoskeleton NAEIES on the right.

Exoskeletons such as BLEEX - *Biomechanical design of the Berkeley lower extremity exoskeleton* (ZOSS; KAZEROONI; CHU, 2006), and NAEIES - *Naval Aeronautical Engineering Institute Exoskeleton Suit*, as shown in Figure 13, were developed to assist users in carrying large loads on different types of terrain. They are able to increase human resistance and facilitate the transport of loads over long distances, since, using less energy, the user will be able to walk longer, (YANG *et al.*, 2009).

HAL - *Hybrid Assistive Lims* is an exoskeleton that in addition to assisting users by increasing strength in their joints, was developed with the aim of also helping people affected by gait disorders to move and perform daily life activities. as healthy individuals, Figure 14. In assistance cases, the hip and knee joints are assisted by an autonomous controller based on two stages of gait: the swing phase and the support phase, while the ankle joints behave passively with a spring (SANKAI, 2010).

Another device developed to rehabilitate individuals with gait disturbance is the MINDWALKER, Figure15. It is an exoskeleton with 5 DoFs in each leg, with three DoFs fed by elastic actuators in series and the other two passive DoFs, but with some rigidity. The control method developed, provides walking assistance from auxiliary torques and is able to withstand weight variations when climbing stairs. (WANG *et al.*, 2013).

With the use of MINDWALKER, in a study carried out by Sylos-Labini *et al.* (2014), six healthy individuals were able to walk using only the exoskeleton, but in the case of the four patients with motor impairment, they had to hold on to a handrail. The muscular forces of the lower and upper limbs of these individuals were also analyzed through elec-

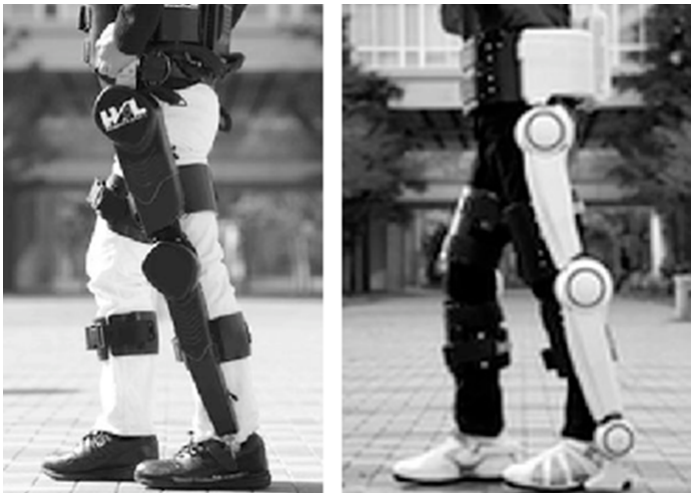

Figure 14 – Exoesqueleto HAL.

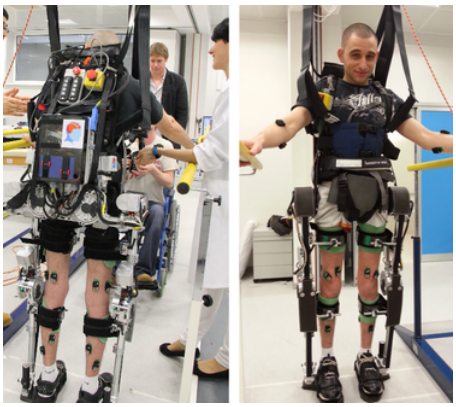

Figure 15 – MINDWALKER exoskeleton.

tromyography - EMG. In the case of healthy individuals, the electromyographic activities with and without the exoskeleton were similar, while in the case of patients with motor problems, the electromyographic activity of their upper limbs was higher when stepping on the ground wearing the exoskeleton, since these patients were unable to walk without support.

A passive exoskeleton for lower limbs, Figure 16, highly adjustable and instrumented to evaluate new design ideas and investigate how certain characteristics of the exoskeleton influence the user's movement, was developed by (BARTENBACH *et al.*, 2015). The project was coordinated by the University Hospital Balgrist and the University of Zurich and sought to investigate how changes in the characteristics of the exoskeleton affect the user.

In this doctoral thesis, an exoskeleton called ExoTao was used. More details on this device will be provided in subsection 2.6.1 below.

Figure 16 – ExoH.

2.7 Biomechanics of the Gait

Walking is the way or way in which you move from place to place with your feet, and walking is the process or components of walking. This is a simple activity of daily life and one of the main skills of the human being that requires balance on one leg while the other moves forward and also requires combined movements of the dorso and arms with joint movements and muscle performance. A better understanding of the characteristics of gait patterns has been the focus of study (SANTOS *et al.*, 2007).

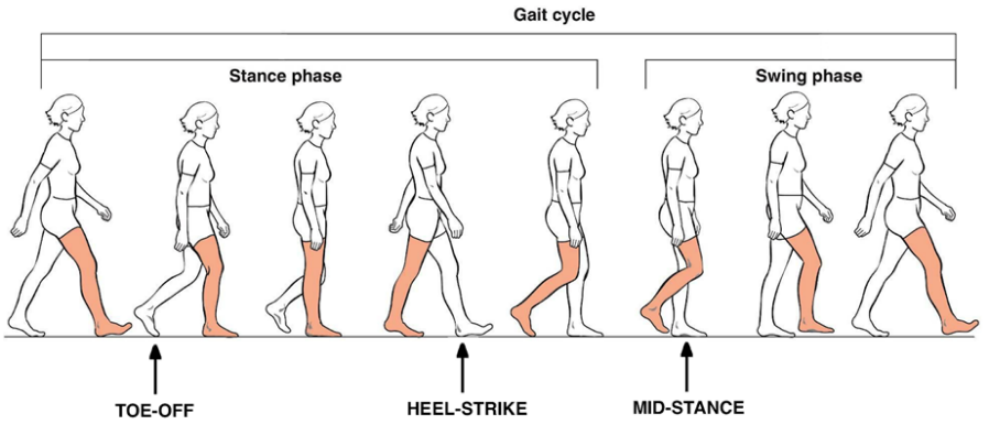

Figure 17 – Phases and subphases of the gait cycle.

The gait cycle can be divided into two phases: support phase and balance phase. In each of these phases different muscles are activated in an isometric or dynamic way. Below, the phases and their subphases will be detailed.

- ❏ Support phase: Corresponds to 60% of the gait cycle and occurs when the foot is in direct contact with the ground. This phase begins when the heel of a foot touches the ground and ends when that foot leaves the ground. This phase is traditionally

divided into five subphases: 1) heel touch; 2) full support of the foot; 3) medium support; 4) exit or elevation of the heel; and 5) exit or elevation of the fingers, according to Figure 17. The start of the support phase (subphase 1) occurs at the touch of the heel on the ground (right foot), at this point the ankle joint will be in a neutral position, that is, between a dorsiflexion and a plantar flexion, and the knee flexion (subphase 2). This slight knee flexion will partially absorb the shock when the foot touches the ground. The hip joint will be flexed at approximately 25 ° and the torso will be erect and will remain so throughout the cycle. When the ankle is in a neutral position (subphase 3 - Medium Support), the dorsiflexor muscles of the foot will be active while the quadriceps femoris muscles, which had concentric contraction, start to contract in an eccentric manner in order to minimize the degree of flexion of the knee. The flexor muscles of the hip joint will now be active.

The balance phase has three sub-phases; acceleration, average balance and deceleration. All of these subphases are weightless.

- Balance phase: In the acceleration phase (subphase 6) the lower limbs will be behind the body and will move to reach it, dorsiflexion of the foot will occur, knee and hip flexion will continue, which will move the lower limb forward. The initial balance is the period between the end of the exit (elevation of the toes of the right foot from the ground) and the end of the acceleration. At the moment of medium balance (subphase 7), the dorsiflexor muscles of the foot will displace the ankle joint in a neutral position. This subphase is the period between the end of the acceleration and the end of the average balance. At that moment, knee and hip flexion are maximal, this one is approximately 65 ° and this one is approximately 25°. The terminal balance deceleration subphase (subphase 8) is the period between the end of the average balance and the end of the deceleration. It is when the deceleration occurs, the dorsiflexor muscles of the foot will have active action to maintain the ankle joint in a neutral position in preparation for the heel touch on the ground. At that moment, knee extension and eccentric contraction of the hamstring muscles will occur to decelerate the lower limb, avoiding a sudden extension. The lower limb will reach the maximum point of swing forward and the knee will continue to flex.

Chapter 3

Experimental Setup

This chapter describes the system components used to validate the methodologies proposed in this work. The main components are the EMG Delsys - Trigno signal measurement system, the kinematic profiles that have been evaluated by processing data from 7 IMUs from XSens Technologies Netherlands and the ExoTao exoskeleton.

3.1 Delsys Electromyograph - Trigno Systems

In order to measure the signals from the muscles of the lower limbs, the Trigno Wireless EMG system (Delsys Inc., Natick, MA, USA) was used. The system has wireless sensors that are positioned with special double-sided adhesives to simplify fixation and minimize movement artifacts, Figure 18. The Trigno System has, in total, 16 differential sensors with detection geometry in parallel bars, which integrate an EMG channel and three accelerometers each.

EMG signals are sampled at 2KHz with 16 bit resolution and a bandwidth of 20 to 450Hz. Five sensors are used, which will capture the excitation of the selected muscles: rectus femoris (RF), vastus medialis (VM), tibialis anterior (TA), biceps femoris (BF) and gastrocnemius lateralis (GL).

Figure 18 – Delsys Electromyograph - Trigno Systems.

3.1.1 Muscle Analysis

The quadriceps femoris muscles are the most affected after neuronal disorders and the weakness of these muscles involved in walking has been reported as one of the biggest problems in different areas of rehabilitation. One of the strongest muscle groups in the body, the quadriceps is innervated by the femoral nerve and its main function is knee extension.

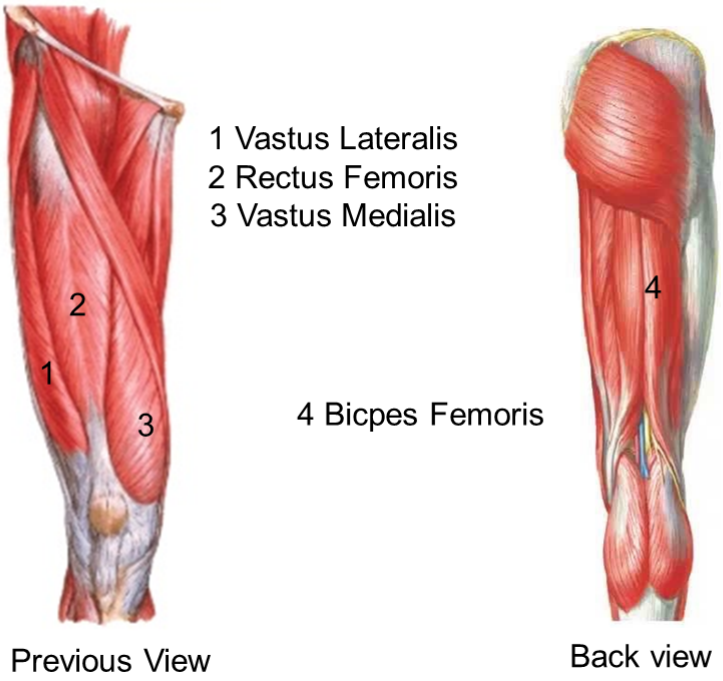

Figure 19 – Muscles selected for analysis. The anterior view, on the left side, shows the extensor muscles, and the right is the posterior view, the flexor muscle.

The quadriceps is composed of four muscular bellies (contractile portion of the muscle), they are: the vastus lateralis (VL), the vastus medialis (VM), the rectus femoris (RF) and the vastus intermedius (VI). Here in this work, we will analyze the vastus medialis (VM), rectus femoris (RF), and biceps femoris (BF), Figure 19 and a sural triceps muscle: lateral gastrocnemius (GL) and the tibialis anterior (TA), Figure 20.

The gastrocnemius lateralis is a muscle located in the posterior region of the leg below the knees and is part of the sural triceps or calf. The sural triceps muscles act as plantar flexors by moving the foot down and also act as knee flexors when the leg is not supporting the weight. The tibialis anterior muscle is a leg muscle that extends laterally to the anterior edge of the tibia. He is responsible for the dorsiflexion and inversion of the foot, stabilizes the ankle as the foot hits the ground during the support phase and then acts to pull the foot off the ground during the swing phase (STANDRING, 2009). The electrodes were positioned according to the specifications below:

❏ Vastus Medialis: Positioned at 80% of the distance between the antero-superior iliac

spine and the joint space at the anterior edge of the medial ligament;

- ❏ Rectus Femoris: Positioned at the median longitude between the joint space at the anterior border of the medial ligament and antero-superior iliac spine;
- ❏ Biceps Femoris: Positioned at 50% of the ischial tuberosity of the line, in the lateral epicondyle of the tibia;
- ❏ Gastrocnemius Lateralis: Positioned 1/3 of the fibula head - heel line. Parallel to the head of the fibula line - heel;
- ❏ Tibialis Anterior: Positioned at 1/3 of the tip of the fibular line, at the tip of the medial malleolus. Parallel to the tip of the fibula line - tip of the medial malleolus.

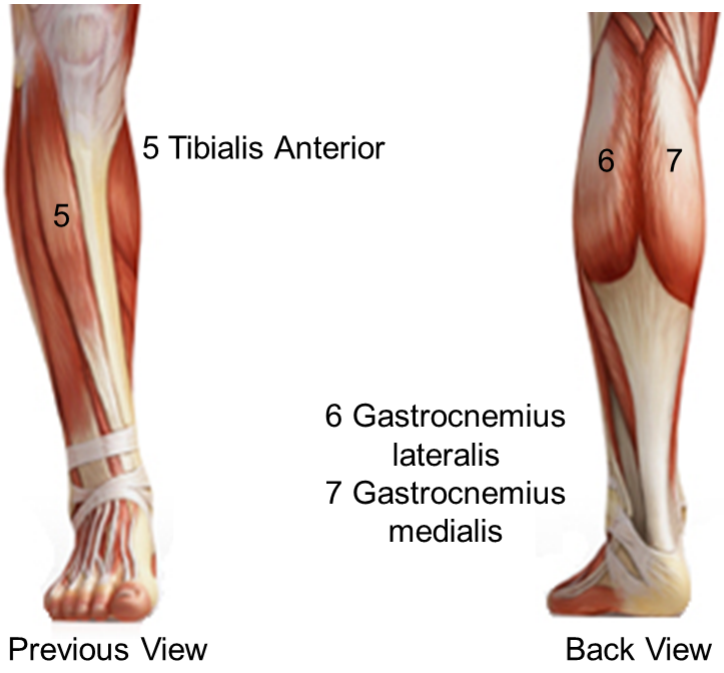

Figure 20 – Muscles selected for analysis. The anterior view, on the left side, shows the anterior tibial, and the right is the posterior view, with the Gastrocnemius Lateralis.

3.2 Inertial Measurement Units - IMU

Inertial Measurement Units - IMU are wireless measurement units that incorporate accelerometers (provide measurements of the components of linear acceleration), gyroscopes (angular velocity), magnetometers (magnetic field) and barometer (atmospheric pressure).

In this study, a scale model was generated, according to the anthropometric measurements and body mass of the individual who wore the exoskeleton. This model will be one of the inputs of the Inverse Dynamics for the calculation of the torques.

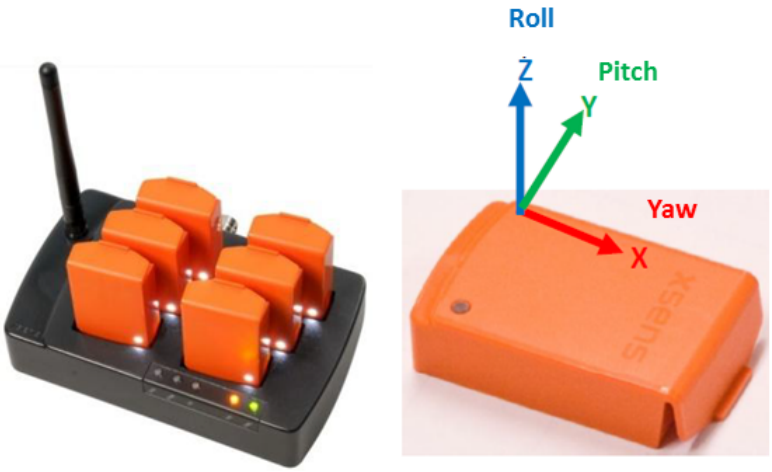

Figure 21 – Inertial Measurement Units Sensors - IMUs

The Euler *angles (roll, pitch and yaw)* describe the rotation of a rigid body by means of three successive rotations in a sequence. The sequence of rotations for Euler's angles follows the aerospace convention (sequence Z-Y-X) for rotation from the global reference coordinate system (L) to the sensor coordinate system (S), Figure 21.

There are numerous areas of application that these inertial measures can be used, such as biomechanics and rehabilitation. And because they have no wires, they improve the speed of use and make it possible to treat patients. The supplied software has the codes C, C ++, LabView, MATLAB and Linux.

In this work, the kinematic profiles for the lower limbs were evaluated by processing data from 7 IMUs (MTx, static RMS-error <1, and dynamic RMS-error <2) from XSens Technologies, Netherlands. The sensors were attached to the torso, thigh, leg and foot, Figure 22.

3.3 OpenSim

OpenSim[1] is free software that allows you to build, exchange and analyze models of the neuro-musculoskeletal system and dynamic movement simulations. It was introduced in 2007 at the American Biomechanical Society conference and has since been used in a wide variety of applications including research in biomechanics, medical device design, rehabilitation and orthopedics, neuroscience, ergonomic analysis, robotics, biology and education. OpenSim also has an API (from English, textit Application Programming Interface) that allows integration with other software and different programming languages (C++, Python and Matlab).

[1]http://opensim.stanford.edu

Figure 22 – IMUs on the user's torso, thigh, shin and foot.

Several devices and tools have been used in the search to obtain parameters that provide better results, such as the use of motion capture technology, dynamometer, force platforms and medical images that, used in conjunction with neuro-musculoskeletal models, provide a solid basis in biomechanical analysis (LLOYD; BESIER, 2003).

In this sense, the use of models allows to know analytically each musculoskeletal and neurophysiological component, in addition to the functional relationships between its variables, allowing to abstract how the input variables are processed by each component, in order to produce an output (SARTORI; LLYOD; FARINA, 2016).

The model used in the development of this study corresponds to the OpenSim Gait2392 model, a three-dimensional computational model of the human musculoskeletal system, with 23 degrees of freedom and 92 muscle-tendon actuators representing 76 muscles of the lower limbs and torso. The dimensionless muscle model adopted in this model is based on the implementation of (THELEN, 2003) and it can be changed and modified. The dimensions of the standard model, without scale, correspond to a 1.80 m tall subject with a mass of 75.16 kg.

3.3.1 Scaling

The Scaling process fits the generic musculoskeletal models offered by OpenSim to the characteristics of the individual. With the anthropometric characteristics of the individual, it is possible to modify the dimensions of the body segments and their properties (body mass and inertia tensor) and the elements that compose it (muscles and tendons).

Scaling is based on a combination of measured distances between marker locations (X, Y and Z) and manually specified scale factors. The locations of the markers are usually obtained using motion capture equipment. The non-scale model has a set of virtual markers placed in the same anatomical locations as the experimental markers.

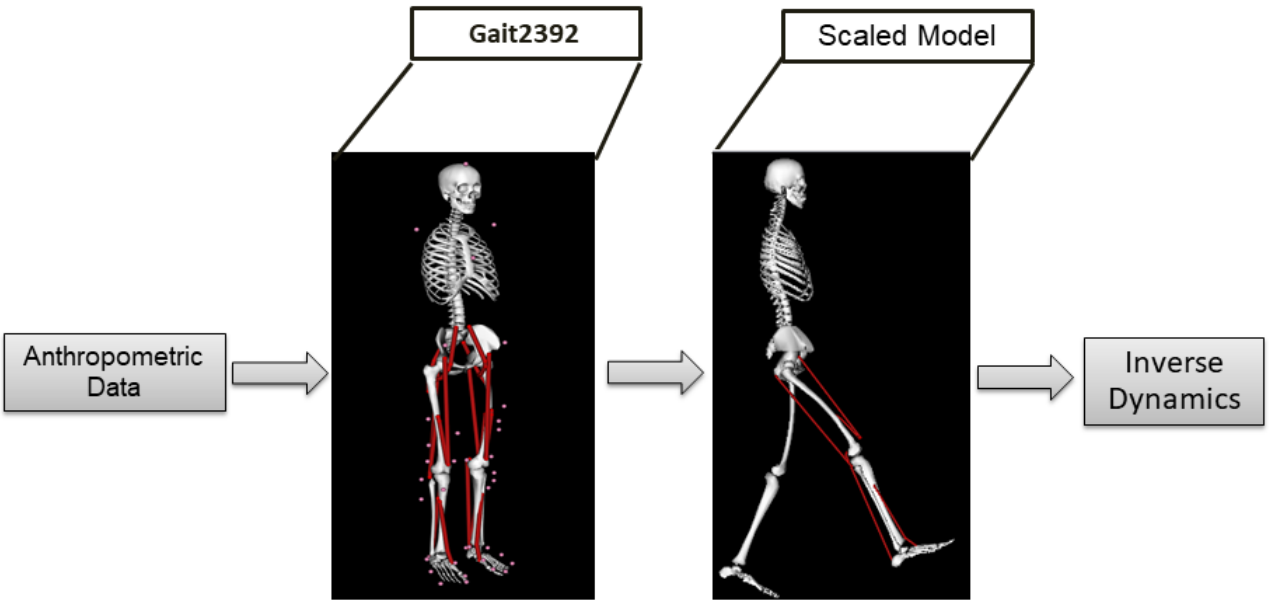

Figure 23 – Scaling the model for Inverse Dynamics.

After obtaining the model with the individual's adjustments, it is possible to obtain the parameters that define each body segment (length, mass) for the calculation of the inverse dynamics. In addition to the parameters of the muscles used to estimate strength and contribution to joint torque, Figure 23.

3.3.2 Inverse Dynamics

The Inverse Dynamics (DI) tool determines the set of torques in the joints responsible for a given movement, making use of the kinematics that describe it (position, speed and acceleration) and the external forces applied to the model. In this work, for the calculation of the DI, the angular position data of the joints were obtained with the IMUs, with the subject without the exoskeleton and then, wearing the device at two speeds (2.5 km/h and 3.0 km/h).

Three data files are needed as input for the Inverse Dynamics tool, as shown in Figure 24:

- ❏ Subject01-walk1ik.mot: Motion file that contains the generalized coordinates that describe the movement of the model (Angles);

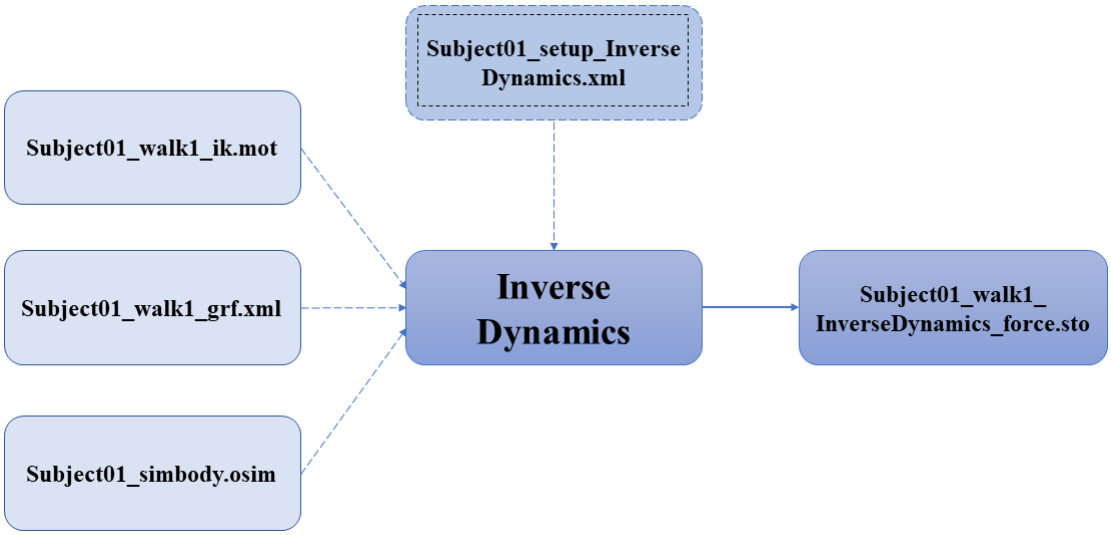

Figure 24 – Diagram of Inverse Dynamics.

- ❏ Subject01-walk1grf.xml: External force data (ground reaction forces, moments and center of the pressure location);

- ❏ Subject-01simbody.osim: OpenSim model specific to the subject with its anthropometric characteristics, generated from the scale of a generic model with the Scale Tool (inertial parameters).

The generated .sto file is a storage file that contains the time histories of the joint torques and the forces acting along the coordinate axes. The Setup-InverseDynamics.xml file is a configuration file for the reverse dynamics tool.

3.4 Lower Limbs Exoskeleton

The exoskeleton utilized in this work is the ExoTao (DOS SANTOS; SIQUEIRA, 2019). This robotic device comprises six rotary, one-degree-of-freedom joints, which can track the hip, knee and ankle joint movement on the sagittal plane, with the aid of magnetic encoders. For the time being, only the right leg of the robot is considered. The only active joint is the knee, whereas the hip and the ankle work passively. The knee joint consists of a module with a rotary Series Elastic Actuator (SEA), as presented in (DOS SANTOS; CAURIN; SIQUEIRA, 2017), which can be configured to work in impedance and force control modes. Its motor is connected to an EPOS controller board, which communicates with the control algorithm running on a desktop computer via Controller Area Network (CAN) ports. In order to prevent the subject from slipping while walking, and to compensate for part of weight of the exoskeleton, a mechanical structure was installed as depicted in Figure 25.

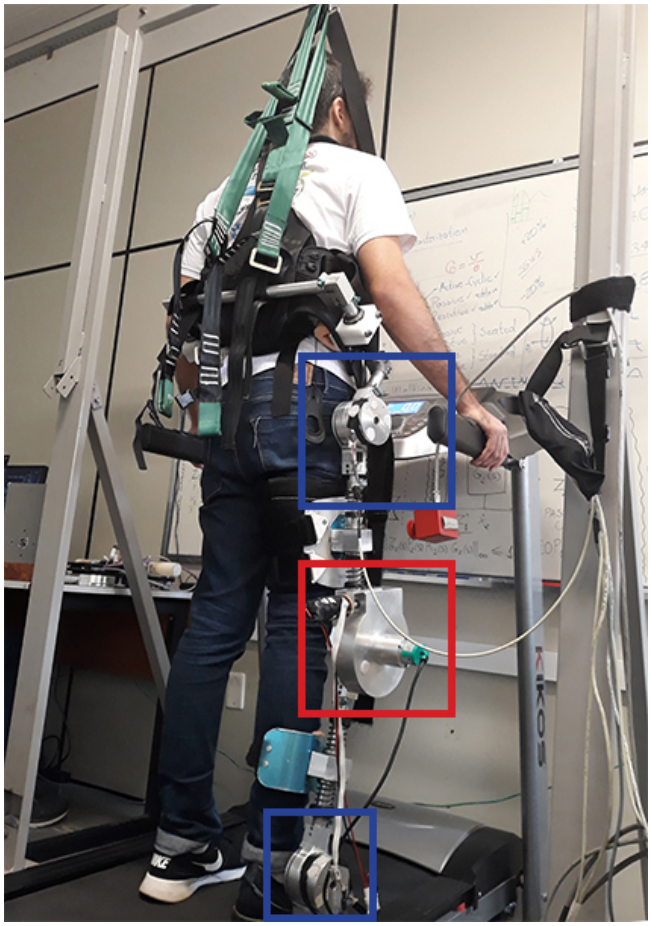

Figure 25 – Test setup with healthy subject wearing the right leg of the lower limbs exoskeleton ExoTao. The red box delimits the rotary SEA at the knee joint. The blue boxes depict the hip and ankle joints, which are not actuated. The robot is suspended by a mechanical structure in order to compensate for part of its weight, which leads to a more comfortable walk on the treadmill.

The joints were designed to attend different ranges of motion with respect to different tasks. However, they can be limited by adjustable end-stops to prevent hyperextension of the joints. The exoskeleton contains Velcro straps and telescopic links, which make it adjustable to different body heights from 1.60 m to 1.90 m, in order to align the exoskeleton and the subject joints (DOS SANTOS *et al.*, 2017).

3.5 Influence of the Exoskeleton on Profiles of Kinetic and Muscular Activity

In this section, the objective was to evaluate the influence of the structure of the exoskeleton for lower limbs on the motor primitives during walking and to find relationships between motor primitives and weights in two conditions: with and without the exoskeleton.

A set of experiments was carried out to evaluate the influence of the structure of the exoskeleton on the profiles of kinematic and muscular activity during the walk. A

healthy subject (29 years old, 84 kg, 1.77 m) was instructed to walk on the treadmill for 2 minutes at a comfortable speed in two conditions: first, not wearing the ExoTao, and then, wearing it.

Average speeds were 3.3 km/h and 2.5 km/h. The subject walked at a speed of 3.3 km/h without wearing the exoskeleton and later, wearing the exoskeleton, walked at two different speeds, 2.5 km/h and 3.3 km/h. The first and last twenty steps were discarded in the analysis, 40 steps were considered for each condition. The kinematic profiles of the lower limbs were evaluated by processing data from 7 IMU sensors attached to the torso, thigh, shank and foot.

Electromyographic signals - EMG of five lower limb muscles were measured: rectus femoris (RF), vastus medialis (VM), tibialis anterior (TA), biceps femoris (BF), and gastrocnemius lateralis (GL). EMG data was collected at 2 kHz on a separate computer using Delsys EMGworks software and further processed using MATLAB. First, the moving average of the signal is subtracted to eliminate the DC bias. Then, the corrected signal is fully rectified, filtered with low pass and normalized considering the maximum value obtained in the experiments. The low-pass filter corresponds to a second order *butterworth* with a cutoff frequency of 2 Hz.

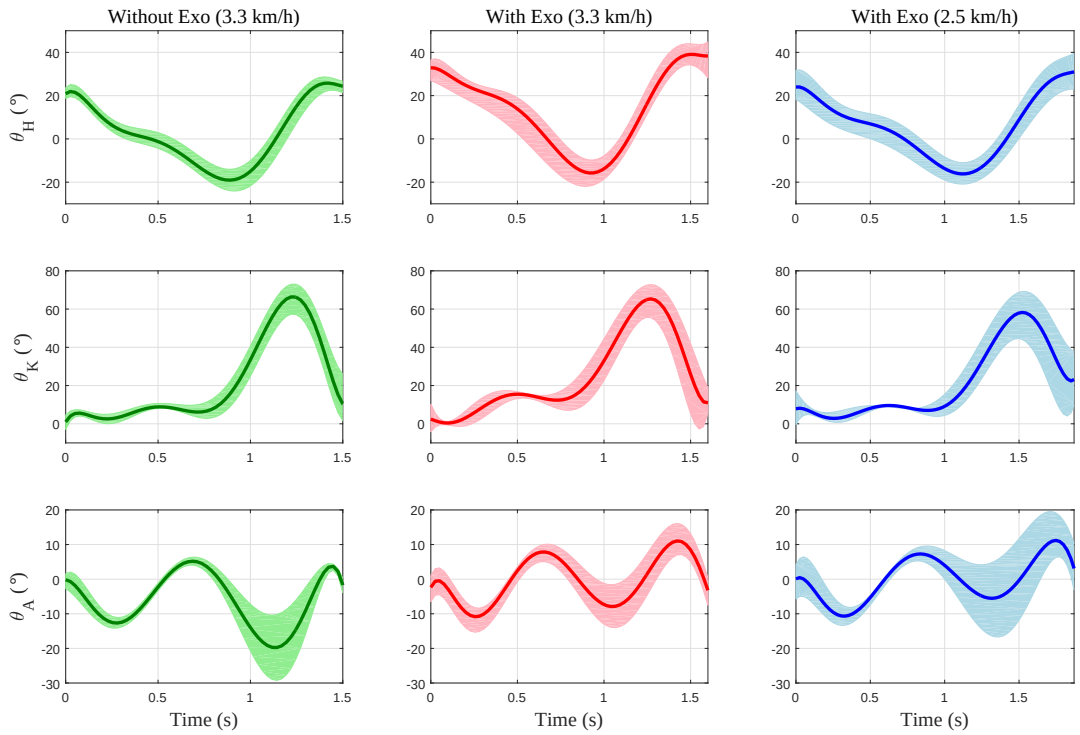

Figure 26 – Articular angles of a subject in the sagittal plane in three different situations: without the exoskeleton (green); with the exoskeleton 3.3 km/h (red) ; and with the exoskeleton 2.5 km/h (blue).

Figure 26 shows the articular angles in the sagittal plane, it is possible to notice that the average kinematic profiles are similar, but the variability of the data when the

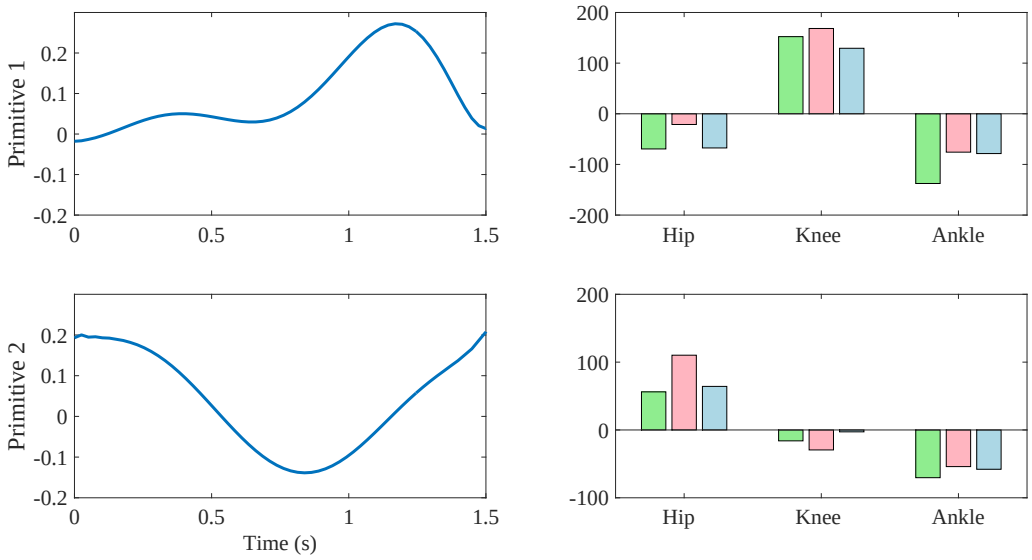

Figure 27 – On the left the primitives of the joint angles and on the right the weights of the subject's joints (hip, knee and ankle) in three different situations: without the exoskeleton (green); with the exoskeleton 3.3 km/h (red); and with the exoskeleton 2.5 km/h (blue).

individual used the exoskeleton is greater, mainly at the speed of 3.3 km/h, indicating that the user healthy is always opposing the structure of the exoskeleton to impose its own walking profile.

The primitives of the joint angles are shown in Figure 27. When the subject is using the exoskeleton and walking at a speed of 3.3 km/h, the maximum amplitude of hip flexion is increased, as illustrated by the greater weight for primitive 2 (light red bar). In relation to the ankle joint, there is a greater dorsiflexion in the swing phase, validated by a lower weight for Primitive 1.

The Figure 28 shows the normalized EMG signs, which correspond to the subject's muscular activity during the walk. As for kinematic data, the greatest variability is observed for the condition in which the user is using the exoskeleton.

It is observed that in the support phase, the vastus medialis and the gastrocnemius lateralis showed greater activation. Muscle responsible for balance, the vastus medialis has a greater activation at the beginning of the support phase (start of stage), according to the weights of primitives 3 and 4.

The rectus femoris showed greater activation at the beginning of the balance phase, because it initiates the hip knee flexion and extension movement in preparation for contact with the ground and impact absorption. The biceps femoris, responsible for balance and stabilize the knee joint immediately after heel contact (start of step), presented a more lasting activation in the early stance phase.

The results indicate computational advantages for the PCA-based approach. Note that the algorithm reconstructed responses with a high degree of fidelity, where the variance in all sets was greater than 98%. Thus, the results suggest that, from a minimum set of

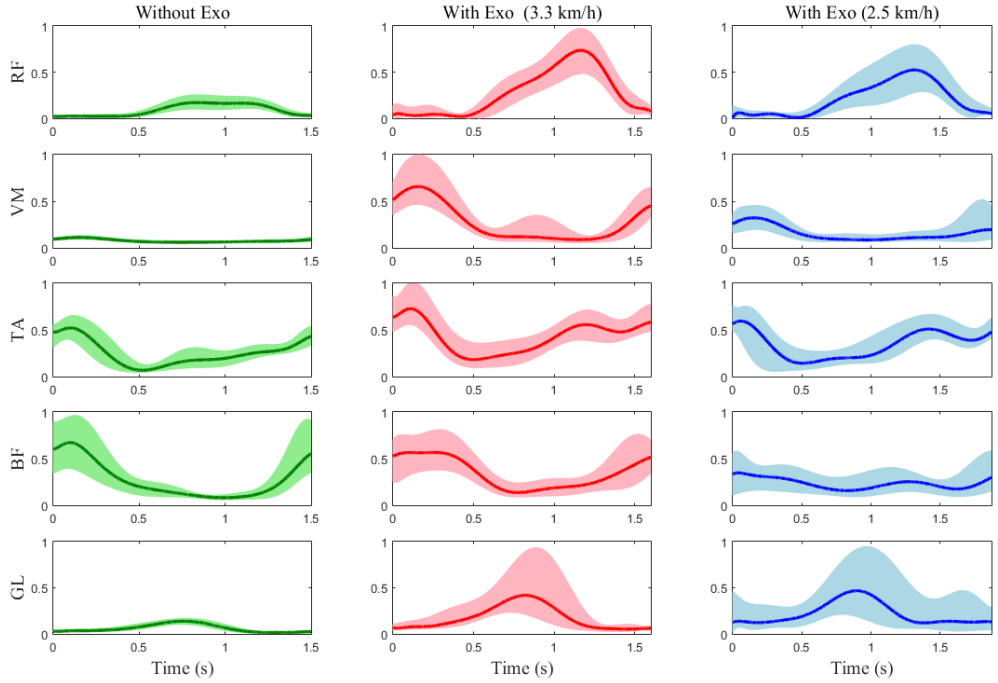

Figure 28 – Normalized EMG signals of activation of the subject's leg muscles (rectus femoris, vastus medialis, tibialis anterior, biceps femoris and lateral gastrocnemius) during walking in three different situations: without the exoskeleton (green); with the exoskeleton 3.3 km/h (red); and with the exoskeleton 2.5 km/h (blue).

components (two EMG primitives and four IMUs), it is possible to reconstruct all possible muscle stimulations or position profiles.

After evaluating the influence of the exoskeleton on the primitives, the influence of the structure of the exoskeleton on the kinetic and muscular characteristics was evaluated through the relationships between motor primitives and their respective weights for the different conditions of use. The experiments mentioned in section 7.1 were used.

To extract the motor primitives in order to analyze the data and reduce its dimensionality and eliminate unnecessary characteristics, of the Non-negative Matrix Factorization (NMF) was used, in the case of the analysis of the muscle primitives and in the case of the torques, the Principal Component Analysis (PCA) was used.

From the same EMG signals as the Figure 28, three primitives and their respective weights were extracted using the other factoring technique, NMF. The Figure 29 shows the primitives that were obtained.

To estimate the torques, OpenSim was used, and the model used in the development of this study corresponds to the OpenSim Gait2392 model. The dimensions of the standard model, not to scale, corresponding to a subject 1.80 m high with a weight of 75.16 kg.

As shown in Figure 29, Primitive 1, right at the end of the equilibrium phase and the beginning of the support phase, the tibialis anterior muscle has a greater activation, especially when the user walks wearing the exoskeleton. As it is a muscle that extends

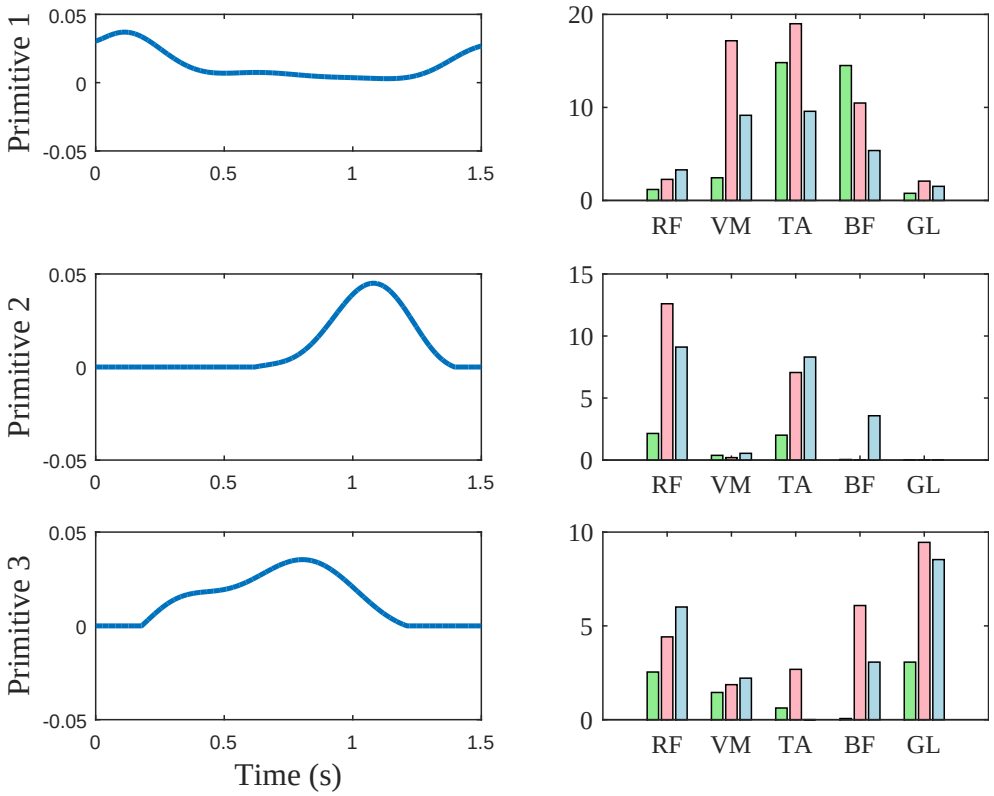

Figure 29 – On the left the EMG signal primitives and on the right the EMG signal weights of the muscles (rectus femoris, vastus medialis, tibialis anterior, biceps femoris and gastrocnemius lateralis) of the subject, extracted with the non-negative matrix factation technique, in three different situations: without the exoskeleton (green); with the exoskeleton 3.3 km/h (red); and with the exoskeleton 2.5 km/h (weights).

on the side of the tibia, it helps in the dorsiflexion of the foot, preventing the toes from dragging on the floor. In Primitive 1, a longer lasting activation of the biceps femoris (thigh muscle) can also be observed when the foot touches the floor. On the other hand, the gastrocnemius lateralis presents greater activation in the final phase of support and beginning of balance (terminal support), according to the weight of the primitive 2. When the user walked wearing the exoskeleton, the activations of this muscle were also greater. The rectus femoris, hip flexion and knee extension, showed greater activation at the end of the support and the beginning of the balance phase, in preparation for contact with the ground and impact absorption, according to primitive 3.

The Figure 30 shows the calculated torques of the hip, knee and ankle calculated using Inverse Dynamics of Opensim and the Figure 31 shows the primitives obtained from the calculated torques. The primitives of the joint torques were obtained using PCA, and when analyzing the weights of the primitives in the three walking conditions of the user, it is possible to notice that the user makes a greater effort to maintain his natural gait pattern when walking with the exoskeleton. In primitive 2, in the support phase (end of phase), when the hip tends to remain neutral when extending the knee, it is noted that the user makes a greater effort when using the exoskeleton, which can be confirmed by analyzing the weights of the rectus femoris muscle of the primitive 2, Figure, since the

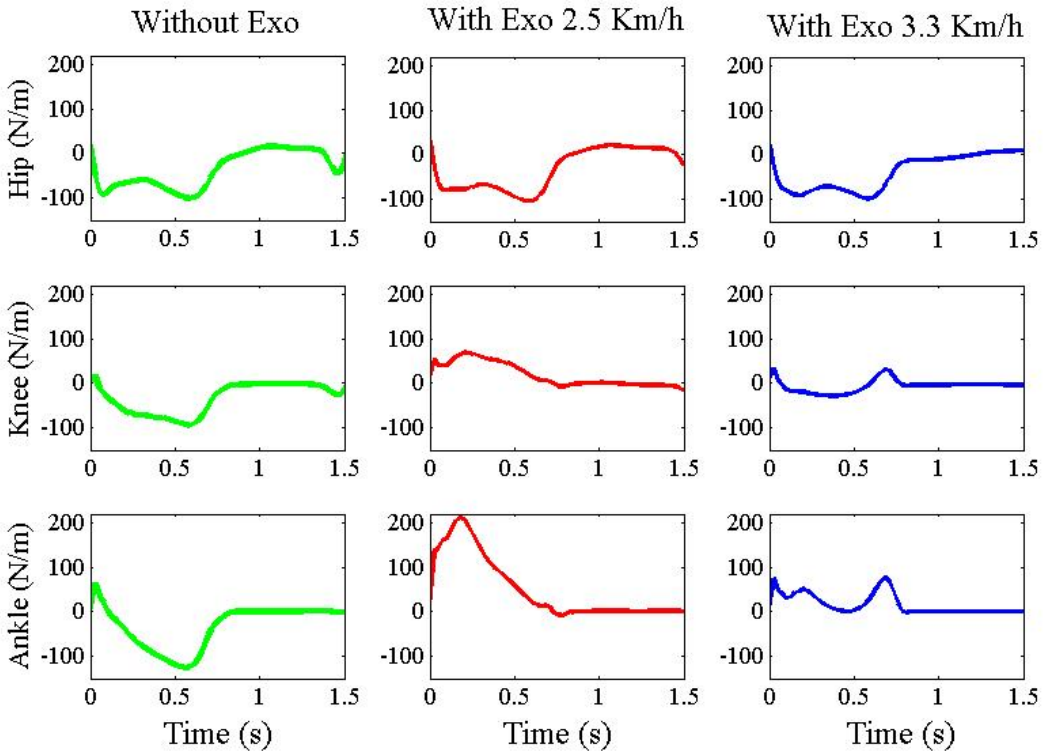

Figure 30 – Torques calculated using Inverse Dynamics of OpenSim of the subject's hip, knee and ankle joints.

rectus femoris is related to the knee extension movement.

It is observed that in all joints a greater weight when the user walks wearing the exoskeleton, for example, primitive 1 at a speed of 3.3 km / h, when the user takes the step and extends the hip joint at the beginning of the support phase and when placing the foot on the floor after flattening the foot, the user applies greater strength to the ankle joint (dorsiflexion) also in the support phase. The responses reconstructed by the algorithms have a high degree of fidelity, and the variation in all sets was greater than 98%, indicating clear advantages in computational efficiency for the approach based on NMF and PCA.

Thus, the results suggest that, based on a minimum set of components (three EMG primitives and two torque primitives), it is possible to reconstruct all possible muscle stimulations or kinetic activity for various conditions of use of the exoskeleton.

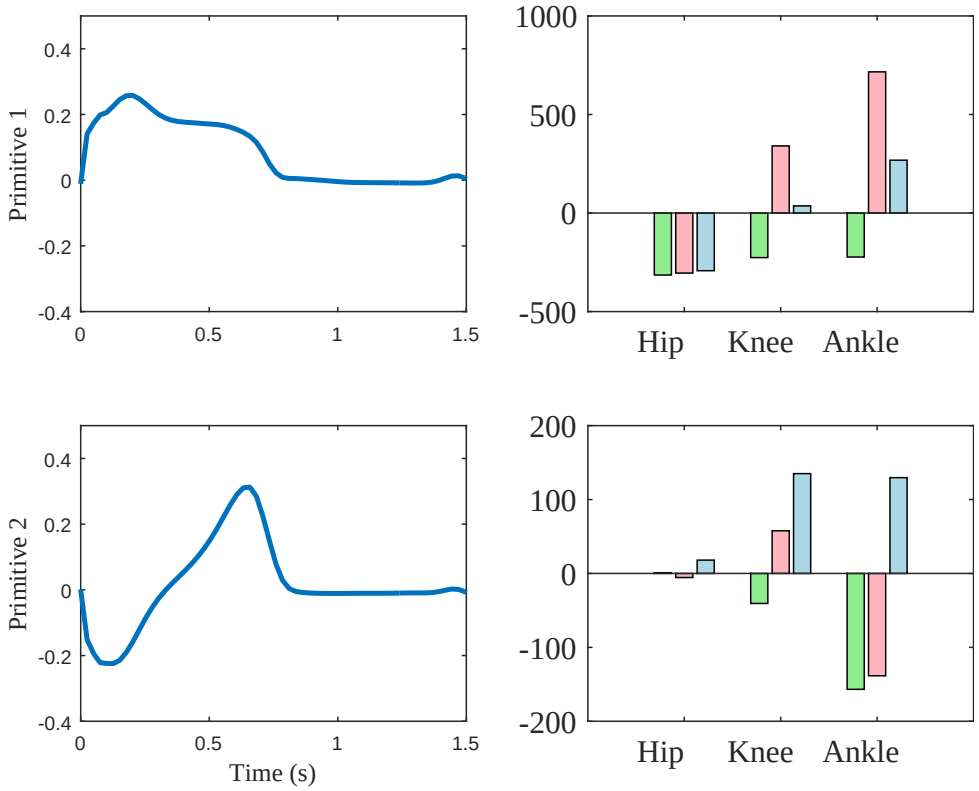

Figure 31 – To the left the torque primitives and to the right the torque weights of the subject's joints, in three different situations: without the exoskeleton (weights); with the exoskeleton 3.3 km/h (red); and with the exoskeleton 2.5 km/h (blue).

Chapter 4

Adaptive Control Strategy based on Motor Primitives

In this chapter, the extraction of the motor primitives will be discussed, using Principal Component Analysis, to obtain the reference values and later to analyze the data. Aditionaly, the bio-inspired adaptive control strategy will be explained in details.

4.1 Motor Primitives Extraction

To extract the primitives and analyze the data, aiming at the reduction of dimensionality and elimination of unnecessary characteristics, the Principal Component Analysis (PERSON, 1901) was employed. The PCA was chosen because it proved to be an accurate estimate to obtain a linear combination of primitives and their respective weights, in order to minimize the difference between the original and reconstructed signals (NUNES; OSTAN; SIQUEIRA, 2020).

The calculation, Equation 9, extracts a linear combination between primitives $\mathbf{p} = [\mathbf{p_1}, \mathbf{p_2}, ..., \mathbf{p_n}]$ where $\mathbf{p} \in \mathbb{R}^{t \times n}$ and their corresponding weights $\mathbf{w} = [\mathbf{w_1}, \mathbf{w_2}, ..., \mathbf{w_n}]$ where $\mathbf{w} \in \mathbb{R}^{n \times m}$, to minimize the difference between the original and reconstructed signals, which, in this case, are torque profiles $\mathcal{T} \in \mathbb{R}^{t \times n}$:

$$\mathcal{T} = \mathbf{P} \cdot \mathbf{w} \tag{9}$$

The motor primitives of four healthy subjects (1 female, 3 male, 30 $\pm$ 6 years, 73 $\pm$ 6 kg, 1.78 $\pm$ 0.04 m) were extracted in order to be further used by the control algorithm as reference. To extract these motor primitives, the subjects walked on a treadmill using the right leg of the exoskeleton for two minutes at 1.0 km/h. The knee joint of the robot was adjusted to impedance mode, thus, the knee of the subjects followed a desired

pre-recorded trajectory, according to the control law:

$$\tau_{r,imp} = K_v(\theta^d - \theta), \tag{10}$$

where K_v is the virtual stiffness of the impedance controller (set to 20 N.m/rad), $\tau_{r,imp}$ is the torque of the robot, while θ^d and θ are the desired trajectory and the knee joint measurement, respectively. An inner Proportional-Integral (PI) torque controller ensures that the robot torque is exerted at the joint.

The torques exerted by the subject ate the hip and ankle are estimated by means of an estimation algorithm that employs a generalized momentum-based disturbance observer (DOB) approach along with an Extended Kalman Filter. The Kalman Filter returns a time-varying gain at the end of every iteration, which ensures robustness with regards to the time-varying characteristics of the patient-exoskeleton model, as described by (DOS SANTOS; SIQUEIRA, 2019). The knee torque is obtained directly from the SEA.

This procedure yields the motor primitives, $\mathbf{p_h}$, and their respective weights, $\mathbf{w_h}$, with respect to each joint. Further auxiliary data considered by the control algorithm are also generated, such as maximum primitive torque, $\tau_{h,max}$, and constant torque offset values, $\tau_{\mathbf{h,dc}}$. The subscript $\mathbf{h}$ healthy subject-related variables.

4.2 Bio-inspired Adaptive Control Algorithm

With the use of primitive motors, the computational load can be significantly reduced during motor control over the CNS. This is because with a basic set of primitives, it is possible to reconstruct different conditions and tasks related to movement, Figure 32. That is, at the end of every step, the control algorithm computes the subject's motor primitive weights, based on the primitive torques extracted beforehand and on the joint torque measurements during the last swing phase. The subject's weights that are below the reference value are identified and, during the next swing phase, the robot actuates in order to compensate for the lack of weight. The following paragraphs explain in details the calculations performed by the control algorithm.

The algorithm is provided with the data from the procedure described in Section 6.2, i.e. the reference values. After the right leg of the subject has performed the k^{th} swing, his torque curves, $\tau_{\mathbf{pat}}$, with respect to the hip, knee and ankle joints are obtained by the estimation algorithm and the SEA. These torque curves are treated before being employed to compute the subject's motor primitive weights. First, their constant offset value, $\tau_{\mathbf{pat,dc}}$, is subtracted. Afterward, they are divided by the extreme torque value obtained from the reference, $\tau_{max,h}$, resulting in a normalized torque profile, $\tau_{\mathbf{pat,n}}$. This extreme value is the maximum value within each torque curve, and among torque curves. Due to the characteristic of the torque curves during the swing phase, it is known beforehand that

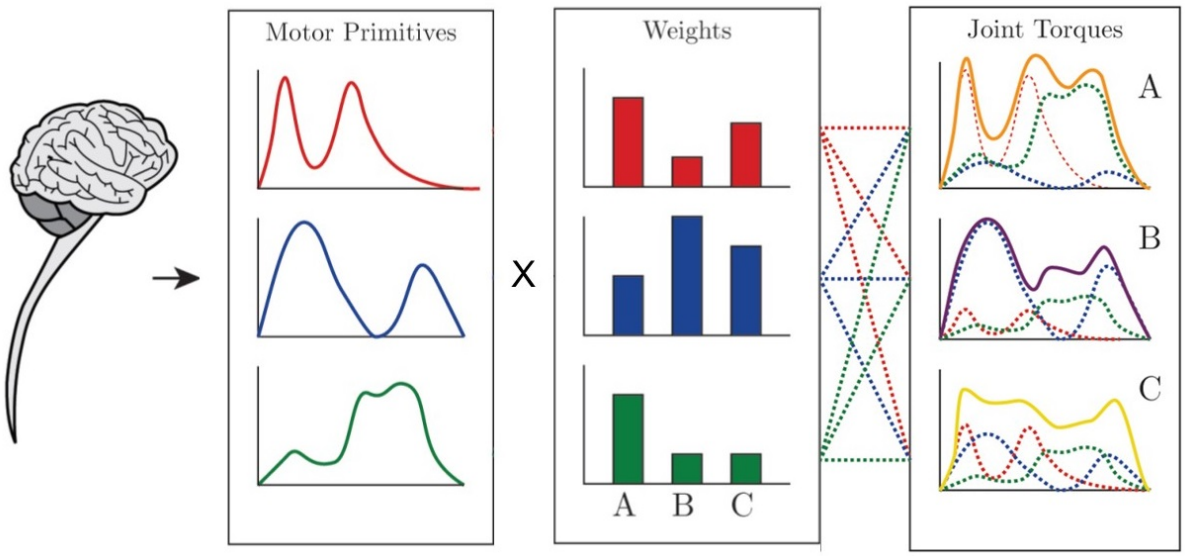

Figure 32 – Joint torques are constructed through a weighted sum of motor primitives by the CNS. Drawing based on (TING *et al.*, 2015).

this value is positive and related to the hip joint. However, in case other gait phases or tasks are analyzed, the algorithm handles the circumstance in which this value is a global minimum instead.

The aforementioned manipulations are summarized by the following equation:

$$\tau_{\mathbf{pat,n}}{}^{k} = \left(\frac{1}{\tau_{h,max}}\right)(\tau_{\mathbf{pat}}{}^{k} - \tau_{\mathbf{pat,dc}}{}^{k}). \tag{11}$$

Therefore, the motor primitive weights of the subject, $\mathbf{w_{pat}}$, are extracted as in:

$$\mathbf{w_{pat}}{}^{k} = \mathbf{p_h}{}^{\dagger}\tau_{\mathbf{pat,n}}{}^{k}, \tag{12}$$

where $\mathbf{p_h}{}^{\dagger}$ denotes the Moore-Penrose inverse of the motor primitives extracted from the gait used as reference.

The subject weights, $\mathbf{w_{pat}}$, are compared with the reference weights, $\mathbf{w_h}$, element-by-element. The relative error between these weights provides a measurement of how distant the subject's gait is from the reference gait. This disparity, $\mathbf{\Delta w}$, should be addressed by the robotic device during the next swing phase and is denoted simply as:

$$\mathbf{\Delta w}^{k} = \mathbf{w_h} - \mathbf{w_{pat}}{}^{k} \tag{13}$$

Subsequently, the relative error, $\mathbf{\Delta w}$, is multiplied by the reference motor primitives, $\mathbf{p_h}$, for the next balance phase. It is important to remember that the primitives were extracted from the normalized torque so it is necessary to multiply them by the maximum primitive torque, $\tau_{h,max}$. The difference between the constant offset values is also addressed

by the robot, subtracting the constant torque offset values, $\tau_{\mathbf{h,dc}}$, by the constant offset value the patient, $\tau_{\mathbf{pat,dc}}$.

$$\tau_{\mathbf{r}}{}^{k+1} = \tau_{h,max}\mathbf{p_h}\boldsymbol{\Delta}\mathbf{w}^k + \left(\tau_{\mathbf{h,dc}} - \tau_{\mathbf{pat,dc}}{}^k\right) \tag{14}$$

All quantities related to the subject are denoted by the subscript **pat**. Though no patient was subjected to the test, the variables were named after this word to illustrate the purpose of the control algorithm, which is aimed at people with some sort of motor impairment.

To avoid abrupt oscillations, the effective torque to be exerted by the robot, $\tau_{\mathbf{r,e}}$, considers the weight deficieny from the last step and the step before the last one. This approach leads to the computation of an exponentially weighted moving average (EWMA). A diagonal matrix, α, composed of α_i factors, $i = 1, 2, 3$ weights the robot torque as in:

$$\tau_{\mathbf{r,e}}{}^{k+1} = \alpha\tau_{\mathbf{r}}{}^{k+1} + (\mathbf{I} - \alpha)\tau_{\mathbf{r}}{}^{k}. \tag{15}$$

During the first step, no robot torque is applied, as there is no previous step. During the second step onward, the robot torque is applied. Exceptionally during the second swing, α is set to unit. Afterward, α, is set to 0.15, a value found empirically.

This robot torque is exerted at the robot joint with the aid of an inner PI torque controller, whose gains were set to $k_p = 370$ and $k_i = 3.5$ based on previous works with the robotic device. The robot only acts during the swing phase. During the stance phase transparency is aimed, so the desired robot torque is set to zero and only the inner torque control loop takes place. The phase detection is hard-coded within the control algorithm and is based on pre-recorded trajectories.

All operations are shown in matrix notation because the control algorithm is proposed to work on three joints of each leg. However, because only the knee joint is actuated, here only this component of the robot torque is used.

The robot exerts torque only when the subject weights are not greater than the reference weights. Otherwise, the robot would restrain the subject's movement, applying an opposing torque. This would lead to a control strategy focused on replicating a reference torque curve, which is not the aim of this work. The same is true for the constant component of the torques when they are greater than the reference values.

However, when the subject exerts more torque than necessary, but in the opposing direction, which in practice results in opposed-sign weights of greater magnitude than the reference, the robot does act in order to correct the gait. Figure 33 shows the complete block diagram of the proposed adaptive control algorithm.

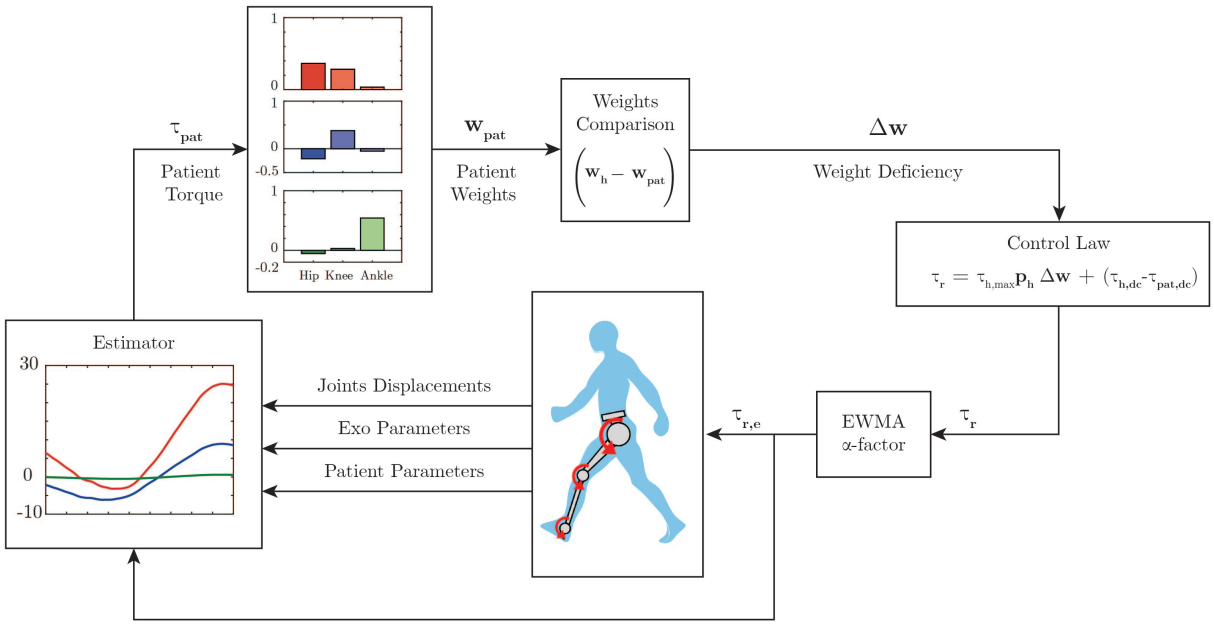

Figure 33 – Control diagram. The patient hip (red), knee (blue) and ankle (green) torques are estimated. Further, the motor primitive weights are extracted according to Equation 12. These weights are compared with reference weights, and then Equation 14 computes the assistive robot torque. The robot will exert an exponentially weighted moving average of the computed torque during the next swing phase.

4.3 Test protocol

Two tests were performed with 5 healthy subjects (1 female, 4 male, 30 ± 6 years, 73 ± 6 kg, 1.77 ± 0.05 m) in order to evaluate the control algorithm and the motor primitive weights behavior, and one test was performed with one healthy subject (male, 25 years old, 71 kg and 1.76 m) to evaluate the algorithm convergence and adaptability to changes in the mode of walk.

In the first test, the subjects were instructed to walk at 1.5 km/h on a treadmill for 2 minutes. This yields data for approximately 50 steps. In this test, the subjects walk in an active manner, as if they were without the exoskeleton. The expected robot torque is small, as the subjects produce all the necessary torque to perform the walk, dispensing further assistance. The joints trajectories and torques are expected to match, to a certain extent, the ones obtained during the procedure to extract motor primitives. Further, the behavior of all weights are analyzed.

In the second test, the subjects walked at 1.0 km/h on a treadmill for 2 minutes. This time, they were instructed to walk slower and also to keep the right leg passive during the swing phase, i.e. to offer no resistance in case the robot tried to move it. Hence, the motor primitive weights relative to the knee joint are expected to result in values lower than the reference, causing the robot to exert an assistive torque over the swing phase. Further, the behavior of all weights are analyzed.

The third test consisted of a combination of the first and the second test and was

performed with one healthy subject. He was instructed to walk actively for 30 seconds at 1.0 km/h, and passively for 30 seconds at the same speed, completing 1 minute of walk. This yields data for 25 steps. Therefore, it could be evaluated whether the control algorithm would adapt to different patient behaviors in real time.

During all tests, the joint displacements, torques, and the motor primitive weights of the subjects were stored for further analysis. The extracted weights of the subject were divided into three categories. The weights could be considered *healthy* weights, which comprised weights with equal or greater magnitude and same direction as the reference weights. In this case, the robot did not actuate. The weights could also be considered *deficient*, which comprised weights below the absolute reference value, regardless of their direction. These weights and their behavior over the first two tests is analyzed. In this case, the robot produced torque during the next swing, in order to assist the subject. Last, the weights could be considered *asynchronous*, which comprised weights with greater magnitude as the reference, but with opposing sign. Although the robot exerted torque in order to correct the subject's gait, these weights are not considered deficient, as their occurrence is rather consequence of a lack of synchrony between the actual gait phase and the phase of the control algorithm, than the consequence of an impaired walk, in which there is a lack of weight to perform the movement.

The primitive extraction procedure and the analysis of data yielded from all tests are processed by means of routines programmed in MATLAB®software (2015a, The MathWorks, Inc., Natick, Massachusetts, United States).

Chapter 5

Results

In this chapter, the results obtained from the adaptive control strategy based on motor primitives for lower limb exoskeletons are presented.

5.1 Adaptive Control Strategy based on Motor Primitives

First, the experimental results obtained from the extraction procedure of the motor primitives will be shown. These data are later used as reference values in the control algorithm. In the sequence, the results of a set of conditions will be presented in which the patient walked actively, passively and later, a combination of the two ways of walking.

5.1.1 Reference Primitive Torques and Weights

Figure 34A shows the average measured joint displacements (solid lines) during the swing phase. Figure 34B shows the average estimated joint torque profiles (solid lines). The shaded region denotes the standard deviation of the measurements.

Figure 35 shows the average primitive torque profiles from the extraction method described in Chapter 4 along with the respective weight regarding each joint. The shaded region denotes the standard deviation of the measurements.

The reference weights employed as reference for the control law are described by the following matrix:

$$\mathbf{w_h} = \begin{bmatrix} \mathbf{w_{h,hip}} \\ \mathbf{w_{h,knee}} \\ \mathbf{w_{h,ankle}} \end{bmatrix} = \begin{bmatrix} 0.8784 & -0.4750 & -0.0539 \\ 0.4768 & 0.8786 & 0.0282 \\ 0.0340 & -0.0505 & 0.9981 \end{bmatrix} \pm \begin{bmatrix} 0.0097 & 0.0142 & 0.0044 \\ 0.0140 & 0.0087 & 0.0574 \\ 0.0284 & 0.0498 & 0.0015 \end{bmatrix}. \quad (16)$$

If one multiplies each primitive curve by the respective joint weight and sum all the three components, the average profile torque can be reconstructed for all joints. It is

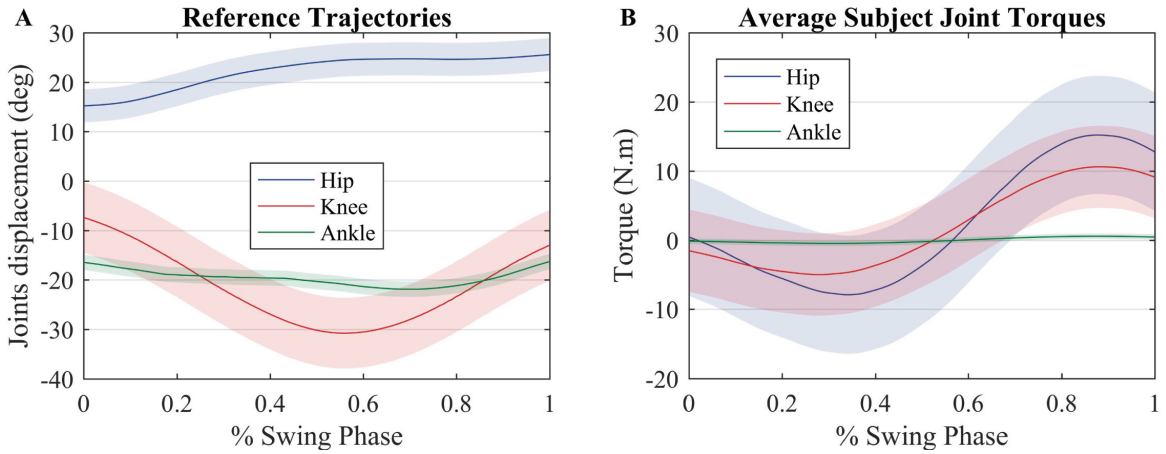

Figure 34 – (**A**) Average measured joint displacements (solid lines) during the swing phase. (**B**) Average estimated joint torque profiles (solid lines). The shaded region denotes the standard deviation of the measurements.

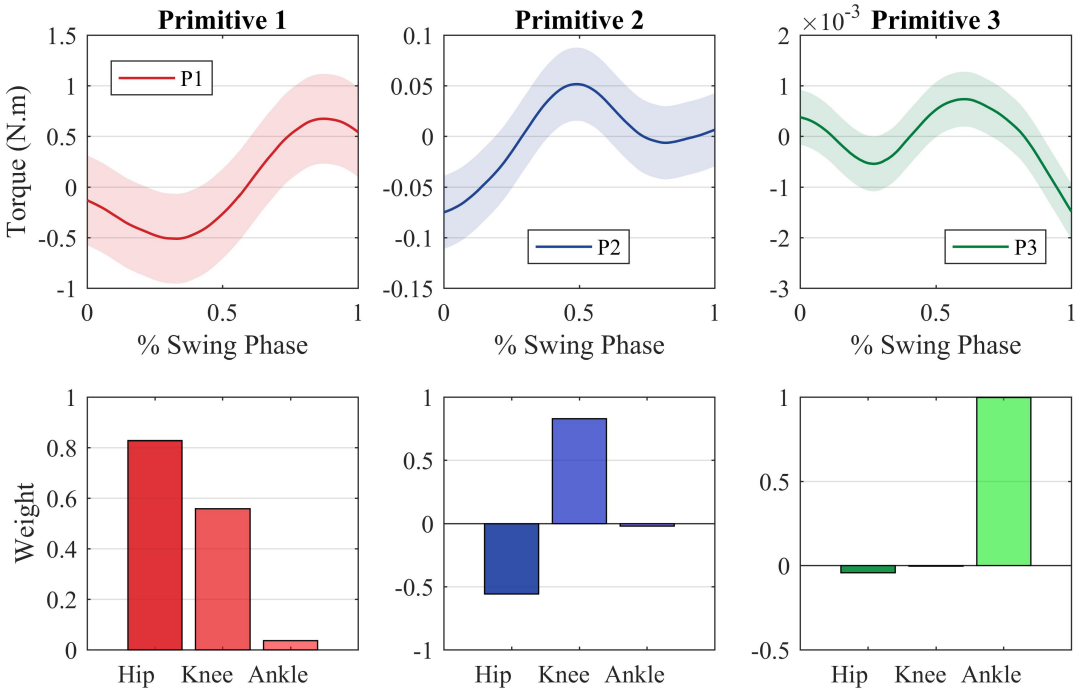

Figure 35 – Motor primitives extracted through the PCA method and the motor primitive weights regarding each joint. The joint torques can be reconstructed by making a weighted sum of each primitive with regards to each joint.

important to notice that each primitive is strictly related to a specific joint. The first primitive, for instance, is tight to the hip joint, which can be noted by the fact that the hip weight of this primitive (0.8784) is greater when compared with the other two weights (0.4768 and 0.0340).

These weights ponder the influence of each primitive on the torque observed at each joint. A negative weight means that the primitive torque must have its direction changed before being multiplied by the weight and being summed to the other primitives that

compose the joint torque. The control algorithm will not provide assistance in the case the subject's weights are at least equal to the reference ones. If his weights are greater than the reference, the subject is exerting more torque than necessary. If the weights are greater in magnitude but with an opposing sign, the subject is exerting more torque than necessary and in the wrong direction. In this case, the subject is not considered necessarily in need of assistance to perform the movement, as he is capable of exerting torque of greater or same magnitude as the reference.

It can be noted that during the swing phase the ankle joint exerts almost no torque. This is due the fact that the exoskeleton shoe is rigid to a certain extent, in order to aid post-stroke patients with foot-drop to perform the walk properly. Therefore, the ankle joint can be left out for this application. Hence, the reference weights matrix is further simplified as

$$\mathbf{w_h} = \begin{bmatrix} \mathbf{w_{h,hip}} \\ \mathbf{w_{h,knee}} \end{bmatrix} = \begin{bmatrix} 0.8784 & -0.4750 \\ 0.4768 & 0.8786 \end{bmatrix} \pm \begin{bmatrix} 0.0097 & 0.0142 \\ 0.0140 & 0.0087 \end{bmatrix} \tag{17}$$

The data extraction also provides an average of the maximum torque, which is the maximum hip torque:

$$\tau_{h,max} = 25.8 \quad \text{Nm.}$$

The constant component regarding the average torque of each joint is given by

$$\tau_{\mathbf{dc}} = \begin{bmatrix} \tau_{dc,hip} & \tau_{dc,knee} \end{bmatrix} = \begin{bmatrix} 12.4 & 4.2 \end{bmatrix} \pm \begin{bmatrix} 9.7 & 1.2 \end{bmatrix} \quad \text{Nm.}$$

It can be noted that there is considerable variation among the torque offset values. This is due to the nuances in the gait pattern of the individuals, as well as their characteristics, such as body mass and leg length.

The constant components of the knee and ankle torques are small when compared with the hip component. Moreover, a steadier robot behavior was achieved when these constant values were not considered, since the robot would abruptly raise its torque to this constant value as soon as the swing phase started. Thus, they were not considered for this test, in order to obtain a smoother robot assistance and steadier gait. To extract the patient weights, $\mathbf{w_{pat}}$, and compare with the reference ones, the algorithm must receive the pseudo-inverse of the primitive torques, $\mathbf{p_h}^{\dagger}$. To reduce computation time, the pseudo-inverse is calculated beforehand and provided to the algorithm. Once the healthy parameters were set, the tests were performed.

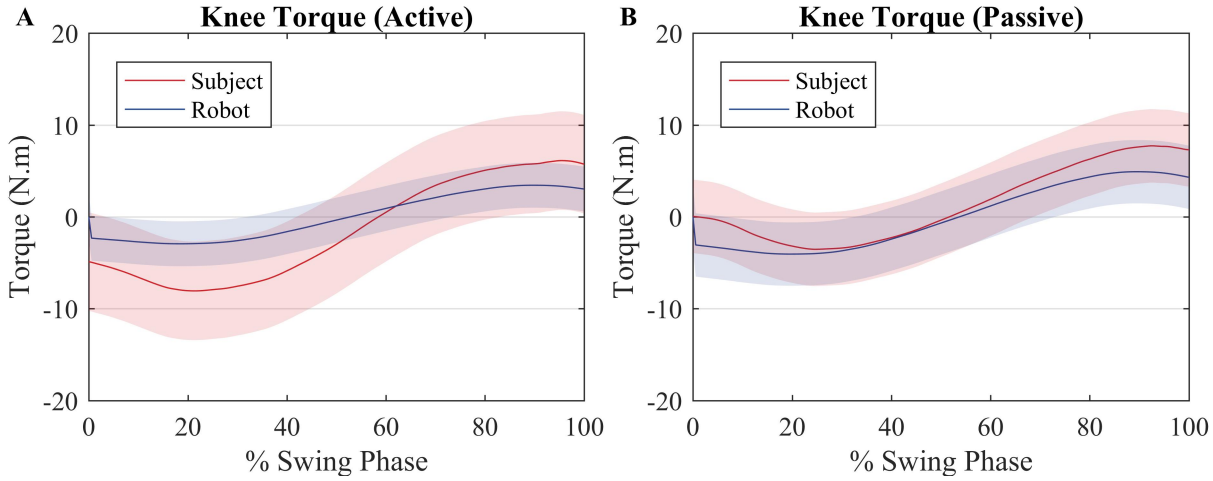

Figure 36 – Average torque exerted by the subjects (red) and by the robot (blue) for an (**A**) active walk and a (**B**) passive walk. Shaded regions denote the standard deviation of the measurements.

5.1.2 Test Results

Though there is not an explicit torque reference value to be tracked by the control algorithm, it is expected that, for the first test, in which the subjects walked actively, the robot exerts less torque than the subject, when compared with the second test, in which the subjects walked passively. In the first case, Figure 36A (active), the robot produces a torque with a RMS value of 2.5 Nm, whereas the user produces a torque with a RMS value of 7.3 Nm, equal to the reference value of 7.3 Nm RMS. In the second case, Figure 36B (passive), the robot produces more torque (RMS = 3.5 Nm) since the user is producing less torque at the knee joint (RMS = 5.6 Nm). It must be noted that it is not possible to prevent the user from exerting torque at the knee joint. When the results of each subject are considered rather than the average among them, for the active walk the minimum RMS torque produced by the robot was 1.2 Nm RMS, when the user was producing a torque of 10.5 Nm RMS. With respect to the passive walk, the maximum torque of the robot was 4 Nm RMS and the subject, 4.4 Nm RMS.

When the subject and the robot torque are compared with the reference, it can be noted that for both scenarios the two torques sum up in order to get closer to the reference torque as depicted by Figures 37A (active) and 37B (passive).

Figure 38 shows a comparison between the hip joint positions of the subject during the primitive extraction procedure (blue) and during the tests (red) and Figure 40 shows the average trajectory error between these joint positions. Despite an offset value, which is due to the position of the exoskeleton around the subject's hip, the trajectories are similar among all subjects, and they relate to the reference profile, though, in the active walk, the amplitude of the movement is greater.

Figure 39 shows a comparison between the knee joint positions of the subject during the primitive extraction procedure (blue) and during the tests (red) and Figure 41 shows the average trajectory error between these joint positions. The trajectories are similar

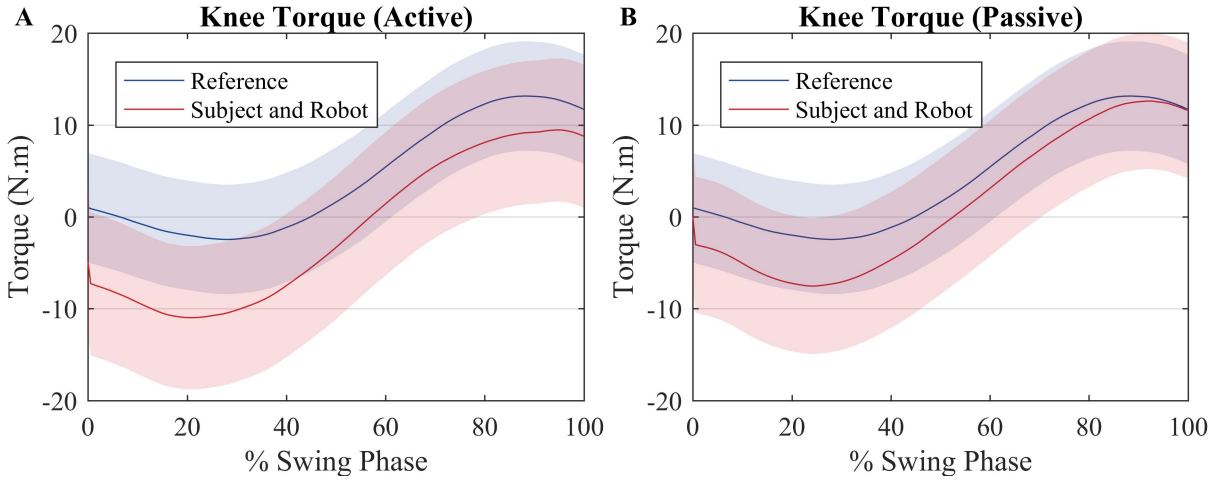

Figure 37 – Average torque exerted by the subjects (red) and average torque value used to compute the reference (blue) for an (**A**) active walk and a (**B**) passive walk. Shaded regions denote the standard deviation of the measurements.

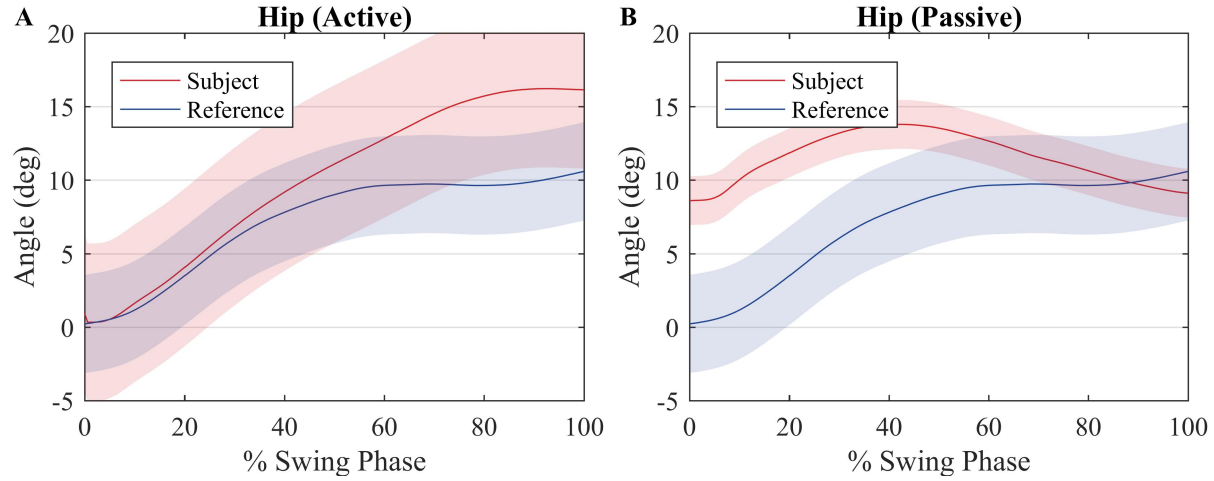

Figure 38 – Average hip joint displacement of the subjects (red) and average hip joint displacement during the procedure to compute the reference values (blue) for an (**A**) active walk and a (**B**) passive walk. Shaded regions denote the standard deviation of the measurements.

among all subjects, and they relate to the reference profile, regardless of the mode of walk, since there is robot actuation at the knee joint. It can be noted that the knee joint is closer to the reference during the passive mode of walk.

With respect to the motor primitive weights, the primitive motor weights of the hip and knee for the first and second primitive motor of each subject are seen in active and passive mode in Appendix A. The gray region denotes the value range over which the weight was considered deficient subsequently, only the weights that were below the reference value, regardless of their signal, were analyzed, in order to evaluate the influence of the robot actuation between the two modes of walk. To simplify this analysis, these weights were summarized in a boxplot and compared with the other subjects, as depicted in Figure 42.

The third test evaluated the algorithm performance during gait with oscillating cha-

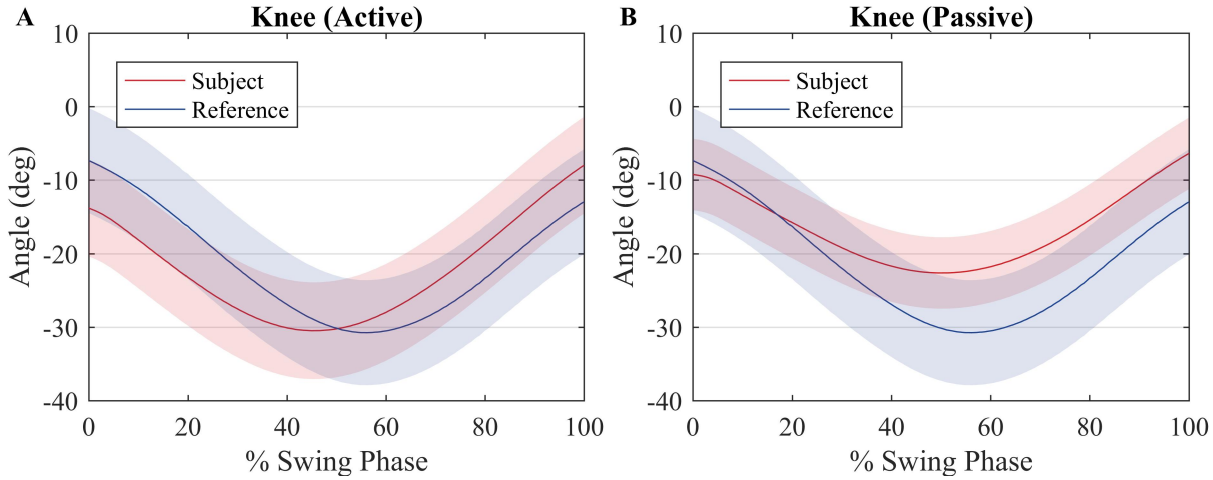

Figure 39 – Average knee joint displacement of the subjects (red) and average hip joint displacement during the procedure to compute the reference values (blue) for an (**A**) active walk and a (**B**) passive walk. Shaded regions denote the standard deviation of the measurements.

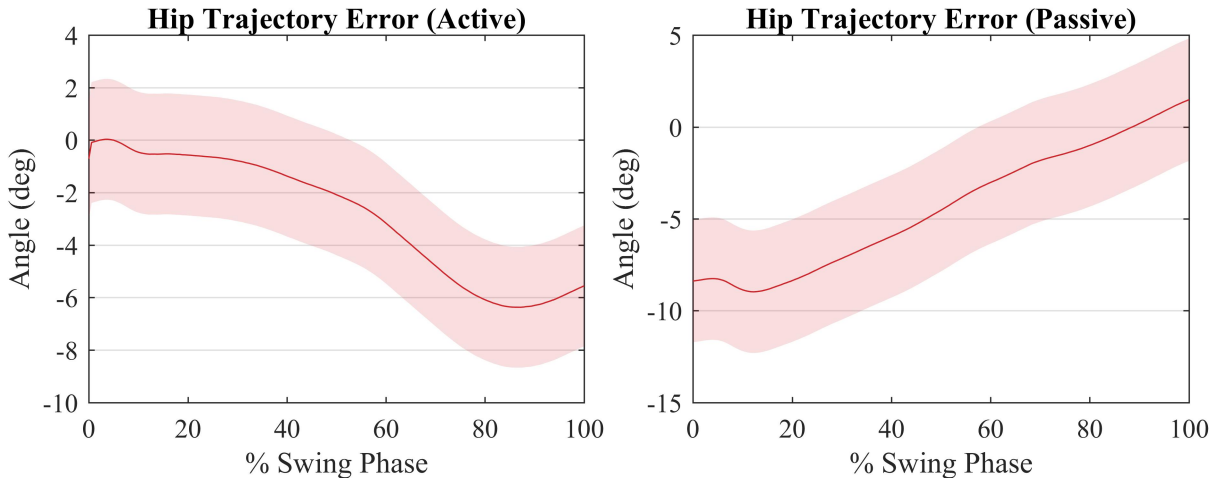

Figure 40 – Error between the average hip joint displacement of the subjects and average hip joint displacement during the procedure to compute the reference values calculation procedure for an active walk (**A**) and a (**B**) passive walk. Shaded regions denote the standard deviation of the measurements.

racteristic. Hence, the user walked actively for 30 seconds and passively for more 30 seconds. Results are depicted in Figure 43.

5.2 Discussion

First, the primitives are extracted from the data of average joint torque profiles, section 5.1.1, and then these are used as reference values in the control algorithm, in which the weights weight the influence of each primitive on the torque observed in each joint. A set of conditions in which the patient walked actively, passively and subsequently a combination of the two ways of walking is presented in section 5.1.2.

As seen in Figure 36, the robot produces less torque during an active mode of walk when compared with the passive mode of walk. However, the robot torque is still present

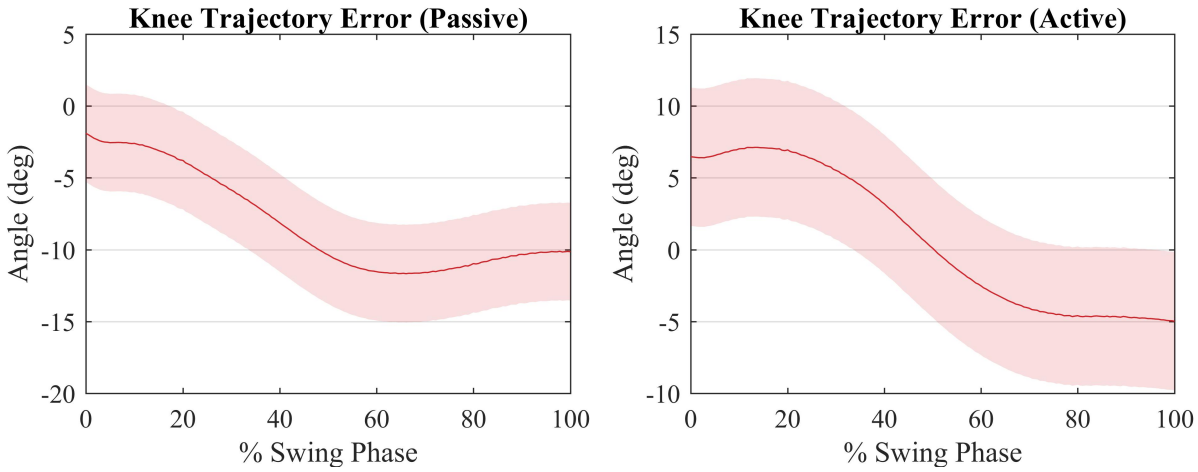

Figure 41 – Error between the average knee joint displacement of the subjects and average knee joint displacement during the procedure to compute the reference values calculation procedure for an active walk (**A**) and a (**B**) passive walk. Shaded regions denote the standard deviation of the measurements.

because even though the subjects produce torque when they walk actively, not always their torques have the exact primitive weights as the reference ones. A better clarification on why the robot acted as such is given further through an analysis of the weights in Appendix A. Therefore, the robot torque is present so that the sum of the subject and the robot torque gets closer to the reference torque value, as in Figure 37.

The trajectory of the hip joint is illustrated in Figure 38 and the trajectory error is illustrated in Figure 10 for an active and passive way of walking. The trajectory is not tracked as accurately when compared to the knee joint due to the lack of activation in this joint, which can be confirmed by analyzing quantitatively in terms of the magnitude of the error. The maximum error of the active trajectory of the hip is 6.37 degrees while the maximum error of the passive trajectory is 8.97 degrees, that is, there is a worsening in the trajectory error of approximately 40% when the subject started to walk passively. This will be reflected in deficient weights in relation to the hip joint and the first primitive engine.

Regarding the trajectory of the knee joint, it can be seen in the Figure 39 that for both walking modes the trajectory is close to the reference, a fact confirmed when analyzing the trajectory error is illustrated in Figure 11. For the active walking mode, the maximum error presented was 8.86 degrees and for the passive mode, it was 7.12 degrees, that is, there was a worsening of approximately 20%. In fact, for the passive walking mode, the trajectory is closer when compared to the active mode, because most of the movement is performed by the robot. During active walking, the user walks at a faster pace and the robot, feeling that the torque of the subject's knee joint is sufficient or greater to perform the movement, is not opposed to the user's movement. This is expected, as the robot should only provide assistance, instead of having the user strictly follow a pre-recorded trajectory.

One can notice that no explicity trajectory or torque tracking is included in the control

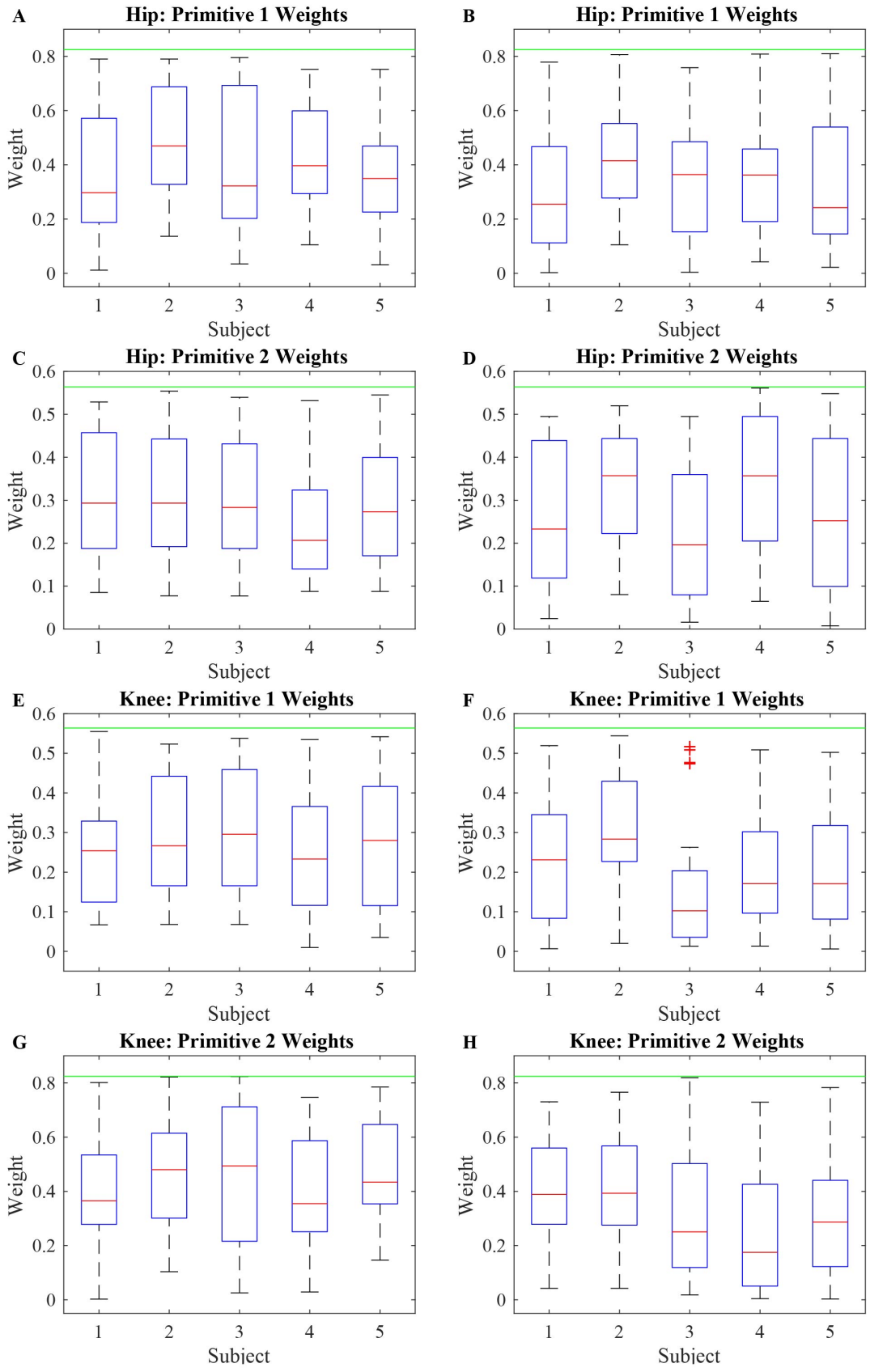

Figure 42 – Boxplot of the absolute value of the defficient weights of five subjects performing two modes of walk: active (left column) and passive (right column).

algorithm. Still, torque and trajectory could still be tracked, indirectly, to a certain extent, so that it matched the reference values.

As the hip joint was not actuated, most hip weights were expected to fall within the range of deficiency. However, due to the knee actuation, the weights of the hip regarding the second primitive were kept at steady values of magnitude during most of the walk.

During the active and passive mode of walk, 58% of the hip weights relative to the first primitive were defficient. With respect to the hip weight relative to the second primitive, during the active walk they were deficient 45% of the test, and, in the passive case, 51%. The knee weights with respect to the first primitive were defficient over 40% of the active walk, as 51% for the passive walk. The knee weights with respect to the second primitive were defficient 53% of the active walk, and 63% of the passive walk. Even though the weights with respect to the knee joint were deficient, the trajectory and torque tracking were ensured by the algorithm. The same is not true with respect to the hip joint, as it was not actuated.

Figure 42 shows the behavior of these weights considered deficient. It is important to analyze the deficient weights with more detail because anything below the threshold value established by the reference value is considered deficient. However, due to the antropomorphic characteristics of each person, if the primitive torques are considered to be the same, the weights must vary in order to account for the gait particularities of each person. It can be noted that most weights during the active phase are located above the median (particularly truth for most subjects in Figures 42 A, C, E and G whereas, for the passive walk, most weights are located below the median, Figure 42 B, or the median values are lower when compared to the Figure beside it, Figures 42 D, F, H.

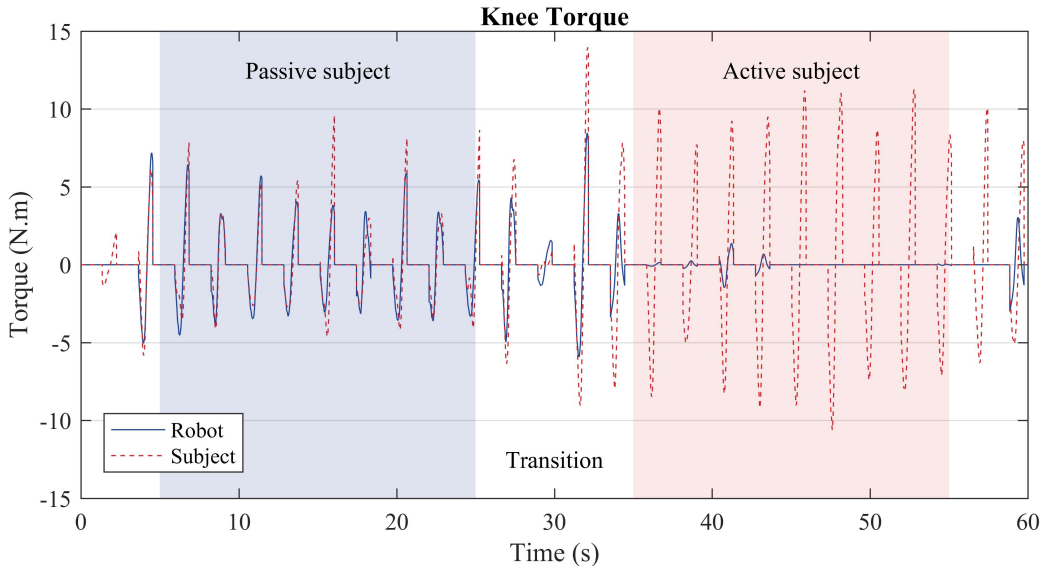

Figure 43 – Subject torque (red dashed lines) and robot torque (solid blue line) in the third test. During the first stage (blue region), the user was instructed to walk passively, i.e. the treadmill slowed down, and the subject prevented from moving more than necessary the knee joint of the right leg.

In the third test the algorithm acted in a way that replicated what was observed in the first and second tests separately. During the transitions, i.e. the white regions of Figure 43, the robot torque is prone to oscillations, as the subject behavior was changing from a passive mode of walk to an active one. Over three to four steps, the robot converges to the expected behavior. During the passive stage (blue region), the robot torque (solid blue line) complements the subject's torque (dashed red line), whereas during the active stage (red region), the robot exerts almost no torque, since the subject is capable of producing the necessary torque by himself.

The hip weights with regards to the first primitives, Figures 42 A and B, presented a behavior similar to the weights of the knee joints regarding the same primitive, Figures 42 E and F. Likewise, there was similarity between the behavior of the hip and knee weights with relation to the second primitive, Figures 42 C and D, and Figures 42 G and H. This shows that the joint weights share characteristics with other joint weights with respect to the same primitives rather than with the weights of the same joint. As a consequence, it can be inferred that the first primitive relates to the hip joint the same way the second primitive relates to the knee joint. Therefore, at the same time it seems rather convenient that the actuation over one joint is capable of propagating its effects over the other joints, which could imply that a smaller number of actuators could be used, the results also suggest that the sole actuation of one joint is not capable of compensating for all weight deficiencies pertaining the actuated joint itself.

The results also show that the sole actuation of the knee could guarantee indirectly, through motor primitive analysis, that the reference joint trajectory was tracked to a certain extent. On the other hand, a position control strategy may not guarantee that the motor primitive weights are close to a reference, though it still may result in functional patient trajectories.

Regarding the convergence and adaptability, the results suggest that the algorithm converges within three to four steps to a steady behavior, once the gait characterists of the subject are analyzed in terms of primitive weights. The robot ceases to actuate once the user produces enough torque, thus sufficient weights, automatically. This ability to adapt guarantees a more comfortable and safe walk, and prevents the scenario in which the subject produces less torque because the robot produces all the necessary torque instead.

The current setup shall be improved in order to extend the results for different modes of walk and before doing tests with impaired individuals. For instance, the actuation of the hip joint is crucial to compensate for weight deficiencies not only at the hip joint, but also at other joints, as concluded with the results exposed here. Extending the number of healthy subjects is important for comparing different motor primitive curves to be used as reference values. The analysis of motor primitives of impaired subjects is also a subject of study, in order to evaluate over therapy how the robotic device assistance affects their

primitives. Moreover, a better comprehension of the motor primitives of an impaired subject may lead to better clues on how to approach the weight deficiency problem. Finally, extensive testing with a greater number of healthy subjects is fundamental to later pursue the validation of the control algorithm with impaired subjects, affected either by stroke, SCI or other types of motor impairments which compromise the lower limbs movement.

Chapter 6

Conclusion

This thesis presents a control algorithm based on motor primitives for a modular lower limbs exoskeleton, in order to aid the rehabilitation of individuals with motor impairment, especially post-stroke victims. First, the influence of the structure of the exoskeleton for lower limbs on the motor primitives during walking on a treadmill was evaluated and the relationships between these primitives and their weights were found in two conditions: with and without the exoskeleton. The kinematic profiles of the lower limbs were evaluated by processing data from 7 IMU sensors attached to the trunk, thigh, shin and foot. Finally, the angular motor primitives were extracted using PCA. After evaluating the influence of the exoskeleton on the angle primitives, the influences of the structure of the exoskeleton on the kinetic and muscular characteristics were evaluated through the relationships between motor primitives and their respective weights for different conditions of use. The EMG signs of five lower limb muscles were measured: rectus femoris (RF), vastus medialis (VM), tibialis anterior (TA), biceps femoris (BF) and gastrocnemius lateralis (GL), and to extract the motor primitives, the Non-negative Matrix Factorization - NMF was used. To estimate the torques the inverse dynamics of OpenSim was used and the primitives of these torque were extracted using the PCA.

And finally, a bio-inspired control algorithm based on motor primitives for the lower limb exoskeleton was proposed, in order to aid the rehabilitation of individuals with motor impairment. In a first step, the motor primitives along with their weights were extracted from four healthy subjects. To perform this task, a torque estimation algorithm together with the Principal Component Analysis were employed. Thereafter, tests with healthy subjects walking on the treadmill wearing the right leg of the exoskeleton were executed to evaluate the controller performance in three different scenarios: when the subject walks actively; when the subject shows some torque deficiency, by walking slower than expected; and when there is a combination of these two cases. In all cases, the algorithm evaluates the motor primitive weights of the current subject comparing them with the weights of a healthy subject (reference). When deficiency is observed, the robot properly exerts a complementary torque during the swing phase, to assist the subject to perform this

movement. It could be noted a relation between weights of different joints with regards to the same primitive. This shows that even though the sole actuation of one joint has influence on the weights of other joints, it is unable to compensate for all the weight deficiencies of the same joint. Moreover, the results suggest that the knee joint trajectory could be tracked indirectly at some extent solely based on the primitive weights analysis. The results showed that the control of primitives was able to adequately adjust the level of assistance of the robot based on user performance and participation.

References

ABDI, H.; WILLIAMS, L. J. Principal component analysis. **Wiley interdisciplinary reviews: computational statistics**, 2010. Wiley Online Library, v. 2, n. 4, p. 433–459, 2010.

ALIBEJI, N. A.; MOLAZADEH, V.; DICIANNO, B. E.; SHARMA, N. A control scheme that uses dynamic postural synergies to coordinate a hybrid walking neuroprosthesis: Theory and experiments. **Frontiers in Neuroscience**, 2018. Frontiers, v. 12, p. 159, 2018.

AN, Q.; ISHIKAWA, Y.; NAKAGAWA, J.; OKA, H.; YAMAKAWA, H.; YAMASHITA, A.; ASAMA, H. Muscle synergy analysis of human standing-up motion with different chair heights and different motion speeds. **2013 IEEE International Conference on Systems, Man, and Cybernetics**, 2013. p. 3579–3584, 2013.

BARBARA, J.; CLARAC, F. Historical concepts on the relations between nerves and muscles. **Brain research**, 2011. Elsevier, v. 1409, p. 3–22, 2011.

BARRECA, S.; WOLF, S. L.; FASOLI, S.; BOHANNON, R. Treatment interventions for the paretic upper limb of stroke survivors: a critical review. **Neurorehabilitation and Neural Repair**, 2003. SAGE Publications, v. 17, n. 4, p. 220–226, 2003.

BARROSO, F. O.; TORRICELLI, D.; MOLINA-RUEDA, F.; ALGUACIL-DIEGO, I. M.; CUERDA, R. Cano-de-la; SANTOS, C.; MORENO, J. C.; MIANGOLARRA-PAGE, J. C.; PONS, J. L. Combining muscle synergies and biomechanical analysis to assess gait in stroke patients. **Journal of Biomechanics**, 2017. Elsevier, v. 63, p. 98–103, 2017.

BARTENBACH, V.; WYSS, D.; SEURET, D.; RIENER, R. A lower limb exoskeleton research platform to investigate human-robot interaction. In: **2015 IEEE International Conference on Rehabilitation Robotics (ICORR), Singapore**. [S.l.: s.n.], 2015. p. 600–605.

BASMAJIAN, J. V.; LUCA, C. D. Muscles fatigue and time-dependent parameters of the surface emg signal. **Muscles alive: their functions revealed by electromyography**, 1985. Williams and Wilkins, v. 278, p. 201–222, 1985.

BAYON, C.; RAMIREZ, O.; SERRANO, J. I.; CASTILLO, M. D.; PÉREZ-SOMARRIBA, A.; BELDA-LOIS, J. M.; MARTÍNEZ-CABALLERO, I.; LERMA-LARA, S.; CIFUENTES, C.; FRIZERA, A. *et al.* Development and evaluation of a

novel robotic platform for gait rehabilitation in patients with cerebral palsy: Cpwalker. **Robotics and Autonomous Systems**, 2017. Elsevier, v. 91, p. 101–114, 2017.

BERGER, D. J.; D'AVELLA, A. Effective force control by muscle synergies. **Frontiers in Computational Neuroscience**, 2014. Frontiers, v. 8, p. 46, 2014.

BERNSTEIN, N. The coordination and regulation of movements: Conclusions towards the study of motor co-ordination. **Biodynamics of Locomotion**, 1967. Pergamon Press 2018: Oxford, p. 104–113, 1967.

BERRY, M. W.; BROWNE, M.; LANGVILLE, A. N.; PAUCA, V. P.; PLEMMONS, R. J. Algorithms and applications for approximate nonnegative matrix factorization. **Computational statistics and data analysis**, 2007. Elsevier, v. 52, n. 1, p. 155–173, 2007.

BIZZI, E.; CHEUNG, V.; D'AVELLA, A.; SALTIEL, P.; TRESCH, M. Combining modules for movement. **Brain Research Reviews**, 2008. Elsevier, v. 57, n. 1, p. 125–133, 2008.

BIZZI, E.; CHEUNG, V. C. The neural origin of muscle synergies. **Frontiers in Computational Neuroscience**, 2013. Frontiers, v. 7, p. 51, 2013.

BRADY, K.; HIDLER, J.; NICHOLS, D.; RYERSON, S. Clinical training and competency guidelines for using robotic devices. In: IEEE. **2011 IEEE International Conference on Rehabilitation Robotics**. [S.l.], 2011. p. 1–5.

BRKIC, L.; SHAW, L.; WIJCK, F. van; FRANCIS, R.; PRICE, C.; FORSTER, A.; LANGHORNE, P.; WATKINS, C.; RODGERS, H. Repetitive arm functional tasks after stroke (raftas): a pilot randomised controlled trial. **Pilot and Feasibility Studies**, 2016. Springer, v. 2, n. 1, p. 1–12, 2016.

CASTLES, S.; HAAS, H. D.; MILLER, M. J. **The age of migration: International population movements in the modern world**. [S.l.]: Palgrave Macmillan: London, UK, 2013.

CHEN, B.; MA, H.; QIN, L.-Y.; GAO, F.; CHAN, K.-M.; LAW, S.-W.; QIN, L.; LIAO, W.-H. Recent developments and challenges of lower extremity exoskeletons. **Journal of Orthopaedic Translation**, 2016. Elsevier, v. 5, p. 26–37, 2016.

CHEUNG, V. C.; PIRON, L.; AGOSTINI, M.; SILVONI, S.; TUROLLA, A.; BIZZI, E. Stability of muscle synergies for voluntary actions after cortical stroke in humans. **Proceedings of the National Academy of Sciences**, 2009. National Acad Sciences, v. 106, n. 46, p. 19563–19568, 2009.

CLANCY, E. A.; BOUCHARD, S.; RANCOURT, D. Estimation and application of emg amplitude during dynamic contractions. **IEEE Engineering in Medicine and Biology Magazine**, 2001. Citeseer, v. 20, n. 6, p. 47–54, 2001.

CLARYS, J. P.; LEWILLIE, L. Clinical and kinesiological electromyography. **Biolocomotion: A Century of Research Using Moving Pictures-Formia. Roma**, 1992. p. 89–114, 1992.

COLOMBO, G.; JOERG, M.; SCHREIER, R.; DIETZ, V. Treadmill training of paraplegic patients using a robotic orthosis. **Journal of Rehabilitation Research and Development**, 2000. Superintendent of Documents, v. 37, n. 6, p. 693, 2000.

CONTRERAS-VIDAL, J. L.; BHAGAT, N. A.; BRANTLEY, J.; CRUZ-GARZA, J. G.; HE, Y.; MANLEY, Q.; NAKAGOME, S.; NATHAN, K.; TAN, S. H.; ZHU, F. *et al.* Powered exoskeletons for bipedal locomotion after spinal cord injury. **Journal of Neural Engineering**, 2016. IOP Publishing, v. 13, n. 3, p. 031001, 2016.

D'AVELLA, A.; SALTIEL, P.; BIZZI, E. Combinations of muscle synergies in the construction of a natural motor behavior. **Nature Neuroscience**, 2003. Nature Publishing Group, v. 6, n. 3, p. 300–308, 2003.

D'AVELLA, A.; TRESCH, M. C. Modularity in the motor system: decomposition of muscle patterns as combinations of time-varying synergies. In: **Advances in Neural Information Processing Systems**. [S.l.: s.n.], 2002. p. 141–148.

DEGALLIER, S.; IJSPEERT, A. Modeling discrete and rhythmic movements through motor primitives: a review. **Biological Cybernetics**, 2010. Springer, v. 103, n. 4, p. 319–338, 2010.

DIAZ, I.; GIL, J. J.; SANCHEZ, E. Lower-limb robotic rehabilitation: literature review and challenges. **Journal of Robotics**, 2011. Hindawi, v. 2011, 2011.

DING, Y.; GALIANA, I.; ASBECK, A.; QUINLIVAN, B.; ROSSI, S. M. M. D.; WALSH, C. Multi-joint actuation platform for lower extremity soft exosuits. In: IEEE. **Robotics and Automation (ICRA), 2014 IEEE International Conference on**. [S.l.], 2014. p. 1327–1334.

DOLLAR, A. M.; HERR, H. Active orthoses for the lower-limbs: challenges and state of the art. In: IEEE. **Rehabilitation Robotics, 2007. ICORR 2007. IEEE 10th International Conference on**. [S.l.], 2007. p. 968–977.

DOLLAR, A. M.; HERR, H. Lower extremity exoskeletons and active orthoses: challenges and state-of-the-art. **IEEE Transactions on robotics**, 2008. v. 24, n. 1, p. 144–158, 2008.

DOS SANTOS, W. M.; CAURIN, G. A.; SIQUEIRA, A. A. Design and control of an active knee orthosis driven by a rotary series elastic actuator. **Control Engineering Practice**, 2017. v. 58, p. 307 – 318, 2017. ISSN 0967-0661.

DOS SANTOS, W. M.; NOGUEIRA, S. L.; OLIVEIRA, G. C. de; PEÑA, G. G.; SIQUEIRA, A. A. Design and evaluation of a modular lower limb exoskeleton for rehabilitation. 2017. p. 447–451, 2017.

DOS SANTOS, W. M.; SIQUEIRA, A. A. Robust torque control based on h infinite criterion of an active knee orthosis. In: IEEE. **5th IEEE RAS/EMBS International Conference on Biomedical Robotics and Biomechatronics**. [S.l.], 2014. p. 644–649.

DOS SANTOS, W. M.; SIQUEIRA, A. A. G. Optimal impedance via model predictive control for robot-aided rehabilitation. **Control Engineering Practice**, 2019. v. 93, p. 1–8, 2019.

DUNCAN, P.; STUDENSKI, S.; RICHARDS, L.; GOLLUB, S.; LAI, S. M.; REKER, D.; PERERA, S.; YATES, J.; KOCH, V.; RIGLER, S. *et al.* Randomized clinical trial of therapeutic exercise in subacute stroke. **Stroke**, 2003. Am Heart Assoc, v. 34, n. 9, p. 2173–2180, 2003.

DUNCAN, P. W. Synthesis of intervention trials to improve motor recovery following stroke. **Topics in Stroke Rehabilitation**, 1997. Taylor and Francis, v. 3, n. 4, p. 1–20, 1997.

DUSCHAU-WICKE, A.; ZITZEWITZ, J. von; CAPREZ, A.; LUNENBURGER, L.; RIENER, R. Path control: a method for patient-cooperative robot-aided gait rehabilitation. **IEEE Transactions on Neural Systems and Rehabilitation Engineering**, 2010. IEEE, v. 18, n. 1, p. 38–48, 2010.

ESQUENAZI, A.; TALATY, M.; PACKEL, A.; SAULINO, M. The rewalk powered exoskeleton to restore ambulatory function to individuals with thoracic-level motor-complete spinal cord injury. **American Journal of Physical Medicine & Rehabilitation**, 2012. LWW, v. 91, n. 11, p. 911–921, 2012.

FAZEKAS, G. Robotics in rehabilitation: Successes and expectations. **International Journal of Rehabilitation Research**, 2013. Wolters Kluwer Health, Lippincott Williams And Wilkins, v. 36, n. 2, p. 95–96, 2013.

FLASH, T.; HOCHNER, B. Motor primitives in vertebrates and invertebrates. **Current Opinion in Neurobiology**, 2005. Elsevier, v. 15, n. 6, p. 660–666, 2005.

FRENCH, B.; THOMAS, L.; LEATHLEY, M.; SUTTON, C.; MCADAM, J.; FORSTER, A.; LANGHORNE, P.; PRICE, C.; WALKER, A.; WATKINS, C. Does repetitive task training improve functional activity after stroke? a cochrane systematic review and meta-analysis. **Journal of rehabilitation medicine**, 2010. Medical Journals Limited, v. 42, n. 1, p. 9–15, 2010.

FRICKE, S. S.; BAYÓN, C.; KOOIJ, H. V. D.; ASSELDONK, E. H. van. Automatic versus manual tuning of robot-assisted gait training in people with neurological disorders. **Journal of Neuroengineering and Rehabilitation**, 2020. Springer, v. 17, n. 1, p. 9, 2020.

FRISOLI, A.; SOLAZZI, M.; LOCONSOLE, C.; BARSOTTI, M. New generation emerging technologies for neurorehabilitation and motor assistance. **Acta Myologica**, 2016. Pacini Editore, v. 35, n. 3, p. 141, 2016.

GARATE, V. R.; PARRI, A.; YAN, T.; MUNIH, M.; LOVA, R. M.; VITIELLO, N.; RONSSE, R. Walking assistance using artificial primitives: a novel bioinspired framework using motor primitives for locomotion assistance through a wearable cooperative exoskeleton. **IEEE Robotics and Automation Magazine**, 2016. v. 23, p. 83–95, 2016.

GARATE, V. R.; PARRI, A.; YAN, T.; MUNIH, M.; LOVA, R. M.; VITIELLO, N.; RONSSE, R. Experimental validation of motor primitive-based control for leg exoskeletons during continuous multi-locomotion tasks. **Frontiers in Neurorobotics**, 2017. Frontiers, v. 11, p. 15, 2017.

GISZTER, S. F. Motor primitives new data and future questions. **Current Opinion in Neurobiology**, 2015. Elsevier, v. 33, p. 156–165, 2015.

GRINYAGIN, I. V.; BIRYUKOVA, E. V.; MAIER, M. A. Kinematic and dynamic synergies of human precision-grip movements. **Journal of Neurophysiology**, 2005. American Physiological Society, v. 94, n. 4, p. 2284–2294, 2005.

GUERRA, J.; UDDIN, J.; NILSEN, D.; MCLNERNEY, J.; FADOO, A.; OMOFUMA, I. B.; HUGHES, S.; AGRAWAL, S.; ALLEN, P.; SCHAMBRA, H. M. Capture, learning, and classification of upper extremity movement primitives in healthy controls and stroke patients. In: IEEE. **2017 International Conference on Rehabilitation Robotics (ICORR)**. [S.l.], 2017. v. 2017, p. 547–554.

GUTIERREZ-MARTINEZ, J.; NUNEZ-GAONA, M.; CARRILLO-MORA, P. Technological advances in neurorehabilitation. **Revista de investigacion clinica; organo del Hospital de Enfermedades de la Nutricion**, 2014. v. 66, p. S8–23, 2014.

HALL, J. E. **Guyton E Hall Tratado De Fisiologia Médica**. [S.l.]: GEN Guanabara Koogan; XIII Edição, 2017.

HART, C. B.; GISZTER, S. F. A neural basis for motor primitives in the spinal cord. **Journal of Neuroscience**, 2010. v. 30, n. 4, p. 1322–1336, 2010.

HATANO, S. Experience from a multicentre stroke register: a preliminary report. **Bulletin of the World Health Organization**, 1976. World Health Organization, v. 54, n. 5, p. 541, 1976.

HESSE, S. Treadmill training with partial body weight support after stroke: a review. **NeuroRehabilitation**, 2008. IOS Press, v. 23, n. 1, p. 55–65, 2008.

HOGAN, N. Physical interaction via dynamic primitives. In: **Geometric and Numerical Foundations of Movements**. [S.l.]: Springer, 2017. p. 269–299.

HOGAN, N.; STERNAD, D. Dynamic primitives of motor behavior. **Biological Cybernetics**, 2012. Springer, v. 106, n. 11-12, p. 727–739, 2012.

HUANG, V. S.; KRAKAUER, J. W. Robotic neurorehabilitation: a computational motor learning perspective. **Journal of Neuroengineering and Rehabilitation**, 2009. BioMed Central, v. 6, n. 1, p. 5, 2009.

IBARRA, J. C. P.; SANTOS, W. M. dos; KREBS, H. I.; SIQUEIRA, A. A. Adaptive impedance control for robot-aided rehabilitation of ankle movements. In: IEEE. **5th IEEE RAS/EMBS International Conference on Biomedical Robotics and Biomechatronics**. [S.l.], 2014. p. 664–669.

IKAI, T.; KAMIKUBO, T.; TAKEHARA, I.; NISHI, M.; MIYANO, S. Dynamic postural control in patients with hemiparesis. **American Journal of Physical Medicine and Rehabilitation**, 2003. LWW, v. 82, n. 6, p. 463–469, 2003.

IVANENKO, Y. P.; POPPELE, R. E.; LACQUANITI, F. Five basic muscle activation patterns account for muscle activity during human locomotion. **The Journal of physiology**, 2004. Wiley Online Library, v. 556, n. 1, p. 267–282, 2004.

JAMES, W. **Psychology, briefer course**. [S.l.]: Harvard University Press, 1984.

JIMENEZ-FABIAN, R.; VERLINDEN, O. Review of control algorithms for robotic ankle systems in lower-limb orthoses, prostheses, and exoskeletons. **Medical Engineering & Physics**, 2012. Elsevier, v. 34, n. 4, p. 397–408, 2012.

JUTINICO, A. L.; JAIMES, J. C.; ESCALANTE, F. M.; PEREZ-IBARRA, J. C.; TERRA, M. H.; SIQUEIRA, A. A. Impedance control for robotic rehabilitation: A robust markovian approach. **Frontiers in Neurorobotics**, 2017. Frontiers, v. 11, p. 43, 2017.

KARGO, W. J.; GISZTER, S. F. Individual premotor drive pulses, not time-varying synergies, are the units of adjustment for limb trajectories constructed in spinal cord. **Journal of Neuroscience**, 2008. Soc Neuroscience, v. 28, n. 10, p. 2409–2425, 2008.

KAZEROONI, H.; RACINE, J.-L.; HUANG, L.; STEGER, R. On the control of the berkeley lower extremity exoskeleton (bleex). In: IEEE. **Proceedings of the 2005 IEEE International Conference on Robotics and Automation**. [S.l.], 2005. p. 4353–4360.

KLEIM, J. A.; JONES, T. A. Principles of experience-dependent neural plasticity: implications for rehabilitation after brain damage. **Journal of Speech, Language, and Hearing Research**, 2008. ASHA, v. 51, n. 1, p. S225–S239, 2008.

KOBAYASHI, T.; SINGER, M. L.; ORENDURFF, M. S.; GAO, F.; DALY, W. K.; FOREMAN, K. B. The effect of changing plantarflexion resistive moment of an articulated ankle–foot orthosis on ankle and knee joint angles and moments while walking in patients post stroke. **Clinical Biomechanics**, 2015. Elsevier, v. 30, n. 8, p. 775–780, 2015.

KONG, K.; TOMIZUKA, M. Control of exoskeletons inspired by fictitious gain in human model. **IEEE/ASME Transactions on Mechatronics**, 2009. IEEE, v. 14, n. 6, p. 689–698, 2009.

KREBS, H. I.; DIPIETRO, L.; LEVY-TZEDEK, S.; FASOLI, S. E.; RYKMAN-BERLAND, A.; ZIPSE, J.; FAWCETT, J. A.; STEIN, J.; POIZNER, H.; LO, A. C. *et al.* A paradigm shift for rehabilitation robotics. **IEEE Engineering in Medicine and Biology Magazine**, 2008. v. 27, n. 4, p. 61–70, 2008.

KWAKKEL, G.; KOLLEN, B. J.; KREBS, H. I. Effects of robot-assisted therapy on upper limb recovery after stroke: a systematic review. **Neurorehabilitation and Neural Repair**, 2008. SAGE Publications Sage CA: Los Angeles, CA, v. 22, n. 2, p. 111–121, 2008.

KWAKKEL, G.; WAGENAAR, R. C.; KOELMAN, T. W.; LANKHORST, G. J.; KOETSIER, J. C. Effects of intensity of rehabilitation after stroke: a research synthesis. **Stroke**, 1997. Am Heart Assoc, v. 28, n. 8, p. 1550–1556, 1997.

KWAKKEL, G.; WAGENAAR, R. C.; TWISK, J. W.; LANKHORST, G. J.; KOETSIER, J. C. Intensity of leg and arm training after primary middle-cerebral-artery stroke: a randomised trial. **The Lancet**, 1999. Elsevier, v. 354, n. 9174, p. 191–196, 1999.

LAMBERT-SHIRZAD, N.; LOOS, H. M. Van der. Data sample size needed for analysis of kinematic and muscle synergies in healthy and stroke populations. In: IEEE. **Rehabilitation Robotics (ICORR), 2017 International Conference on**. [S.l.], 2017. p. 777–782.

LAMBRECHT, S.; NOGUEIRA, S. L.; BORTOLE, M.; SIQUEIRA, A. A.; TERRA, M. H.; ROCON, E.; PONS, J. L. Inertial sensor error reduction through calibration and sensor fusion. **Sensors**, 2016. Multidisciplinary Digital Publishing Institute, v. 16, n. 2, p. 235, 2016.

LANGHORNE, P.; BERNHARDT, J.; KWAKKEL, G. Stroke rehabilitation. **The Lancet**, 2011. Elsevier, v. 377, n. 9778, p. 1693–1702, 2011.

LEMAY, M. A.; CALAGAN, J.; HOGAN, N.; BIZZI, E. Modulation and vectorial summation of the spinalized frog's hindlimb end-point force produced by intraspinal electrical stimulation of the cord. **IEEE Transactions on Neural Systems and Rehabilitation Engineering**, 2001. IEEE, v. 9, n. 1, p. 12–23, 2001.

LI, S.; ZHUANG, C.; NIU, C. M.; BAO, Y.; XIE, Q.; LAN, N. Evaluation of functional correlation of task-specific muscle synergies with motor performance in patients poststroke. **Frontiers in Neurology**, 2017. Frontiers, v. 8, p. 337, 2017.

LI, Z.; HAYASHIBE, M.; GUIRAUD, D. Forward estimation of joint torque from emg signal through muscle synergy combinations. 2013. p. 806–809, 2013.

LLOYD, D. G.; BESIER, T. F. An emg-driven musculoskeletal model to estimate muscle forces and knee joint moments in vivo. **Journal of Biomechanics**, 2003. Elsevier, v. 36, n. 6, p. 765–776, 2003.

LOZANO, R.; NAGHAVI, M.; FOREMAN, K.; LIM, S.; SHIBUYA, K.; ABOYANS, V.; ABRAHAM, J.; ADAIR, T.; AGGARWAL, R.; AHN, S. Y. *et al.* Global and regional mortality from 235 causes of death for 20 age groups in 1990 and 2010: a systematic analysis for the global burden of disease study 2010. **The Lancet**, 2012. Elsevier, v. 380, n. 9859, p. 2095–2128, 2012.

LUCA, C. J. D. Physiology and mathematics of myoelectric signals. **IEEE Transactions on Biomedical Engineering**, 1979. IEEE, n. 6, p. 313–325, 1979.

LUCA, C. J. D. The use of surface electromyography in biomechanics. **Journal of Applied Biomechanics**, 1997. v. 13, n. 2, p. 135–163, 1997.

LUCAS, K. The all or none contraction of the amphibian skeletal muscle fibre. **The Journal of Physiology**, 1909. Wiley Online Library, v. 38, n. 2-3, p. 113–133, 1909.

LUM, P.; REINKENSMEYER, D.; MAHONEY, R.; RYMER, W. Z.; BURGAR, C. Robotic devices for movement therapy after stroke: current status and challenges to clinical acceptance. **Topics in stroke rehabilitation**, 2002. Taylor and Francis, v. 8, n. 4, p. 40–53, 2002.

MACKAY, J.; MENSAH, G. A.; GREENLUND, K. **The atlas of heart disease and stroke**. [S.l.]: World Health Organization: Geneva, Switzerland, 2004.

MACKO, R. F. Short-term ankle motor performance with ankle robotics training in chronic hemiparetic stroke. **Journal of Rehabilitation Research and Development**, 2011. Superintendent of Documents, v. 48, n. 4, p. 417, 2011.

MAGGIONI, S.; REINERT, N.; LÜNENBURGER, L.; MELENDEZ-CALDERON, A. An adaptive and hybrid end-point/joint impedance controller for lower limb exoskeletons. **Frontiers in Robotics and AI**, 2018. Frontiers, v. 5, p. 104, 2018.

MANG, C. S.; CAMPBELL, K. L.; ROSS, C. J.; BOYD, L. A. Promoting neuroplasticity for motor rehabilitation after stroke: considering the effects of aerobic exercise and genetic variation on brain-derived neurotrophic factor. **Physical therapy**, 2013. Oxford University Press, v. 93, n. 12, p. 1707–1716, 2013.

MEHRHOLZ, J.; HADRICH, A.; PLATZ, T.; KUGLER, J.; POHL, M. Electromechanical and robot-assisted arm training for improving generic activities of daily living, arm function, and arm muscle strength after stroke. **Cochrane Database Syst Rev**, 2012. Wiley Online Library, v. 6, n. 6, 2012.

MEHRHOLZ, J.; POHL, M.; PLATZ, T.; KUGLER, J.; ELSNER, B. Electromechanical and robot-assisted arm training for improving activities of daily living, arm function, and arm muscle strength after stroke. **The Cochrane Library**, 2015. Wiley Online Library, 2015.

MEHRHOLZ SIMONE THOMAS, C. W. J. K. M. P. B. E. Electromechanical-assisted training for walking after stroke. **The Cochrane Library**, 2017. Wiley Online Library, 2017.

MOSCONI, D.; NUNES, P. F.; SIQUEIRA, A. A. G. Modeling and control of an active knee orthosis using a computational model of the musculoskeletal system. **Journal of Mechatronics Engineering**, 2018. v. 1, n. 3, p. 12–19, 2018.

MURRAY, C. J.; BARBER, R. M.; FOREMAN, K. J.; OZGOREN, A. A.; ABD-ALLAH, F.; ABERA, S. F.; ABOYANS, V.; ABRAHAM, J. P.; ABUBAKAR, I.; ABU-RADDAD, L. J. *et al.* Global, regional, and national disability-adjusted life years (dalys) for 306 diseases and injuries and healthy life expectancy (hale) for 188 countries, 1990–2013: quantifying the epidemiological transition. **The Lancet**, 2015. Elsevier, v. 386, n. 10009, p. 2145–2191, 2015.

MURRAY, C. J.; VOS, T.; LOZANO, R.; NAGHAVI, M.; FLAXMAN, A. D.; MICHAUD, C.; EZZATI, M.; SHIBUYA, K.; SALOMON, J. A.; ABDALLA, S. *et al.* Disability-adjusted life years (dalys) for 291 diseases and injuries in 21 regions, 1990–2010: a systematic analysis for the global burden of disease study 2010. **The lancet**, 2012. Elsevier, v. 380, n. 9859, p. 2197–2223, 2012.

NAH, M. C.; KROTOV, A.; RUSSO, M.; STERNAD, D.; HOGAN, N. Dynamic primitives facilitate manipulating a whip. In: IEEE. **2020 8th IEEE RAS/EMBS International Conference for Biomedical Robotics and Biomechatronics (BioRob)**. [S.l.], 2020. p. 685–691.

NOGUEIRA, S. L.; LAMBRECHT, S.; INOUE, R. S.; BORTOLE, M.; MONTAGNOLI, A. N.; MORENO, J. C.; ROCON, E.; TERRA, M. H.; SIQUEIRA, A. A.; PONS, J. L. Global kalman filter approaches to estimate absolute angles of lower limb segments. **Biomedical Engineering Online**, 2017. Springer, v. 16, n. 1, p. 58, 2017.

NOGUEIRA, S. L.; SIQUEIRA, A. A.; INOUE, R. S.; TERRA, M. H. Markov jump linear systems-based position estimation for lower limb exoskeletons. **Sensors**, 2014. Multidisciplinary Digital Publishing Institute, v. 14, n. 1, p. 1835–1849, 2014.

NUNES, P. F.; OSTAN, I.; SANTOS, W. M. d.; SIQUEIRA, A. A. Analysis of matrix factorization techniques for extraction of motion motor primitives. 2020. **XXVII Edição do Congresso Brasileiro de Engenharia Biomédica - CBEB**. Espírito Santo, Brazil, p. 1–9, 2020.

NUNES, P. F.; OSTAN, I.; SIQUEIRA, A. A. Evaluation of motor primitive-based adaptive control for lower limb exoskeletons. **Frontiers in Robotics and AI**, 2020. Frontiers, v. 7, p. 201, 2020.

NUNES P. F.; SANTOS, W. M. d.; SIQUEIRA, A. A. G. Influence of an exoskeleton on kinetic characteristics and muscles during the march using motion primitives. 2018. **Procceedings of the 6th Encontro Nacional de Engenharia Biomecânica.**, p. 1–7, 2018.

OLSON, W. H. Basic concepts of medical instrumentation. **Medical Instrumentation Application and Design**, 1998. p. 1–55, 1998.

ORGANIZATION, W. H. **World health statistics 2015**. [S.l.]: World Health Organization, 2015.

PATTON, J. L.; MUSSA-IVALDI, F. A. Robot-assisted adaptive training: custom force fields for teaching movement patterns. **IEEE Transactions on Biomedical Engineering**, 2004. IEEE, v. 51, n. 4, p. 636–646, 2004.

PEKNA, M.; PEKNY, M.; NILSSON, M. Modulation of neural plasticity as a basis for stroke rehabilitation. **Stroke**, 2012. Am Heart Assoc, v. 43, n. 10, p. 2819–2828, 2012.

PEÑA, G. G.; CONSONI, L. J.; SANTOS, W. M. dos; SIQUEIRA, A. A. Feasibility of an optimal emg-driven adaptive impedance control applied to an active knee orthosis. **Robotics and Autonomous Systems**, 2019. Elsevier, v. 112, p. 98–108, 2019.

PEPPEN, R. P. V.; KWAKKEL, G.; WOOD-DAUPHINEE, S.; HENDRIKS, H. J.; WEES, P. J. Van der; DEKKER, J. The impact of physical therapy on functional outcomes after stroke: what's the evidence? **Clinical Rehabilitation**, 2004. SAGE Publications Sage CA: Thousand Oaks, CA, v. 18, n. 8, p. 833–862, 2004.

PEREZ-IBARRA, J. C.; SIQUEIRA, A. A.; SILVA-COUTO, M. A.; RUSSO, T. L. de; KREBS, H. I. Adaptive impedance control applied to robot-aided neuro-rehabilitation of the ankle. **IEEE Robotics and Automation Letters**, 2018. IEEE, v. 4, n. 2, p. 185–192, 2018.

PERSON, K. On lines and planes of closest fit to system of points in space. **Philiosophical Magazine**, 1901. v. 2, p. 559–572, 1901.

PORT, I. G. van de; WOOD-DAUPHINEE, S.; LINDEMAN, E.; KWAKKEL, G. Effects of exercise training programs on walking competency after stroke: a systematic review. **American Journal of Physical Medicine and Rehabilitation**, 2007. LWW, v. 86, n. 11, p. 935–951, 2007.

PRANGE, G. B.; JANNINK, M. J.; GROOTHUIS-OUDSHOORN, C. G.; HERMENS, H. J.; IJZERMAN, M. J. Systematic review of the effect of robot-aided therapy on recovery of the hemiparetic arm after stroke. **Journal of rehabilitation research and development**, 2006. Superintendent of Documents, v. 43, n. 2, p. 171, 2006.

RICHARDS, L.; POHL, P. Therapeutic interventions to improve upper extremity recovery and function. **Clinics in geriatric medicine**, 1999. v. 15, n. 4, p. 819–832, 1999.

ROBINSON, C. A.; SHUMWAY-COOK, A.; CIOL, M. A.; KARTIN, D. Participation in community walking following stroke: subjective versus objective measures and the impact of personal factors. **Physical Therapy**, 2011. Oxford University Press, v. 91, n. 12, p. 1865–1876, 2011.

ROH, J.; RYMER, W. Z.; BEER, R. F. Evidence for altered upper extremity muscle synergies in chronic stroke survivors with mild and moderate impairment. **Frontiers in Human Neuroscience**, 2015. Frontiers, v. 9, p. 6, 2015.

ROHRER, B.; FASOLI, S.; KREBS, H. I.; HUGHES, R.; VOLPE, B.; FRONTERA, W. R.; STEIN, J.; HOGAN, N. Movement smoothness changes during stroke recovery. **Journal of Neuroscience**, 2002. Soc Neuroscience, v. 22, n. 18, p. 8297–8304, 2002.

RONSSE, R.; ROSSI, S. M. M. D.; VITIELLO, N.; LENZI, T.; CARROZZA, M. C.; IJSPEERT, A. J. Real-time estimate of velocity and acceleration of quasi-periodic signals using adaptive oscillators. **IEEE Transactions on Robotics**, 2013. IEEE, v. 29, n. 3, p. 783–791, 2013.

RONSSE, R.; VITIELLO, N.; LENZI, T.; KIEBOOM, J. van den; CARROZZA, M. C.; IJSPEERT, A. J. Human–robot synchrony: flexible assistance using adaptive oscillators. **IEEE Transactions on Biomedical Engineering**, 2011. IEEE, v. 58, n. 4, p. 1001–1012, 2011.

ROY, A.; KREBS, H. I.; BEVER, C. T.; FORRESTER, L. W.; MACKO, R. F.; HOGAN, N. Measurement of passive ankle stiffness in subjects with chronic hemiparesis using a novel ankle robot. **Journal of Neurophysiology**, 2011. Am Physiological Soc, v. 105, n. 5, p. 2132–2149, 2011.

ROY, A.; KREBS, H. I.; WILLIAMS, D. J.; BEVER, C. T.; FORRESTER, L. W.; MACKO, R. M.; HOGAN, N. Robot-aided neurorehabilitation: a novel robot for ankle rehabilitation. **IEEE Transactions on Robotics**, 2009. IEEE, v. 25, n. 3, p. 569–582, 2009.

SALTIEL, P.; WYLER-DUDA, K.; D'AVELLA, A.; TRESCH, M. C.; BIZZI, E. Muscle synergies encoded within the spinal cord: evidence from focal intraspinal nmda iontophoresis in the frog. **Journal of Neurophysiology**, 2001. American Physiological Society Bethesda, MD, v. 85, n. 2, p. 605–619, 2001.

SANKAI, Y. Hal: Hybrid assistive limb based on cybernics. In: **Robotics Research**. [S.l.]: Springer, 2010. p. 25–34.

SANTELLO, M.; BAUD-BOVY, G.; JORNTELL, H. Neural bases of hand synergies. **Frontiers in Computational Neuroscience**, 2013. Frontiers, v. 7, p. 23, 2013.

SANTOS, J.; PALHANO, R.; DETÃ¢NICO, R.; HAUPENTHAL, A.; MELO, S.; ANDRADE, M.; AVILA, A. Análise das variáveis cinéticas da marcha em duas diferentes velocidades. **Tecnicouro**, 2007. v. 28, p. 46–9, 2007.

SARTORI, M.; LLYOD, D. G.; FARINA, D. Neural data-driven musculoskeletal modeling for personalized neurorehabilitation technologies. **IEEE Transactions on Biomedical Engineering**, 2016. IEEE, v. 63, n. 5, p. 879–893, 2016.

SCHAAL, S.; SCHWEIGHOFER, N. Computational motor control in humans and robots. **Current Opinion in Neurobiology**, 2005. Elsevier, v. 15, n. 6, p. 675–682, 2005.

SHERRINGTON, C. S. *et al.* Remarks on some aspects of reflex inhibition. **Proc. R. Soc. Lond. B**, 1925. The Royal Society, v. 97, n. 686, p. 519–545, 1925.

SMITH, L. I. A tutorial on principal components analysis. 2002. Cornell University. USA, February, v. 51, n. 52, p. 21–28, 2002.

SOMMERFELD, D. K.; EEK, E. U.-B.; SVENSSON, A.-K.; HOLMQVIST, L. W.; ARBIN, M. H. von. Spasticity after stroke: its occurrence and association with motor impairments and activity limitations. **Stroke**, 2004. Am Heart Assoc, v. 35, n. 1, p. 134–139, 2004.

SQUIRE, L.; BERG, D.; BLOOM, F. E.; LAC, S. D.; GHOSH, A.; SPITZER, N. C. **Fundamental neuroscience**. [S.l.]: Academic Press, 2012.

STANDRING, S. **Anatomia del Gray. Le basi anatomiche per la pratica clinica**. [S.l.]: Elsevier srl, 2009.

STEELE, K. M.; TRESCH, M. C.; PERREAULT, E. J. The number and choice of muscles impact the results of muscle synergy analyses. **Frontiers in Computational Neuroscience**, 2013. Frontiers, v. 7, p. 105, 2013.

STEIN, J. Robotics in rehabilitation: technology as destiny. **American Journal of Physical Medicine & Rehabilitation**, 2012. Wolters Kluwer, v. 91, p. S199–S203, 2012.

STEPHENSON, A.; STEPHENS, J. An exploration of physiotherapists experiences of robotic therapy in upper limb rehabilitation within a stroke rehabilitation centre. **Disability and Rehabilitation: Assistive Technology**, 2017. Taylor and Francis, p. 1–8, 2017.

STEULTJENS, E. M.; DEKKER, J.; BOUTER, L. M.; NES, J. C. van de; CUP, E. H.; ENDE, C. H. van den; LANDI, F.; BERNABEI, R. Occupational therapy for stroke patients: When, where, and how? **Stroke**, 2003. Am Heart Assoc, v. 34, n. 3, p. 676–687, 2003.

STUART, D. G.; BROWNSTONE, R. M. The beginning of intracellular recording in spinal neurons: facts, reflections, and speculations. **Brain research**, 2011. Elsevier, v. 1409, p. 62–92, 2011.

SYLOS-LABINI, F.; SCALEIA, V. L.; D'AVELLA, A.; PISOTTA, I.; TAMBURELLA, F.; SCIVOLETTO, G.; MOLINARI, M.; WANG, S.; WANG, L.; ASSELDONK, E. van *et al.* Emg patterns during assisted walking in the exoskeleton. **Frontiers in Human Neuroscience**, 2014. Frontiers, v. 8, p. 423, 2014.

TEASELL, R. W.; FOLEY, N. C.; BHOGAL, S. K.; SPEECHLEY, M. R. An evidence-based review of stroke rehabilitation. **Topics in Stroke Rehabilitation**, 2003. Taylor and Francis, v. 10, n. 1, p. 29–58, 2003.

THELEN, D. G. Adjustment of muscle mechanics model parameters to simulate dynamic contractions in older adults. **Journal of Biomechanical Engineering**, 2003. American Society of Mechanical Engineers, v. 125, n. 1, p. 70–77, 2003.

TING, L. H.; CHIEL, H. J.; TRUMBOWER, R. D.; ALLEN, J. L.; MCKAY, J. L.; HACKNEY, M. E.; KESAR, T. M. Neuromechanical principles underlying movement modularity and their implications for rehabilitation. **Neuron**, 2015. v. 86, n. 1, p. 38 – 54, 2015. ISSN 0896-6273.

TRESCH, M. C.; SALTIEL, P.; BIZZI, E. The construction of movement by the spinal cord. **Nature Neuroscience**, 1999. Nature Publishing Group, v. 2, n. 2, p. 162, 1999.

TURVEY, M. T. Action and perception at the level of synergies. **Human Movement Science**, 2007. Elsevier, v. 26, n. 4, p. 657–697, 2007.

VERGHESE, J.; LEVALLEY, A.; HALL, C. B.; KATZ, M. J.; AMBROSE, A. F.; LIPTON, R. B. Epidemiology of gait disorders in community-residing older adults. **Journal of the American Geriatrics Society**, 2006. Wiley Online Library, v. 54, n. 2, p. 255–261, 2006.

WANG, L.; WANG, S.; ASSELDONK, E. H. van; KOOIJ, H. van der. Actively controlled lateral gait assistance in a lower limb exoskeleton. In: IEEE. **Intelligent Robots and Systems (IROS), 2013 IEEE/RSJ International Conference on**. [S.l.], 2013. p. 965–970.

WEVERS, L.; PORT, I. V. D.; VERMUE, M.; MEAD, G.; KWAKKEL, G. Effects of task-oriented circuit class training on walking competency after stroke: a systematic review. **Stroke**, 2009. Am Heart Assoc, v. 40, n. 7, p. 2450–2459, 2009.

WIELOCH, T.; NIKOLICH, K. Mechanisms of neural plasticity following brain injury. **Current Opinion in Neurobiology**, 2006. Elsevier, v. 16, n. 3, p. 258–264, 2006.

WOLDAG, H.; HUMMELSHEIM, H. Evidence-based physiotherapeutic concepts for improving arm and hand function in stroke patients. **Journal of Neurology**, 2002. Springer, v. 249, n. 5, p. 518–528, 2002.

YAN, T.; CEMPINI, M.; ODDO, C. M.; VITIELLO, N. Review of assistive strategies in powered lower-limb orthoses and exoskeletons. **Robotics and Autonomous Systems**, 2015. Elsevier, v. 64, p. 120–136, 2015.

YANG, N.; AN, Q.; YAMAKAWA, H.; TAMURA, Y.; YAMASHITA, A.; TAKAHASHI, K.; KINOMOTO, M.; YAMASAKI, H.; ITKONEN, M.; ALNAJJAR, F. *et al.* Clarification of muscle synergy structure during standing-up motion of healthy young, elderly and post-stroke patients. In: IEEE. **Rehabilitation Robotics (ICORR), 2017 International Conference on**. [S.l.], 2017. p. 19–24.

YANG, Z.; ZHU, Y.; YANG, X.; ZHANG, Y. Impedance control of exoskeleton suit based on adaptive rbf neural network. In: IEEE. **Intelligent Human-Machine Systems and Cybernetics, 2009. IHMSC'09. International Conference on**. [S.l.], 2009. v. 1, p. 182–187.

ZOSS, A. B.; KAZEROONI, H.; CHU, A. Biomechanical design of the berkeley lower extremity exoskeleton (bleex). **IEEE/ASME Transactions On Mechatronics**, 2006. IEEE, v. 11, n. 2, p. 128–138, 2006.

Appendix

Appendix A

The Figures below represent the values of hip and knee weights during the emulation of paretic and non-paretic walking, in relation to the first and second primitives of the 50 steps of the walk. The gray region represents the range of values over which the weights are considered impaired and the dotted lines have the upper and lower limits, which are limited by the value of the reference weight and its counterpart of the opposite sign. Blue crosses represent healthy weights, those with a magnitude equal to or greater than the reference weights and in the same direction. The red crosses are the deficient weights, which are below the absolute reference value, regardless of the direction and finally, the green crosses represent the moments of lack of synchrony between the subject's walk and the gait phase detection algorithm. Whenever there was a lack of synchrony, that is, the weights of the subjects with a sign opposite the reference values and with greater magnitude, it means that the robot acted in order to reduce them.

During the non-paretic walking mode, the robot produces less torque compared to the paretic walking mode, however, the robot's torque is still present, as shown in Figure 38, because although the subjects produce torque when they walk actively, not always their torques have the exact weights as the reference. This can be analyzed in subject 1, primitive 1 related to the hip, Figure 44A, in its paretic mode presented deficient weights, weights below the reference value, for 30 steps while in the non-paretic mode, Figures 48A, deficient weights were found in 23 stages of the walk. Therefore, in the active mode there was a reduction in degeneration in 7 steps and the asynchrony was also reduced by 50%. In primitive 2 related to the knee of subject 1, there was also a reduction in degeneration from 32, Figure 44D, to 26 steps, Figure 48D, during the walk. Similar results to that of subject 1, were found in all other subjects.

It is important to note that in the weights of other subjects, both the knee (joint acted) and the hip (joint not acted) showed less degradation in passive walking. This result (less deficient weights and more healthy weights) was expected for the knee joint for having the actuator, but in relation to the hip joint it was not expected. This shows that the weights of a joint can share characteristics with other weights of other joints with respect to the same primitives. Therefore, it seems quite convenient that the actuation on one

joint is able to propagate its reach over the other joints, which could imply that a smaller number of actuators could be used, however the results also showed that the actuation of a single joint is not able to compensate for all the weight deficiencies pertaining to the actuated joint itself.

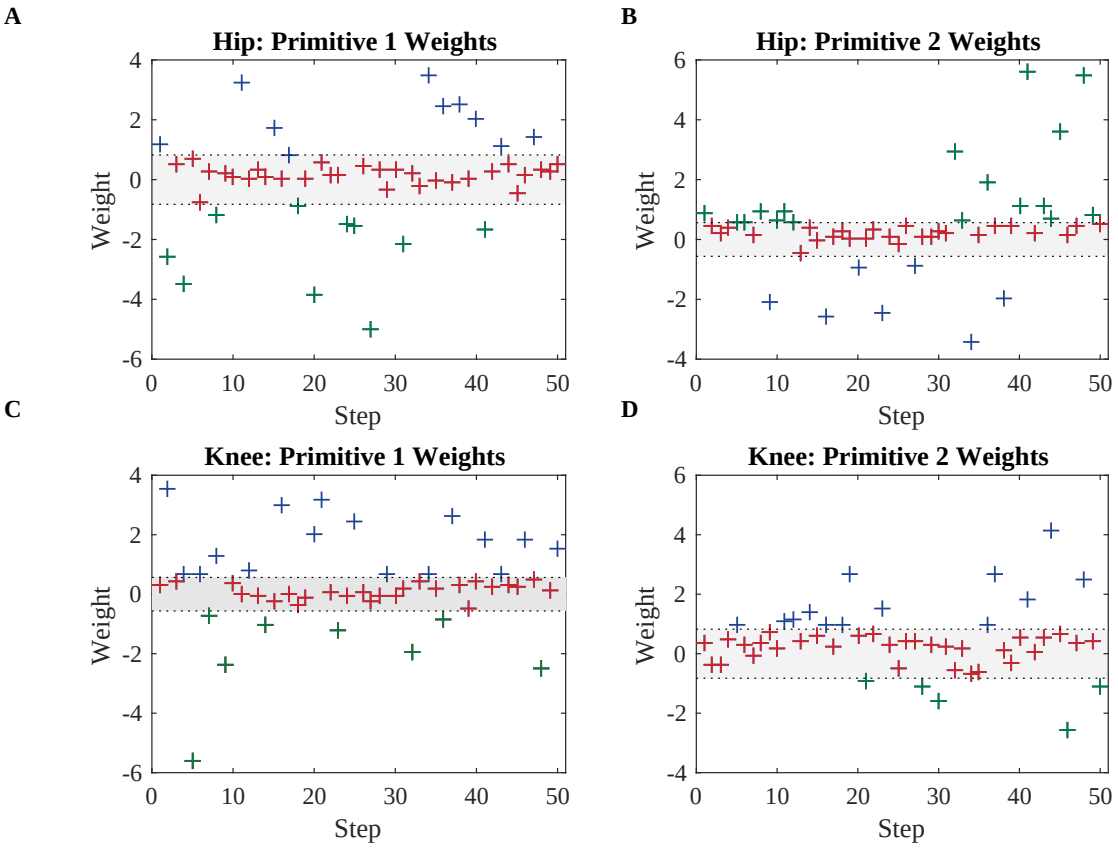

Figure 44 – Hip and knee weight values during the emulation of a paretic walk, of subject 1, with relation to the first and second hip and knee primitives.

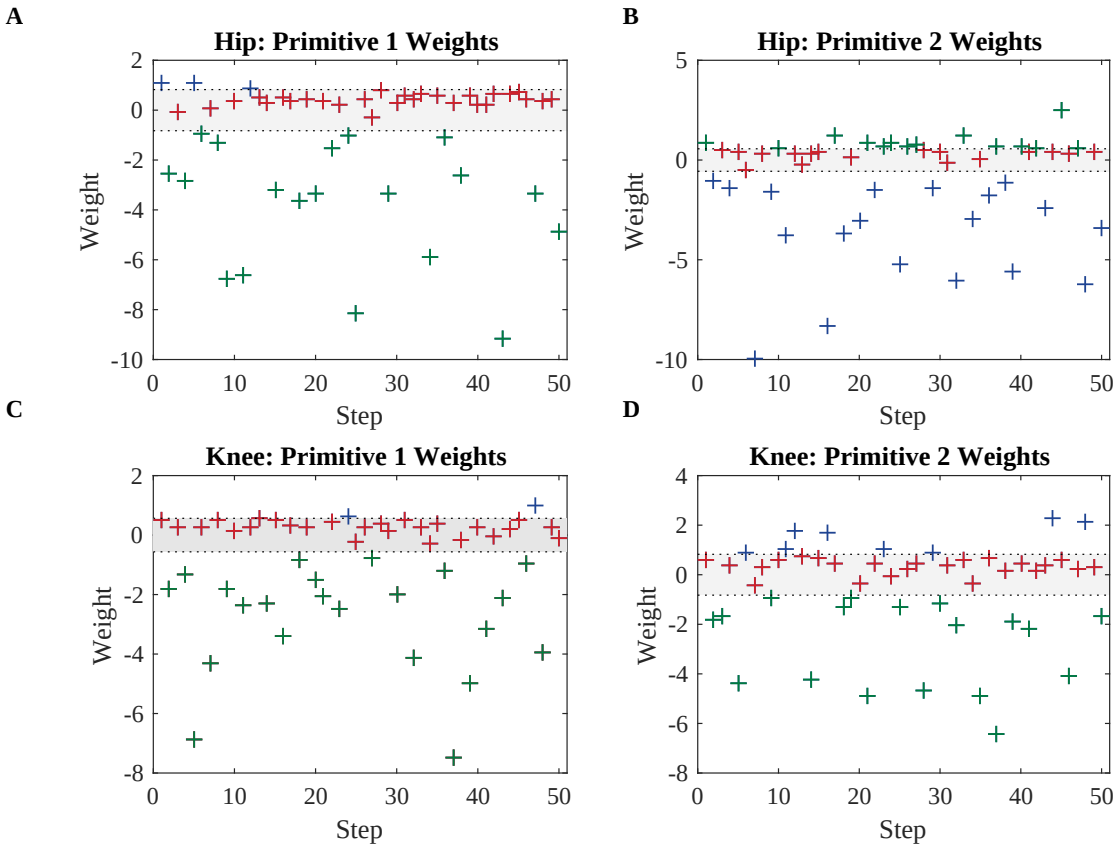

Figure 45 – Hip and knee weight values during the emulation of a paretic walk, of subject 2, with relation to the first and second hip and knee primitives.

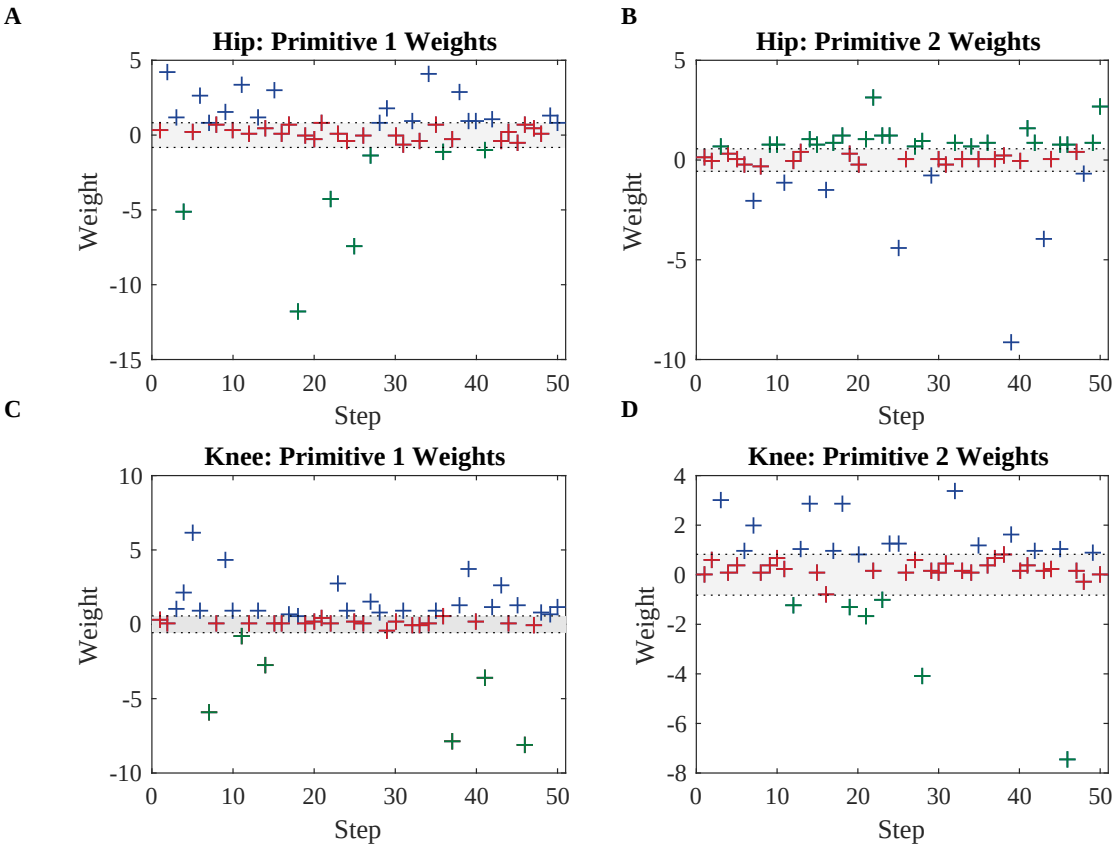

Figure 46 – Hip and knee weight values during the emulation of a paretic walk, of subject 3, with relation to the first and second hip and knee primitives.

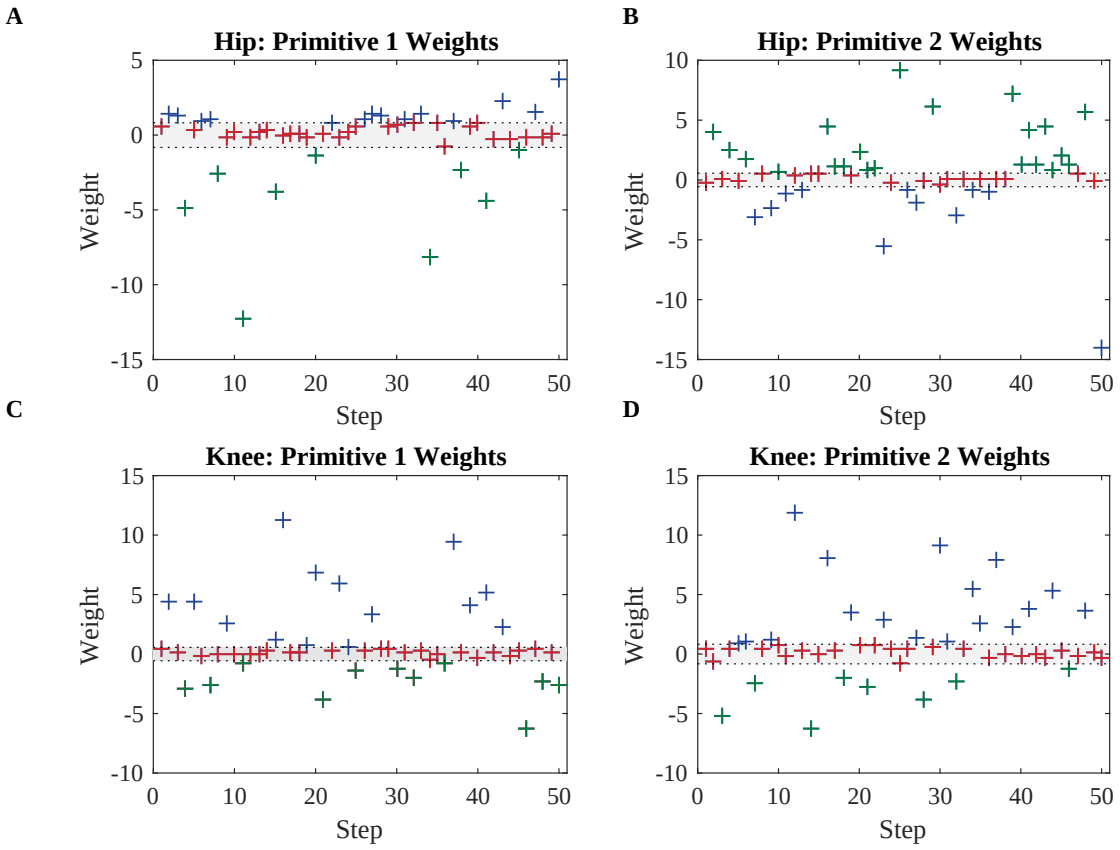

Figure 47 – Hip and knee weight values during the emulation of a paretic walk, of subject 5, with relation to the first and second hip and knee primitives.

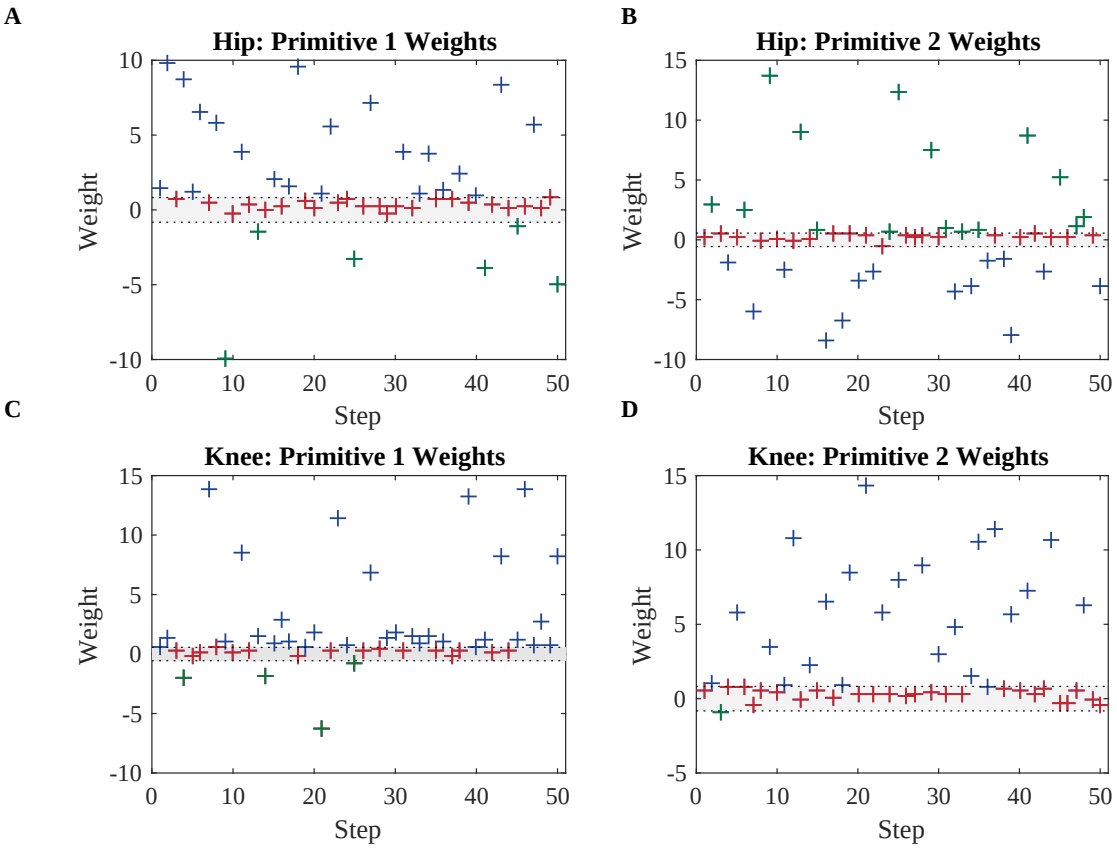

Figure 48 – Hip and knee weight values during the emulation of a non-paretic walk, of subject 1, with relation to the first and second hip and knee primitives.

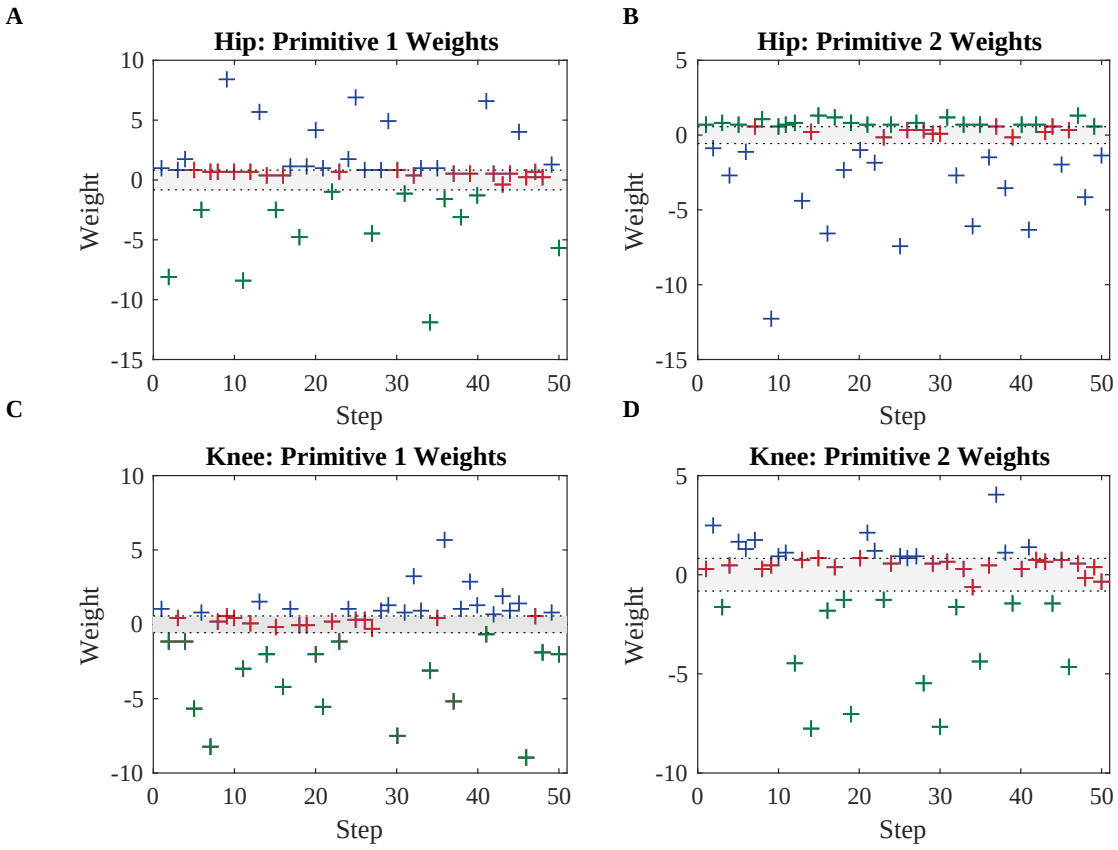

Figure 49 – Hip and knee weight values during the emulation of a non-paretic walk, of subject 2, with relation to the first and second hip and knee primitives.

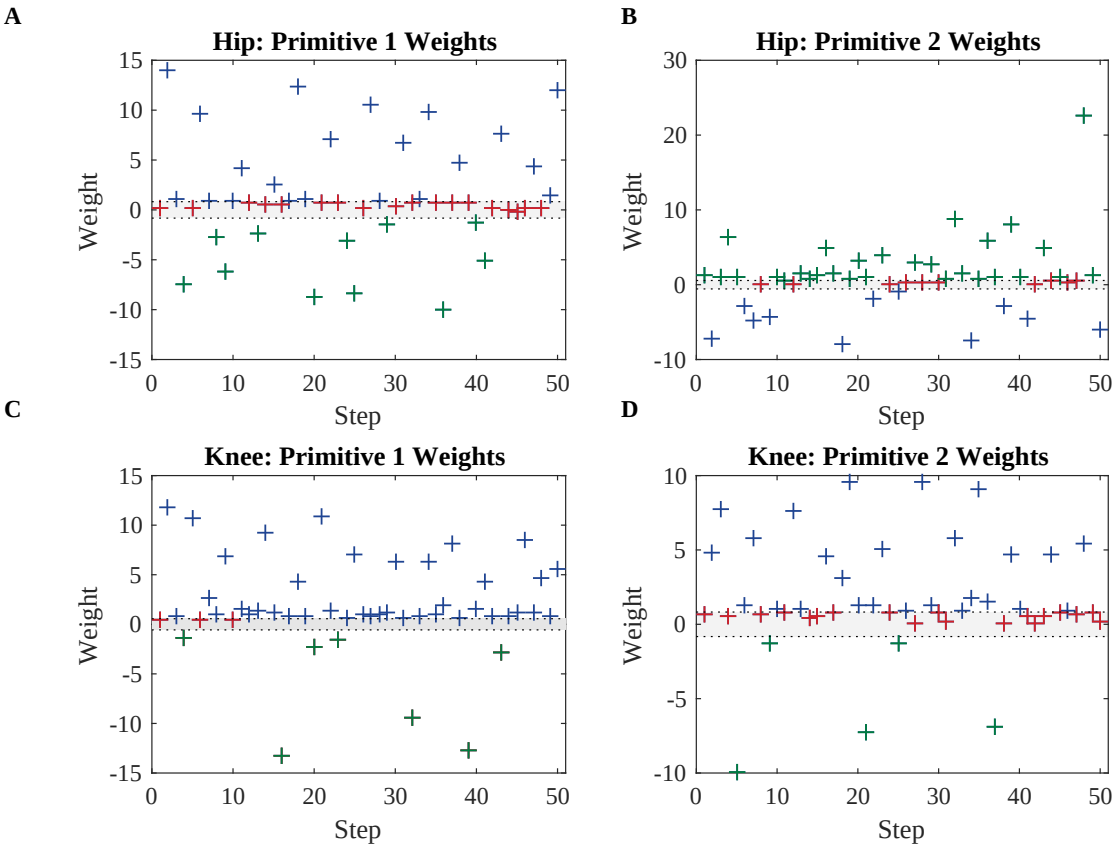

Figure 50 – Hip and knee weight values during the emulation of a non-paretic walk, of subject 3, with relation to the first and second hip and knee primitives.

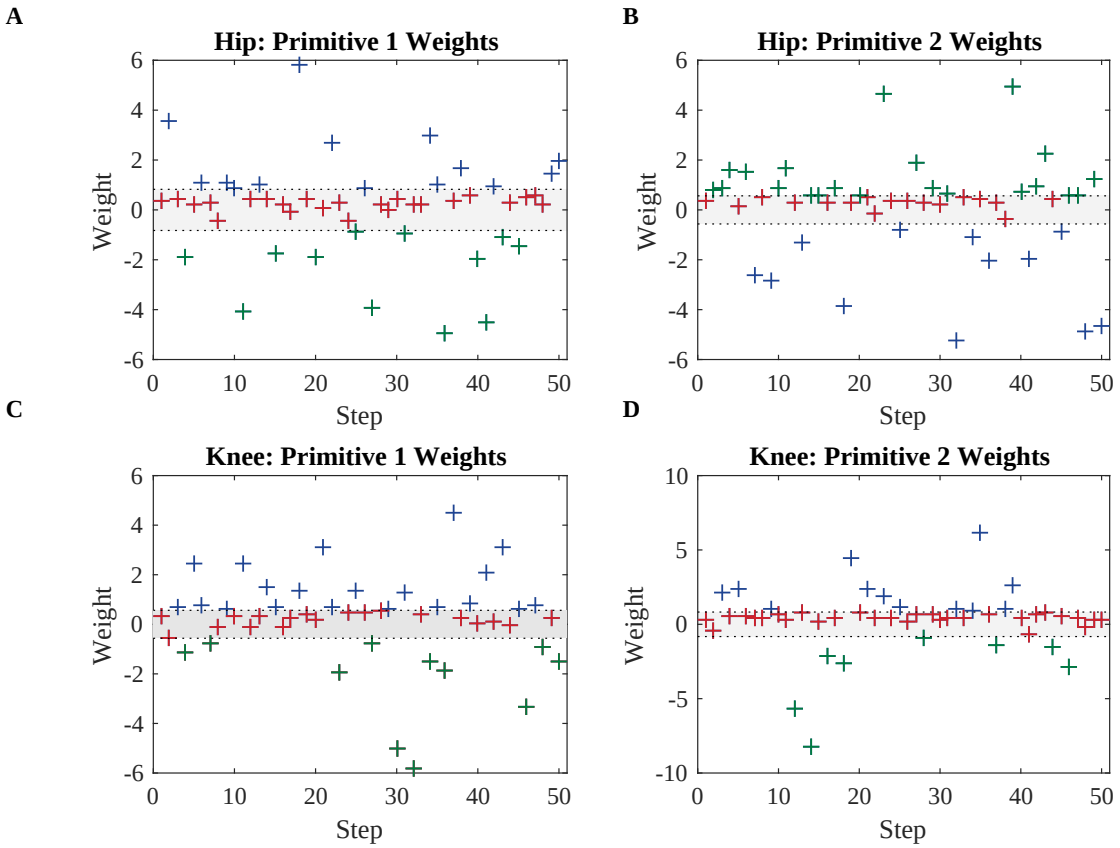

Figure 51 – Hip and knee weight values during the emulation of a non-paretic walk, of subject 5, with relation to the first and second hip and knee primitives.